Importance of axion-like particles for very- high-energy astrophysics

Marco Roncadelli

INFN and University of Pavia, Pavia, Italy

SUMMARY

1 – AXION-LIKE PARTICLES (ALPs)

Aesthetic reasons and conceptual problems lead to regard the Standard Model (SM) as the LOW-ENERGY EFFECTIVE THEORY (LEET) of some more FUNDAMENTAL THEORY (FT) characterized by a very large energy scale $M \gg G_F^{-1/2}$, containing both light ϕ and heavy Φ particles and defined by the lagrangian $\mathcal{L}_{\rm FT}(\phi, \Phi)$.

This view is made COMPELLING by the observational evidence for NONBARYONIC DARK MATTER responsible for the formation of cosmic structures and for DARK ENERGY presumably triggering the present accelerated cosmic expansion.

Denoting by

$$Z_{\rm FT}[J,K] \propto \int \mathcal{D}\phi \int \mathcal{D}\Phi \exp\left(i \int d^4x \left[\mathcal{L}_{\rm FT}(\phi,\Phi) + \phi J + \Phi K \right] \right) \tag{1}$$

the generating functional of the FT, the resulting LEET emerges

by integrating out the heavy particles and so its lagrangian $\mathcal{L}_{\rm eff}(\phi)$ is defined by

$$\exp\left(i\int d^4x\,\mathcal{L}_{\rm eff}(\phi)\right)\equiv\int\mathcal{D}\Phi\exp\left(i\int d^4x\,\mathcal{L}_{\rm FT}(\phi,\Phi)\right)\ . \quad (2)$$

Hence, $\mathcal{L}_{\rm eff}(\phi)$ not only contains $\mathcal{L}_{\rm SM}(\phi)$ but also includes nonrenormalizable terms involving ϕ that are suppressed by inverse powers of M. So the SM is embedded in the LEET whose generating functional reads

$$Z_{\rm eff}[J,K]\propto\int\mathcal{D}\phi\,\exp\left(i\int d^4x\left[\mathcal{L}_{\rm eff}(\phi)+\phi J\right]\right)\ . \quad (3)$$

Any sufficiently rich gauge structure such as the FT contains some GLOBAL symmetry $\mathcal{G}$ which is an accidental consequence of gauge invariance. As a rule, when gauge invariance gets spontaneously broken $\mathcal{G}$ gets SPONTANEOUSLY broken as well. Therefore some massless Goldstone bosons show up in the physical

spectrum. Yet, typically $\mathcal{G}$ is also slightly EXPLICITLY broken, e.g. this happens when Planck-scale effects are included since black holes do not carry definite global quantum numbers. As a consequence Goldstone bosons $\longrightarrow$ pseudo-Goldstone bosons with mass $\ll G_F^{-1/2}$, which must be present in the LEET even though they arise from physics at energies $\gg G_F^{-1/2}$. In conclusion, denoting by a the pseudo-Goldstone bosons and splitting up $\phi \longrightarrow \{\phi_{\rm SM}, a\}$ we have

$$\begin{aligned} \mathcal{L}_{\rm eff}(\phi_{\rm SM}, a) = \mathcal{L}_{\rm SM}(\phi_{\rm SM}) + \mathcal{L}_{\rm nonren}(\phi_{\rm SM}) + \\ + \mathcal{L}_{\rm ren}(a) + \mathcal{L}_{\rm ren}(\phi_{\rm SM}, a) + \mathcal{L}_{\rm nonren}(\phi_{\rm SM}, a) \ , \end{aligned} \tag{4}$$

where $\mathcal{L}_{\rm ren}(\phi_{\rm SM}, a)$ stands for possible renormalizable soft-breaking terms.

Natural Lorentz-Heaviside units with with $\hbar = c = k_{\rm B} = 1$ are employed throughout (unless otherwise stated).

An important example of this strategy is provided by the Peccei-Quinn $U(1)$ symmetry – giving rise to the AXION as a pseudo-Goldstone boson – which was proposed as a natural solution to the strong CP problem. Accordingly, we have

$$\mathcal{L}_{\rm ren}(a) = \frac{1}{2}\,\partial^\mu a\,\partial_\mu a - \frac{1}{2}\,m^2\,a^2\ , \tag{5}$$

where m is the axion mass and

$$\mathcal{L}_{\rm nonren}(\phi_{\rm SM}, a) = \mathcal{L}_{a\gamma\gamma} + \text{couplings of } a \text{ to fermions}\ , \tag{6}$$

with

$$\mathcal{L}_{a\gamma\gamma} = -\frac{1}{4M}\,F^{\mu\nu}\,\tilde{F}_{\mu\nu}\,a = \frac{1}{M}\,\mathbf{E}\cdot\mathbf{B}\,a\ , \tag{7}$$

where $F^{\mu\nu} \equiv (\mathbf{E}, \mathbf{B}) \equiv \partial^\mu A^\nu - \partial^\nu A^\mu$ is the usual electromagnetic field strength and $\tilde{F}^{\mu\nu} \equiv \frac{1}{2}\epsilon^{\mu\nu\rho\sigma}F_{\rho\sigma}$. Finally, the scale at which the Peccei-Quinn symmetry is spontaneously broken is proportional to M and a STRICT RELATIONSHIP exists between m and M.

Remarkably enough, many attempts to extend the SM – in the manner skeyched above – along very different directions such as four-dimensional ordinary and SUSY models, Kaluza-Klein theories and superstring theories all converge in generically predicting the existence of AXION-LIKE PARTICLES (ALPs).

ALPs are a straightforward generalization of the axion but important differences exist, since the axion arises in a very specific context while in dealing with ALPs the aim is to bring out their properties in a model-independent fashion as much as possible. This attitude has two main consequences:

- ONLY ALP-photon interaction terms are taken into account. Therefore, any other possible coupling of ALPs to SM particles is presently discarded and this entails that $\mathcal{L}_{\rm nonren}(\phi_{\rm SM}, a)$ in Eq. (4) ONLY includes $\mathcal{L}_{a\gamma\gamma}$ as defined by Eq. (7). Observe that such an ALP coupling to two photons $a\gamma\gamma$ is just supposed to exist without further worrying about its origin.

- The parameters m and M are to be regarded as UNRELATED for ALPs, and it is merely assumed that $m \ll G_F^{-1/2}$ and $M \gg G_F^{-1/2}$.

As a result, ALPs are described by the Lagrangian

$$\mathcal{L}_{\rm ALP} = \mathcal{L}_{\rm ren}(a) + \mathcal{L}_{a\gamma\gamma} = \tag{8}$$
$$= \frac{1}{2}\,\partial^\mu a\,\partial_\mu a - \frac{1}{2}\,m^2\,a^2 - \frac{1}{M}\,\mathbf{E}\cdot\mathbf{B}\,a\ .$$

So, the ONLY new interaction is of 1 ALP with 2 photons and the corresponding vertex is $a\gamma\gamma$.

Depending on the values of m and M, ALPs can be good candidates for either NONBARYONIC DARK MATTER or QUINTESSENTIAL DARK ENERGY.

2 – PHOTON-ALP MIXING

Because of the $\gamma\gamma a$ vertex, in the presence of an EXTERNAL magnetic field an OFF-DIAGONAL element in the mass matrix for the photon-ALP system shows up. Therefore, the interaction eigenstates DIFFER from the propagation eigenstates and photon-ALP MIXING occurs, which depends ONLY on B/M. The situation is analogous to what happens in the case of massive neutrinos with different flavours, apart from an important difference. All neutrinos have equal spin, and so neutrino oscillations can freely occur. Instead, ALPs are supposed to have spin zero whereas the photon has spin one, and so one of them can transform into the other only if the spin mismatch is compensated for by an external field.

Observe that since the vertex $\gamma\gamma a$ goes like $\mathbf{E}\cdot\mathbf{B}$, in the presence of an EXTERNAL magnetic field $\mathbf{B}$ ONLY the component $\mathbf{B}_T$ orthogonal to the photon momentum $\mathbf{k}$ matters. In addition,

photons $\gamma_\perp$ with linear polarization **E** orthogonal to the plane defined by **k** and **B** do NOT mix with an ALP, and so only photons $\gamma_\parallel$ with linear polarization in that plane DO mix.

Thus, photon-ALP mixing in the presence of an EXTERNAL magnetic field produces 2 different effects:

- photon-ALP OSCILLATIONS;
- CHANGE of the photon POLARIZATION state.

We consider throughout a monochromatic photon/ALP beam of energy E propagating along the z-direction – to be interpreted as the line-of sight – in a cold medium with the following properties:

- a HOMOGENEOUS magnetic field **B** is present;
- matter is IONIZED, and denoting by n_e the electron density the associated plasma frequency is $\omega_{\rm pl}^2 = 4\pi\alpha n_e/m_e$;
- photons CAN be ABSORBED – so that they have a FINITE mean free path $\lambda_\gamma(E)$ – but ALPs CANNOT.

Because we are interested in the regime $E \gg m$, the short-wavelength approximation (WKB) can be meaningfully applied, and so the beam propagation equations – which would be SECOND-ORDER coupled generalized Klein-Gordon and Maxwell equations – become FIRST-ORDER equations of the form

$$\left(i \frac{d}{dz} + E + \mathcal{M} \right) \begin{pmatrix} A_x(z) \\ A_y(z) \\ a(z) \end{pmatrix} = 0 \ , \tag{9}$$

where $A_x(z)$ and $A_y(z)$ are the two photon linear polarization amplitudes along the x and y axis, respectively, $a(z)$ denotes the ALP amplitude and $\mathcal{M}$ represents the photon-ALP mixing matrix which fails to be self-adjoint when photon absorption occurs. Observe that this is a Schrödinger-like equation, which entails that the beam is formally described as a NONRELATIVISTIC 3-LEVEL UNSTABLE QUANTUM SYSTEM with $H = -(E + \mathcal{M})$.

We will employ the generalized polarization density matrix

$$\rho(z) = \begin{pmatrix} A_x(z) \\ A_y(z) \\ a(z) \end{pmatrix} \otimes \begin{pmatrix} A_x(z) & A_y(z) & a(z) \end{pmatrix}^* \tag{10}$$

which obeys the Liouville-Von Neumann equation

$$i\frac{d\rho}{dz} = \rho\,\mathcal{M}^\dagger - \mathcal{M}\rho \tag{11}$$

associated with Eq. (9), whose solution is

$$\rho(z) = \mathcal{U}(z, z_0)\,\rho(z_0)\,\mathcal{U}^\dagger(z, z_0) \tag{12}$$

in terms of the transfer matrix $\mathcal{U}(z, z_0)$, namely the solution of Eq. (9) with initial condition $\mathcal{U}(z, z_0) = 1$. Then the probability that a photon/ALP beam initially in the state ρ_1 will be found in the state ρ_2 after a distance z is

$$P^{(0)}_{\rho_1 \to \rho_2}(z) = \frac{\mathrm{Tr}\left(\rho_2\,\mathcal{U}(z,0)\,\rho_1\,\mathcal{U}^\dagger(z,0)\right)}{\mathrm{Tr}\left(\rho_1\,\mathcal{U}^\dagger(z,0)\mathcal{U}(z,0)\right)}\ . \tag{13}$$

What is the form of $\mathcal{M}$? It is instructive to proceed as follows.

PARTICULAR CASE 1: **B** along the y-axis – to be interpreted as a fixed fiducial direction on the plane of the sky – with no absorption.

$$\mathcal{M}_0^{(0)} = \begin{pmatrix} \Delta_{\rm pl} & 0 & 0 \\ 0 & \Delta_{\rm pl} & \Delta_{a\gamma} \\ 0 & \Delta_{a\gamma} & \Delta_{aa} \end{pmatrix} \ , \tag{14}$$

with

$$\Delta_{\rm pl} = -\frac{\omega_{\rm pl}^2}{2E} \ , \quad \Delta_{a\gamma} \equiv \frac{B}{2M} \ , \quad \Delta_{aa} \equiv -\frac{m^2}{2E} \ . \tag{15}$$

It is useful to define the photon-ALP mixing angle

$$\alpha = \frac{1}{2}\,{\rm arctg}\left[\left(\frac{B}{M}\right)\left(\frac{2E}{m^2-\omega_{\rm pl}^2}\right)\right] \ . \tag{16}$$

In this case transfer matrix is

$$\mathcal{U}_0(z, z_0; 0) = e^{i\lambda_1(z-z_0)}\, T_0^1(0) + e^{i\lambda_2(z-z_0)}\, T_0^2(0) + e^{i\lambda_3(z-z_0)}\, T_0^3(0)\,, \tag{17}$$

where $\lambda_{1,2,3}$ are the eigenvalues of $\mathcal{M}_0^{(0)}$ and the T matrices are

$$T_0^1(0) \equiv \begin{pmatrix} 1 & 0 & 0 \\ 0 & 0 & 0 \\ 0 & 0 & 0 \end{pmatrix}\,, \tag{18}$$

$$T_0^2(0) \equiv \begin{pmatrix} 0 & 0 & 0 \\ 0 & \sin^2\alpha & -\sin\alpha\cos\alpha \\ 0 & -\sin\alpha\cos\alpha & \cos^2\alpha \end{pmatrix}\,, \tag{19}$$

$$T_0^3(0) \equiv \begin{pmatrix} 0 & 0 & 0 \\ 0 & \cos^2\alpha & \sin\alpha\cos\alpha \\ 0 & \sin\alpha\cos\alpha & \sin^2\alpha \end{pmatrix}\,. \tag{20}$$

In such a situation the oscillation probability is

$$P^{(0)}_{0,\gamma_y\to a}(z) = \left(\frac{B}{M\,\Delta_{\rm osc}}\right)^2 \sin^2\left(\frac{\Delta_{\rm osc}\,z}{2}\right) \ , \tag{21}$$

with oscillation wavenumber

$$\Delta_{\rm osc} \equiv \left[\left(\frac{m^2-\omega^2_{\rm pl}}{2E}\right)^2 + \left(\frac{B}{M}\right)^2\right]^{1/2} \ . \tag{22}$$

Eq. (21) shows that the photon-ALP oscillation probability becomes both MAXIMAL and ENERGY-INDEPENDENT for

$$\Delta_{\rm osc} \simeq \frac{B}{M} \ , \tag{23}$$

which defines the STRONG-COUPLING REGIME which sets in for $E > E_*$, with

$$E_* \equiv \frac{|m^2-\omega^2_{\rm pl}|M}{2B} \ . \tag{24}$$

PARTICULAR CASE 2: **B** along the y-axis plus absorption.

Including absorption is easy because it is INDEPENDENT of photon-ALP oscillations. Thanks to the analogy with QM, we have to obtain

$$P_{\rm decay} = e^{-z/\lambda_\gamma(E)} \ , \tag{25}$$

where $\lambda_\gamma(E)$ denotes the photon mean free path. As is well known, such a decay probability arises from the inclusion of an absorbitive term $-\Delta_{\rm abs}$ into the Hamiltonian, with

$$\Delta_{\rm abs} \equiv \frac{i}{2\,\lambda_\gamma(E)} \ . \tag{26}$$

Because photons undergo absorption but ALPs do not, $\mathcal{M}_0^{(0)}$ becomes

$$\mathcal{M}^{(0)} = \begin{pmatrix} \Delta_{\rm pl} + \Delta_{\rm abs} & 0 & 0 \\ 0 & \Delta_{\rm pl} + \Delta_{\rm abs} & \Delta_{a\gamma} \\ 0 & \Delta_{a\gamma} & \Delta_{aa} \end{pmatrix} , \qquad (27)$$

Enforcing the strong-mixing condition, $\mathcal{M}^{(0)}$ takes the simpler form

$$\mathcal{M}^{(0)} = \begin{pmatrix} \Delta_{\rm abs} & 0 & 0 \\ 0 & \Delta_{\rm abs} & \Delta_{a\gamma} \\ 0 & \Delta_{a\gamma} & 0 \end{pmatrix} , \qquad (28)$$

which is denoted by the same symbol for notational simplicity (only Eq. (28) will be used hereafter). Note that m and $\omega_{\rm pl}$ presently drop out of $\mathcal{M}^{(0)}$. Correspondingly, the transfer matrix is

$$\mathcal{U}(z, z_0; 0) = e^{i\lambda_1(z-z_0)}\, T_1(0) + e^{i\lambda_2(z-z_0)}\, T_2(0) + e^{i\lambda_3(z-z_0)}\, T_3(0) , \qquad (29)$$

where $\lambda_{1,2,3}$ are the eigenvalues of $\mathcal{M}^{(0)}$ and the T matrices are

$$T_1(0) \equiv \begin{pmatrix} 1 & 0 & 0 \\ 0 & 0 & 0 \\ 0 & 0 & 0 \end{pmatrix} , \tag{30}$$

$$T_2(0) \equiv \begin{pmatrix} 0 & 0 & 0 \\ 0 & \frac{-1+\sqrt{1-4\delta^2}}{2\sqrt{1-4\delta^2}} & \frac{i\delta}{\sqrt{1-4\delta^2}} \\ 0 & \frac{i\delta}{\sqrt{1-4\delta^2}} & \frac{1+\sqrt{1-4\delta^2}}{2\sqrt{1-4\delta^2}} \end{pmatrix} , \tag{31}$$

$$T_3(0) \equiv \begin{pmatrix} 0 & 0 & 0 \\ 0 & \frac{1+\sqrt{1-4\delta^2}}{2\sqrt{1-4\delta^2}} & -\frac{i\delta}{\sqrt{1-4\delta^2}} \\ 0 & -\frac{i\delta}{\sqrt{1-4\delta^2}} & \frac{-1+\sqrt{1-4\delta^2}}{2\sqrt{1-4\delta^2}} \end{pmatrix} , \tag{32}$$

where we have set

$$\delta \equiv \frac{B\,\lambda_\gamma(E)}{M} . \tag{33}$$

GENERAL CASE: **B** at angle ψ with respect to the y-axis plus absorption.

$$\mathcal{M} = \begin{pmatrix} \Delta_{\rm abs} & 0 & \Delta_{a\gamma}\,\sin\psi \\ 0 & \Delta_{\rm abs} & \Delta_{a\gamma}\,\cos\psi \\ \Delta_{a\gamma}\,\sin\psi & \Delta_{a\gamma}\,\cos\psi & 0 \end{pmatrix} , \qquad (34)$$

yielding the transfer matrix

$$\mathcal{U}(z, z_0; \psi) = e^{i\lambda_1(z-z_0)}\, T_1(\psi) + e^{i\lambda_2(z-z_0)}\, T_2(\psi) + e^{i\lambda_3(z-z_0)}\, T_3(\psi) , \qquad (35)$$

where $\lambda_{1,2,3}$ are the eigenvalues of $\mathcal{M}$ and the T matrices are

$$T_1(\psi) \equiv \begin{pmatrix} \cos^2\psi & -\sin\psi\cos\psi & 0 \\ -\sin\psi\cos\psi & \sin^2\psi & 0 \\ 0 & 0 & 0 \end{pmatrix} , \qquad (36)$$

$$T_2(\psi) \equiv \begin{pmatrix} \frac{-1+\sqrt{1-4\delta^2}}{2\sqrt{1-4\delta^2}} \sin^2\psi & \frac{-1+\sqrt{1-4\delta^2}}{2\sqrt{1-4\delta^2}} \sin\psi\cos\psi & \frac{i\delta}{\sqrt{1-4\delta^2}} \sin\psi \\ \frac{-1+\sqrt{1-4\delta^2}}{2\sqrt{1-4\delta^2}} \sin\psi\cos\psi & \frac{-1+\sqrt{1-4\delta^2}}{2\sqrt{1-4\delta^2}} \cos^2\psi & \frac{i\delta}{\sqrt{1-4\delta^2}} \cos\psi \\ \frac{i\delta}{\sqrt{1-4\delta^2}} \sin\psi & \frac{i\delta}{\sqrt{1-4\delta^2}} \cos\psi & \frac{1+\sqrt{1-4\delta^2}}{2\sqrt{1-4\delta^2}} \end{pmatrix} \tag{37}$$

$$T_3(\psi) \equiv \begin{pmatrix} \frac{1+\sqrt{1-4\delta^2}}{2\sqrt{1-4\delta^2}} \sin^2\psi & \frac{1+\sqrt{1-4\delta^2}}{2\sqrt{1-4\delta^2}} \sin\psi\cos\psi & \frac{-i\delta}{\sqrt{1-4\delta^2}} \sin\psi \\ \frac{1+\sqrt{1-4\delta^2}}{2\sqrt{1-4\delta^2}} \sin\psi\cos\psi & \frac{1+\sqrt{1-4\delta^2}}{2\sqrt{1-4\delta^2}} \cos^2\psi & \frac{-i\delta}{\sqrt{1-4\delta^2}} \cos\psi \\ \frac{-i\delta}{\sqrt{1-4\delta^2}} \sin\psi & \frac{-i\delta}{\sqrt{1-4\delta^2}} \cos\psi & \frac{-1+\sqrt{1-4\delta^2}}{2\sqrt{1-4\delta^2}} \end{pmatrix} \tag{38}$$

We stress that 1-loop QED vacuum polarization effects have been discarded since we shall deal with very weak magnetic fields. Also Faraday rotation is neglected because we are concerned with high-energy photons.

3 – ASTROPHYSICAL IMPLICATIONS

ALPs turn out to be extremely elusive in high-energy experiments and the only way to look for them in the laboratory requires very careful polarimetric measurements to be carried out on a laser beam or alternatively to perform a SHINING-THROUGH-A-WALL experiment. Unfortunately, with PRESENT capabilities successful detection of ALPs requires in either case a fairly large $a\gamma\gamma$ coupling.

Astrophysical manifestations of ALPs appear the best way to discover their existence, since they can give rise to observable effects even for much smaller values of the $a\gamma\gamma$ coupling. In fact, it has been noticed since a long time that for an $a\gamma\gamma$ coupling that looks hopelessly small to be probed in the laboratory stellar evolution would be dramatically altered by the Primakoff process and this fact sets a strong upper

$$M > 10^{10}\,\mathrm{GeV}\ . \tag{39}$$

In addition, the negative result of the CAST experiment designed to detect ALPs emitted by the Sun yields the bound

$$M > 1.14 \cdot 10^{10}\,\mathrm{GeV} \tag{40}$$

for $m < 0.02\,\mathrm{eV}$. Moreover, for $m < 10^{-10}\,\mathrm{eV}$ the failure to observe γ-rays coming from the conversion of ALPs emitted by the supernova SN1987A with the Solar Maximum Mission Gamma-Ray Detector provides the stronger bound

$$M > 10^{11}\,\mathrm{GeV} \tag{41}$$

which is however affected by large uncertainties.

In the last few years it has been realized that photon-ALP oscillations triggered by intervening COSMIC magnetic fields along the line of sight can produce DETECTABLE effects in observations of high-energy gamma-ray sources.

4 – INTERGALACTIC MEDIUM (IGM)

We shall be concerned throughout with the following situation.

Gamma-ray photons are emitted by a distant blazar and are detected on Earth at energies larger than $100\,\mathrm{GeV}$ with the Imaging Atmospheric Cherenkov Telescopes (ICTs) H.E.S.S., MAGIC, CANGAROO III and VERITAS, and in the future also with the Cherenkov Telescope Array (CTA) and the HAWC water Cherenkov γ-ray observatory. On their way to us they propagate inside the IGM.

We do NOT assume that the Universe is dominated by an ALP background.

Still, we ASSUME that INTERGALACTIC MAGNETIC FIELDS (IMFs) exist. Then inside the IGM photon-ALP OSCILLATIONS take place.

We suppose that the IGM consists of the following components:

1 - IONIZED MATTER. Absence of the Gunn-Peterson effect entails that the IGM is ionized. Observations of the primordial abundance of the light elements yields $\bar{n}_{e,0} \simeq 1.8 \cdot 10^{-7}\,\mathrm{cm}^{-3}$, but it has been argued that in the $z < 1$ Universe which is relevant for us $n_e(z)$ ought to be smaller than $\bar{n}_{e,0}$ by a factor 15. Correspondingly we get

$$\omega_{\mathrm{pl}}(z) \simeq 4.04 \cdot 10^{-15}\,(1+z)^{3/2}\ \mathrm{eV}\ , \tag{42}$$

2 - MAGNETIC FIELD. Owing to the notorious lack of information about their morphology, one usually assumes that they have a DOMAIN-LIKE structure. That is, **B** ought to be constant over a domain of size L_{dom} equal to its coherence length, with **B** RANDOMLY changing its direction from one domain to another but keeping approximately the SAME strength. Neglecting AUGER

results because too uncertain, we rely only on well-established upper bounds:

$$B_0 < 3.8\,\mathrm{nG} \quad \text{for} \quad L_{\mathrm{dom}} = 50\,\mathrm{Mpc}\ , \tag{43}$$

$$B_0 < 6.3\,\mathrm{nG} \quad \text{for} \quad L_{\mathrm{dom}} = 1\,\mathrm{Mpc}\ . \tag{44}$$

It is usually supposed that $1\,\mathrm{Mpc} \leq L_{\mathrm{dom}} \leq 10\,\mathrm{Mpc}$, and so we will assume throughout

$$B_0 < 6\,\mathrm{nG}\ . \tag{45}$$

Owing to the high conductivity of the IGM, the magnetic flux lines can be thought as frozen inside the IGM. Therefore, flux conservation during the cosmic expansion entails that B scales like the volume to the power $2/3$, thereby implying the magnetic field strength in a domain at redshift z is

$$B(z) = B_0\ (1+z)^2\ . \tag{46}$$

3 - EXTRAGALACTIC BACKGROUND LIGHT (EBL). This is the light produced by galaxies during the whole cosmic evolution. Basically, five different approaches have been pursued to determine its SED:

- *Forward evolution* – This is the most ambitious approach, since it begins from first principles, namely from semi-analytic models of galaxy formation in order to predict the time evolution of the galaxy luminosity function.
- *Backward evolution* – This starts from observations of the present galaxy population and extrapolates the galaxy luminosity function backward in time. Among others, this strategy has been followed by Stecker, Malkan and Scully (SMS) and by Franceschini, Rodighiero and Vaccari (FRV).
- *Inferred evolution* – This models the EBL by using quantities like the star formation rate, the initial mass function and the dust extinction as inferred from observations.

- *Observed evolution* – This method has the advantage to rely only upon observations by using a very rich sample of galaxies extending over the redshift range $0 \leq z \leq 1$.
- *Compared observations* – This technique has been implemented in two ways. One consists in comparing observations of the EBL itself with blazar observations with IACTs and deducing the EBL level from the VHE photon dimming. Another starts from some γ-ray observations of a given blazar below $100\,\mathrm{GeV}$ where EBL absorption is negligible and infers the EBL level by comparing the IACT observations of the same blazar with the source spectrum as extrapolated from the former observations. In the latter case the main assumption is that the emission mechanism is presumed to be known with great accuracy. In either case, the crucial unstated assumption is that photon propagation in the VHE band is governed by conventional physics.

The latter approach does not apply to the DARMA scenario, and so it will not be considered.

As far as the backward evolution approach is concerned, the models of SMS predict a much higher EBL level as compared to the model of FRV. Recently, the SMS models have been ruled out by Fermi/LAT observations.

On the other hand, a remarkable agreement exists among the FRV model and the other models based on forward evolution, inferred evolution and observed evolution.

Throughout this paper, we adopt the FRV model, whose SED is illustrated in Fig. 1 where regretfully error bars are not reported.

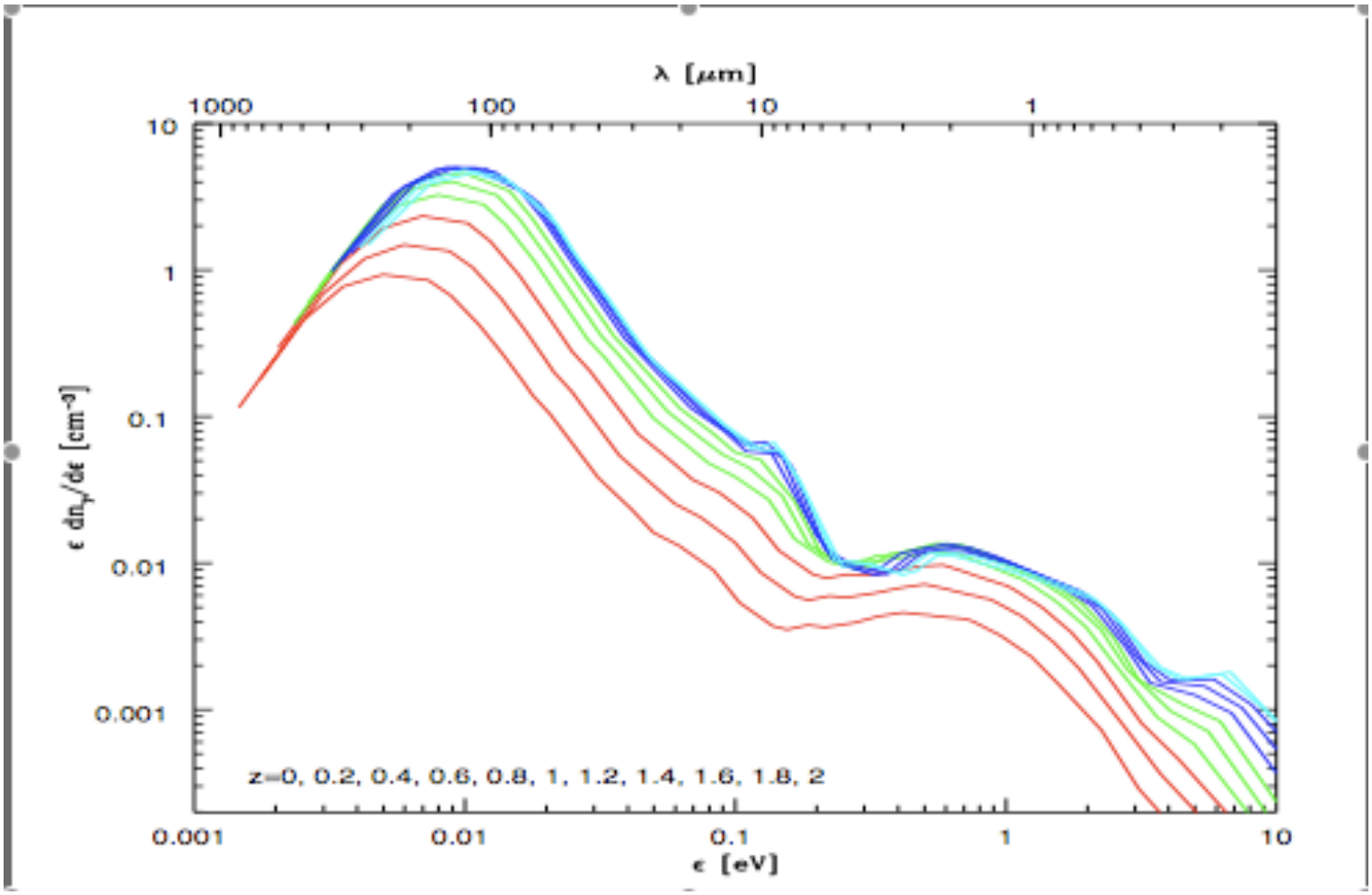

Fig. 1 – SED for the FRV model

According to conventional physics when hard beam photons of energy E scatter off EBL photons of energy ϵ produce e^+e^- pairs through the standard $\gamma\gamma \longrightarrow e^+e^-$ process. The corresponding Breit-Wheeler cross-section is

$$\sigma_{\gamma\gamma}(E,\epsilon,\varphi) \simeq 1.25 \cdot 10^{-25} \left(1-\beta^2\right) \times \tag{47}$$
$$\times \left[2\beta\left(\beta^2-2\right) + \left(3-\beta^4\right) \ln\left(\frac{1+\beta}{1-\beta}\right)\right] \mathrm{cm}^2 \ ,$$

which depends on E, ϵ and φ only through the dimensionless parameter

$$\beta(E,\epsilon,\varphi) \equiv \left[1 - \frac{2\, m_e^2\, c^4}{E\epsilon\,(1-\cos\varphi)}\right]^{1/2} \ , \tag{48}$$

where φ denotes the scattering angle and m_e is the electron mass. The process is kinematically allowed for $\beta^2 > 0$ and $\sigma_{\gamma\gamma}(E,\epsilon,\varphi)$ reaches its maximum $\sigma_{\gamma\gamma}^{\max} \simeq 1.70 \cdot 10^{-25}\,\mathrm{cm}^2$ for $\beta \simeq 0.70$.

Assuming head-on collisions for definiteness ($\varphi = \pi$), it follows that $\sigma_{\gamma\gamma}(E, \epsilon, \pi)$ gets maximized for the EBL photon energy

$$\epsilon(E) \simeq \left(\frac{500\,\mathrm{GeV}}{E}\right)\,\mathrm{eV}\ , \tag{49}$$

where E and ϵ correspond to the same redshift. Throughout, E will be regarded as an independent variable (note that E and ϵ change along the beam in proportion of $1 + z$).

Within the standard ΛCDM cosmological model the optical depth $\tau_\gamma(E_0, z)$ for $\gamma\gamma \to e^+e^-$ arises by first convolving the spectral number density $n_\gamma(\epsilon(z), z)$ of the EBL at a generic redshift with $\sigma_{\gamma\gamma}(E(z), \epsilon(z), \varphi)$ along the line of sight for fixed values of z, φ and $\epsilon(z)$, and next integrating over all these variables. Hence

$$\tau_\gamma(E_0, z) = \int_0^z \mathrm{d}z \, \frac{\mathrm{d}l(z)}{\mathrm{d}z} \int_{-1}^{1} \mathrm{d}(\cos\varphi) \, \frac{1-\cos\varphi}{2} \times \tag{50}$$
$$\times \int_{\epsilon_{\rm thr}(E(z),\varphi)}^{\infty} \mathrm{d}\epsilon(z) \, n_\gamma(\epsilon(z), z) \, \sigma_{\gamma\gamma}\big(E(z), \epsilon(z), \varphi\big) \ ,$$

where the distance travelled by a photon per unit redshift at redshift z is given by

$$\frac{dl(z)}{dz} = \frac{c}{H_0} \frac{1}{(1+z)\left[\Omega_\Lambda + \Omega_M (1+z)^3\right]^{1/2}} \ , \tag{51}$$

with Hubble constant $H_0 \simeq 70\,\mathrm{Km\,s^{-1}\,Mpc^{-1}}$, with $\Omega_\Lambda \simeq 0.7$ and $\Omega_M \simeq 0.3$. Finally, the photon survival probabilty is

$$P^{\rm CP}_{\gamma\to\gamma}(E_0,z) = e^{-\tau_\gamma(E_0,z)} \ , \tag{52}$$

so that the observed and emitted differential photon number fluxes – namely dN/dE – are related by

$$\Phi_{\rm obs}(E_0,z) = P^{\rm CP}_{\gamma\to\gamma}(E_0,z)\,\Phi_{\rm em}\left(E_0(1+z)\right) \ , \tag{53}$$

In terms of $n_\gamma(\epsilon(z),z)$ as exhibited in Fig. 1, using Eq. (50) FRV provide a very detailed numerical evaluation of $\tau^{\rm FRV}_\gamma(E_0,z)$.

Discarding cosmological effects, the source distance is $D = cz/H_0$ and the optical depth becomes

$$\tau_\gamma(E,D) = \frac{D}{\lambda_\gamma(E)} \ , \tag{54}$$

where $\lambda_\gamma(E)$ is the photon mean free path for $\gamma\gamma \to e^+e^-$ referring to the present cosmic epoch. As a consequence, Eq. (52) becomes

$$P^{\rm CP}_{\gamma\to\gamma}(E,D) = e^{-D/\lambda_\gamma(E)} \ , \tag{55}$$

and so Eq. (53) reduces to

$$\Phi_{\rm obs}(E,D) = e^{-D/\lambda_\gamma(E)}\ \Phi_{\rm em}(E) \ . \tag{56}$$

Within the FRV EBL model without cosmological effects $\lambda_\gamma^{\mathrm{FRV}}(E)$ is plotted in Fig. 2.

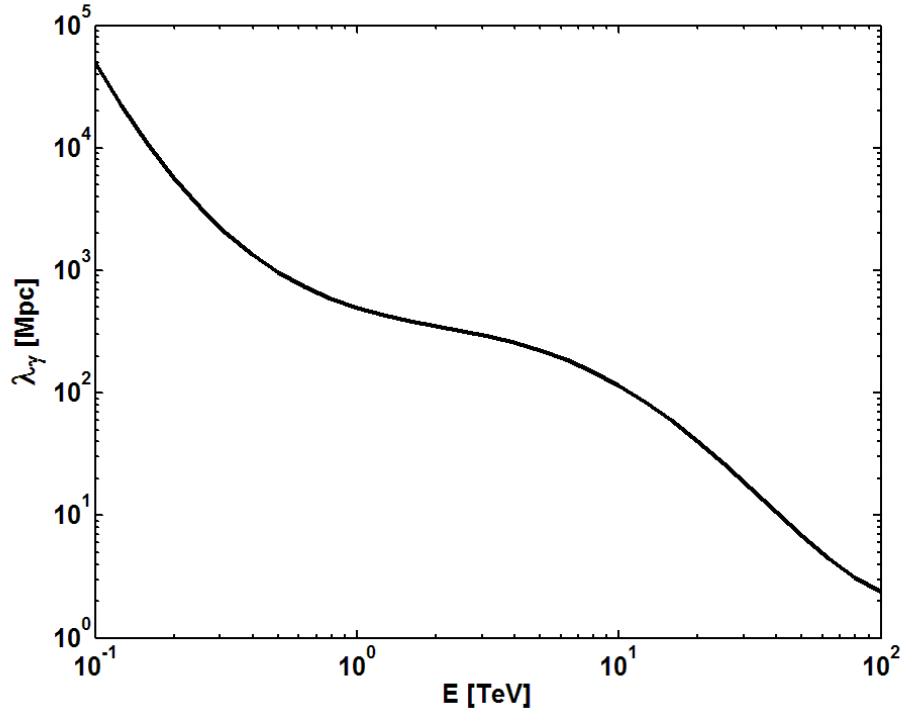

Fig. 2 – The pair-production mean free path $\lambda_\gamma^{\mathrm{FRV}}$ of a VHE photon is plotted versus its energy E. Only conventional physics is assumed.

We will address very-high-energy (VHE) blazars in the range 100 GeV – 100 TeV. Fig. 2 shows that the EBL is VERY IMPORTANT, and so photon absorption takes place. Correspondingly, from Eq. (49) it follows that EBL dimming is maximal for EBL photon energy in the range $0.005\,\mathrm{eV} < \epsilon_0 < 5\,\mathrm{eV}$ ($1.21 \cdot 10^3\ \mathrm{GHz} < \nu_0 < 1.21 \cdot 10^5\,\mathrm{GHz}$, $2.48\,\mu\mathrm{m} < \lambda_0 < 2.48 \cdot 10^2\,\mu\mathrm{m}$).

Most of the blazars observed so far are in the range $0.2\,\mathrm{TeV} < E_0 < 2\,\mathrm{TeV}$ and from Eq. (49) we see that the EBL band where $\sigma_{\gamma\gamma}(E_0, \epsilon_0, \pi)$ becomes maximal is $0.25\,\mathrm{eV} < \epsilon_0 < 2.5\,\mathrm{eV}$ ($6.07 \cdot 10^4\,\mathrm{GHz} < \nu_0 < 6.07 \cdot 10^5\,\mathrm{GHz}$, $0.50\,\mu\mathrm{m} < \lambda_0 < 4.94\,\mu\mathrm{m}$).

5 – BEAM PROPAGATION INSIDE THE IGM

Within the cosmological context, the overall structure of the cellular configuration of large-scale magnetic fields is naturally described by a UNIFORM mesh in redshift space with elementary step Δz, which can be constructed as follows. The magnetic domain closest to us and labelled by $n = 1$ extends from 0 to Δz. Hence, its size $L^{(1)}$ can also be written as

$$L^{(1)} = L(0, \Delta z) = \left(\frac{L^{(1)}}{5\,\mathrm{Mpc}} \right) 5\,\mathrm{Mpc}\ , \tag{57}$$

where $L(0, \Delta z)$ is the domain's proper size and the second equality stresses our preferred choice for $L^{(1)}_{\mathrm{dom}}$. Since the proper length extending over the redshift interval $[z_a, z_b]$ $(z_a < z_b)$ is

$$L(z_a, z_b) \simeq 2.96 \cdot 10^3 \ln \left(\frac{1 + 1.45\, z_b}{1 + 1.45\, z_a} \right)\ \mathrm{Mpc} \tag{58}$$

we infer

$$\Delta z \simeq 1.17 \cdot 10^{-3} \left(\frac{L^{(1)}}{5\,\mathrm{Mpc}} \right) \ , \tag{59}$$

indeed in agreement with the linear Hubble law. Because our mesh in redshift space is uniform, Δz sets the redshift size of ALL magnetic domains. Furthermore, the n-th domain extends from $z = (n-1)\Delta z$ to $z = n\Delta z$ and its proper size can be written as $L^{(n)} = L((n-1)\Delta z, n\Delta z)$. Thanks to Eq. (58)

$$L^{(n)} \simeq 2.96 \cdot 10^{3} \ln \left(1 + \frac{1.45\,\Delta z}{1 + 1.45\,(n-1)\Delta z} \right) \mathrm{Mpc} \ . \tag{60}$$

Manifestly, the WHOLE propagation process of the beam in question can be recovered by ITERATING the propagation over a SINGLE domain as many times as the number of domains crossed by the beam, taking each time a RANDOM value for the angle ψ between **B** and a FIXED fiducial direction and the appropriate value of $B(z)$ as well as the appropriate value of $\lambda_\gamma(E_0(1+z))$.

In this way, the problem is reduced to the much easier one – already solved – of photon-ALP oscillation in a HOMOGENEOUS magnetic field in the presence of photon absorption.

Eventually, such a procedure can be repeated very many times and finally we AVERAGE all these realizations of the propagation process over the random angles. In this way we obtain the PHOTON SURVIVAL PROBABILITY $P_{\gamma\to\gamma}(E_0, z)$ for a source at redshift z and observed at energy E_0.

We work throughout within the STRONG-MIXING REGIME.

6 – DARMA SCENARIO

Once emitted, photons can convert into ALPs and next reconvert back into photons before reaching the Earth. We restrict ourselves to the situation in which photon-ALP oscillations take place in intergalactic space ONLY. As a consequence photons acquire a SPLIT PERSONALITY, travelling for some time as real photons and for some time as ALPs. However, they suffer EBL absorption ONLY when they are real photons, which means that the effective photon mean free path $\lambda_{\gamma,\mathrm{eff}}(E)$ is actually LARGER than $\lambda_{\gamma}(E)$ as predicted by conventional physics. Since the photon survival probability depends exponentially on minus the optical depth – which in turn goes like the source distance divided by $\lambda_{\gamma,\mathrm{eff}}(E)$ – even a SLIGHT INCREASE of $\lambda_{\gamma,\mathrm{eff}}(E)$ with respect to $\lambda_{\gamma}(E)$ produces a SUBSTANTIAL ENHANCEMENT of the photon survival probability and so of the observed flux.

Actually, since the EBL absorption increases with energy whereas the photon-ALP oscillation probability is energy-independent, the observed flux enhancement gets larger and larger as the energy increases. As a consequence, the observed spectra are HARDER than currently expected, thereby making the VHE Universe MORE TRANSPARENT than generally believed.

A more quantitative insight into the DARMA mechanism can be gained as follows. Suppose that VHE photons are both emitted and detected as usual, but that along their way to us they convert into ALPs and back into photons. Accordingly, the number N_c of either $\gamma \longrightarrow a$ or $a \longrightarrow \gamma$ conversions must necessarily be even, and we may schematically regard the beam propagation in large-scale magnetic fields as a succession of such conversions. Assuming ideally that each conversion occurs suddenly at some space point, the source distance D gets divided into a number $N_c + 1$ of steps of equal length L, over which a beam particle behaves either as a real photon or as an ALP.

Hence, a beam particle exhibits an overall behaviour as a real photon over a total length equal to

$$D_\gamma = \frac{N_c + 2}{2\,(N_c + 1)}\,D = \left(1 - \frac{N_c}{2N_c + 2}\right) D\ . \tag{61}$$

We intuitively expect N_c to increase with the photon-ALP oscillation probability which leads to a slight decrease of D_γ starting from D. Correspondingly equation

$$P^{\rm CP}_{\gamma\to\gamma}(E, D) = e^{-D/\lambda_\gamma(E)}\ , \tag{62}$$

gets presently replaced by

$$P^{\rm DARMA}_{\gamma\to\gamma}(E, D) = e^{-D_\gamma/\lambda_\gamma(E)} = e^{-\left(1-\frac{N_c}{2N_c+2}\right)D/\lambda_\gamma(E)}\ , \tag{63}$$

and thanks to its exponential dependence on $D_\gamma/\lambda_\gamma(E)$ even a SMALL DECREASE of D_γ starting from D produces a LARGE ENHANCEMENT of $P^{\rm DARMA}_{\gamma\to\gamma}(E, D)$ as compared to $P^{\rm CP}_{\gamma\to\gamma}(E, D)$.

7 – GENERAL STRATEGY

Our ultimate goal consists in the evaluation of the photon survival probability $P_{\gamma\to\gamma}^{\rm DARMA}(E_0, z)$ from a blazar at redshift z to us when allowance is made for photon-ALP oscillations as well as for EBL photon absorption.

Our strategy can be implemented through the following steps:
1 – We work within the STRONG-MIXING REGIME so as to ensure that the photon-ALP oscillation probability is both maximal and energy-independent. Such a condition requires $E > E_*$, with the energy threshold E_* defined by Eq. (24). But demanding the strong-mixing regime to take place for $E > 100\,{\rm GeV}$ evidently amounts to assume $E_* < 100\,{\rm GeV}$, which sets the upper bound

$$\left| \left(\frac{m}{10^{-10}\,{\rm eV}} \right)^2 - \left(1.14 \cdot 10^{-4} \right)^2 \right|^{1/2} < \tag{64}$$

$$< 1.97 \cdot 10^{-10} \left(\frac{B}{\rm nG} \right)^{1/2} \left(\frac{10^{11}\,{\rm GeV}}{M} \right)^{1/2} {\rm eV} \ .$$

2 – From Eq. (35) it follows that the transfer matrix across the n-th domain can be more suitably be written as

$$\mathcal{U}_n(E_n,\psi_n) \equiv e^{i\left(\lambda_1^{(n)}\, L^{(n)}\right)}\, T_1(\psi_n) + e^{i\left(\lambda_2^{(n)}\, L^{(n)}\right)}\, T_2(\psi_n) + e^{i\left(\lambda_3^{(n)}\, L^{(n)}\right)}\, T_3(\psi_n)\,, \tag{65}$$

with $T_1(\psi_n)$, $T_2(\psi_n)$, $T_3(\psi_n)$ given by Eqs. (36), (37), (38) with $\psi \to \psi_n$. The photon mean free path $\lambda_\gamma^n(E_0)$ over the n-th domain is

$$\lambda_\gamma^{(n)}(E_0) = \left(\frac{4.29\cdot 10^3}{1+1.45\,(n-1)\Delta z}\right) \left(\frac{\Delta z}{\tau_\gamma\,(E_0, n\,\Delta z) - \tau_\gamma\,(E_0,(n-1)\Delta z)}\right) \mathrm{Mpc}\,. \tag{66}$$

Similarly, the energy E_n and the magnetic field B_n pertaining to the n-th domain are

$$E_n \equiv E_0 \left[1 + (n-1)\,\Delta z)\right] , \tag{67}$$

$$B_n = B_0 \left[1 + (n-1)\,\Delta z)\right]^2 , \tag{68}$$

so that the parameter δ_n entering the T matrices and the eigenvalues of $\mathcal{M}$ is

$$\delta_n \equiv \frac{B_n\,\lambda_\gamma^{(n)}(E_0)}{M} \tag{69}$$

Note that $\mathcal{U}_n(E_0, \psi_n)$ depends on E_0 only because of the energy-dependence of EBL absorption.

3 – Iteration of the latter result over the total number N_d of domains crossed by the beam from the blazar to us yields the total transfer matrix

$$\mathcal{U}\left(E_0, z; \psi_1, ..., \psi_{N_d}\right) = \prod_{n=1}^{N_d} \mathcal{U}_n\left(E_n, \psi_n\right) \ . \tag{70}$$

According to Eq. (13), the probability that a photon/ALP beam emitted by a blazar at z in the state ρ_1 will be detected in the state ρ_2 for FIXED orientations $\psi_1, ..., \psi_{N_d}$ of $\mathbf{B}$ in every domain is

$$P_{\rho_1 \to \rho_2}\left(E_0, z; \psi_1, ..., \psi_{N_d}\right) = \tag{71}$$
$$\frac{\mathrm{Tr}\left(\rho_2 \mathcal{U}\left(E_0, z; \psi_1, ..., \psi_{N_d}\right) \rho_1 \mathcal{U}^{\dagger}\left(E_0, z; \psi_1, ..., \psi_{N_d}\right)\right)}{\mathrm{Tr}\left(\rho_1 \mathcal{U}^{\dagger}\left(E_0, z; \psi_1, ..., \psi_{N_d}\right) \mathcal{U}\left(E_0, z; \psi_1, ..., \psi_{N_d}\right)\right)} \ .$$

4 – As a consequence, the actual detection probability for the beam in question emerges by averaging the above expression over all angles, namely

$$P_{\rho_1 \to \rho_2}(E_0, z) = \left\langle P_{\rho_1 \to \rho_2}(E_0, z; \psi_1, ..., \psi_{N_d}) \right\rangle_{\psi_1, ..., \psi_{N_d}} . \quad (72)$$

Because of the fact that the photon polarization cannot be measured at the energies considered here we have to sum this result over the two final polarization states

$$\rho_x = \begin{pmatrix} 1 & 0 & 0 \\ 0 & 0 & 0 \\ 0 & 0 & 0 \end{pmatrix} , \quad (73)$$

$$\rho_z = \begin{pmatrix} 0 & 0 & 0 \\ 0 & 1 & 0 \\ 0 & 0 & 0 \end{pmatrix} . \quad (74)$$

Moreover, we suppose for simplicity that the emitted beam consists 100 % of unpolarized photons, so that the initial beam state is described by

$$\rho_{\mathrm{unpol}} = \frac{1}{2} \begin{pmatrix} 1 & 0 & 0 \\ 0 & 1 & 0 \\ 0 & 0 & 0 \end{pmatrix} \quad . \tag{75}$$

Hence, we ultimately have

$$P_{\gamma\to\gamma}^{\mathrm{DARMA}}(E_0, z) = \left\langle P_{\rho_{\mathrm{unpol}}\to\rho_x}(E_0, z; \psi_1, ..., \psi_{N_d}) \right\rangle_{\psi_1,...,\psi_{N_d}} + \tag{76}$$

$$+ \left\langle P_{\rho_{\mathrm{unpol}}\to\rho_z}(E_0, z; \psi_1, ..., \psi_{N_d}) \right\rangle_{\psi_1,...,\psi_{N_d}} .$$

5 – We implement this procedure as follows. In the first place, we ARBITRARILY choose the angle ψ_n in the n-th domain and we evaluate the corresponding transfer matrix $\mathcal{U}_n\left(E_n, \psi_n\right)$ for a given value of E_0, keeping Eq. (67) in mind. Next, the application of Eqs. (70) and (71) yields the corresponding photon survival probabilities entering Eq. (76) for a SINGLE realization of the propagation process. We REPEAT these steps 5000 times, by RANDOMLY VARYING ALL ANGLES ψ_n EACH TIME, thereby generating 5000 random realizations of the propagation process. Finally, we average the resulting photon survival probabilities over all these realizations of the propagation process, thereby accomplishing the average process in Eq. (76). We find in this way the physical photon survival probability $P_{\gamma\to\gamma}^{\mathrm{DARMA}}\left(E_0, z\right)$.

9 – DISCUSSION

Because all physical predictions depend solely on B/M, it is quite useful to introduce the dimensionless parameter

$$\xi \equiv \left(\frac{B_0}{\mathrm{nG}}\right)\left(\frac{10^{11}\,\mathrm{GeV}}{M}\right) \ . \tag{77}$$

Owing to conditions (41) and (45), it will be assumed

$$\xi < 6 \tag{78}$$

throughout our discussion. Specifically, we will focus our attention on the representative cases $\xi = 5.0$, $\xi = 1.0$, $\xi = 0.5$, $\xi = 0.1$, taking both $L_{\mathrm{dom}} = 4\,\mathrm{Mpc}$ and $L_{\mathrm{dom}} = 10\,\mathrm{Mpc}$ at $z = 0$. Nevertheless, it is important to keep under control which values of B_0 and M are allowed in each case. From the constraints (41) and (45) we find the allowed ranges reported in Table 1

ξ	$M/(10^{11}\,\mathrm{GeV})$	B_0/nG
0.1	1 – 60	0.1 – 6
0.5	1 – 12	0.5 – 6
1.0	1 – 6.0	1 – 6
5.0	1 – 1.2	5 – 6

Table 1 – Allowed values of M and B_0 in the considered cases.

Observe that Eq. (64) can be rewritten as

$$\left| \left(\frac{m}{10^{-10}\,\mathrm{eV}} \right)^2 - \left(1.14 \cdot 10^{-4} \right)^2 \right|^{1/2} < 1.97\,\xi^{1/2} \qquad (79)$$

Thanks to condition (78), we see that within the DARMA scenario ALPs have to be very light, with mass never exceeding $5 \cdot 10^{-10}\,\mathrm{eV}$. In particular, the axion needed to solve the strong CP problem is therefore ruled out by several orders of magnitude.

Observe that for $m < 1.14 \cdot 10^{-14}\,\mathrm{eV}$ the plasma frequency dominates, so that even massless ALPs behave as if their mass where equal to the plasma frequency. The upper bounds on m corresponding to the cases under consideration are reported in Table 2.

Upper bound on m	Value of the ξ parameter
$4.40 \cdot 10^{-10}\,\mathrm{eV}$	$\xi = 5.0$
$1.97 \cdot 10^{-10}\,\mathrm{eV}$	$\xi = 1.0$
$1.39 \cdot 10^{-10}\,\mathrm{eV}$	$\xi = 0.5$
$0.62 \cdot 10^{-10}\,\mathrm{eV}$	$\xi = 0.1$

Table 2 – Upper bounds on the ALP mass in the considered cases.

9 – PREDICTIONS FOR FUTURE OBSERVATIONS

The best way to figure out the relevance of the DARMA scenario for future observations to be performed with the CTA and with the HAWC water Cherenkov γ-ray observatory is to compare the photon survival probability $P_{\gamma\to\gamma}^{\rm DARMA}(E_0, z)$ with the one predicted by conventional physics $P_{\gamma\to\gamma}^{\rm CP}(E_0, z)$, with the EBL described in either case by the FRV model.

We do that for a sample of sources at different redshifts, like $z = 0.031$, $z = 0.188$, $z = 0.444$ and $z = 0.536$. We remark that the case of $z = 0.031$ may look somewhat academic, since its location inside the Local Group is likely to make the morphology of the magnetic field crossed by its line of sight more complicated than assumed in this paper. Nevertheless, we include $z = 0.031$ in the present analysis in order to see what happens for a very nearby blazar even if a drastic simplifying assumption is made.

The results are displayed in the next Figures. For each of the selected sources, we consider the above choices for ξ, which are represented by a solid black line ($\xi = 5.0$), a dotted-dashed line ($\xi = 1.0$), a dashed line ($\xi = 0.5$) and a dotted line ($\xi = 0.1$), while the solid grey line corresponds to conventional physics. We take both $L_{\rm dom} = 4\,{\rm Mpc}$ and $L_{\rm dom} = 10\,{\rm Mpc}$ for the domain size at $z = 0$.

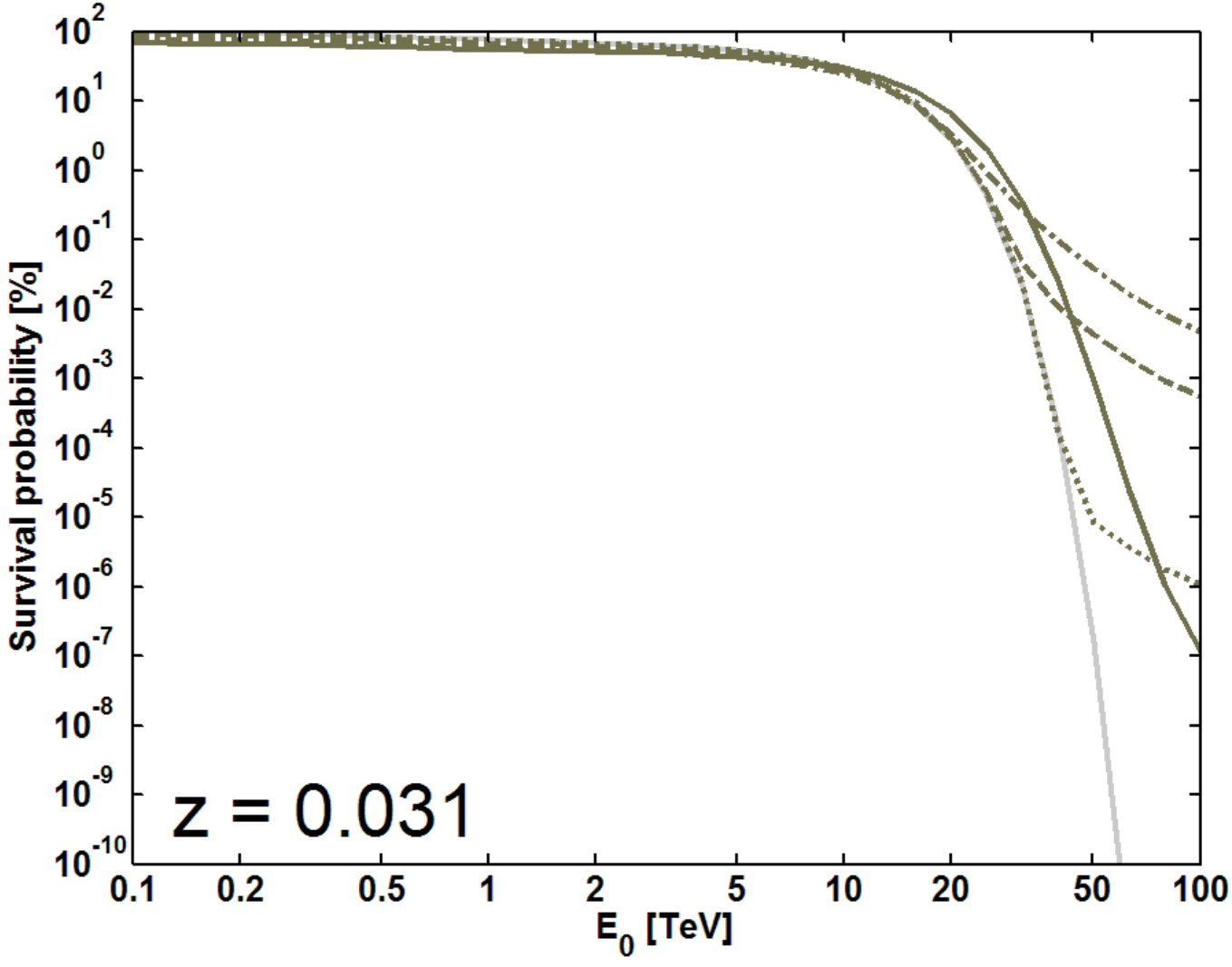

$L_{\mathrm{dom}} = 4\,\mathrm{Mpc}$

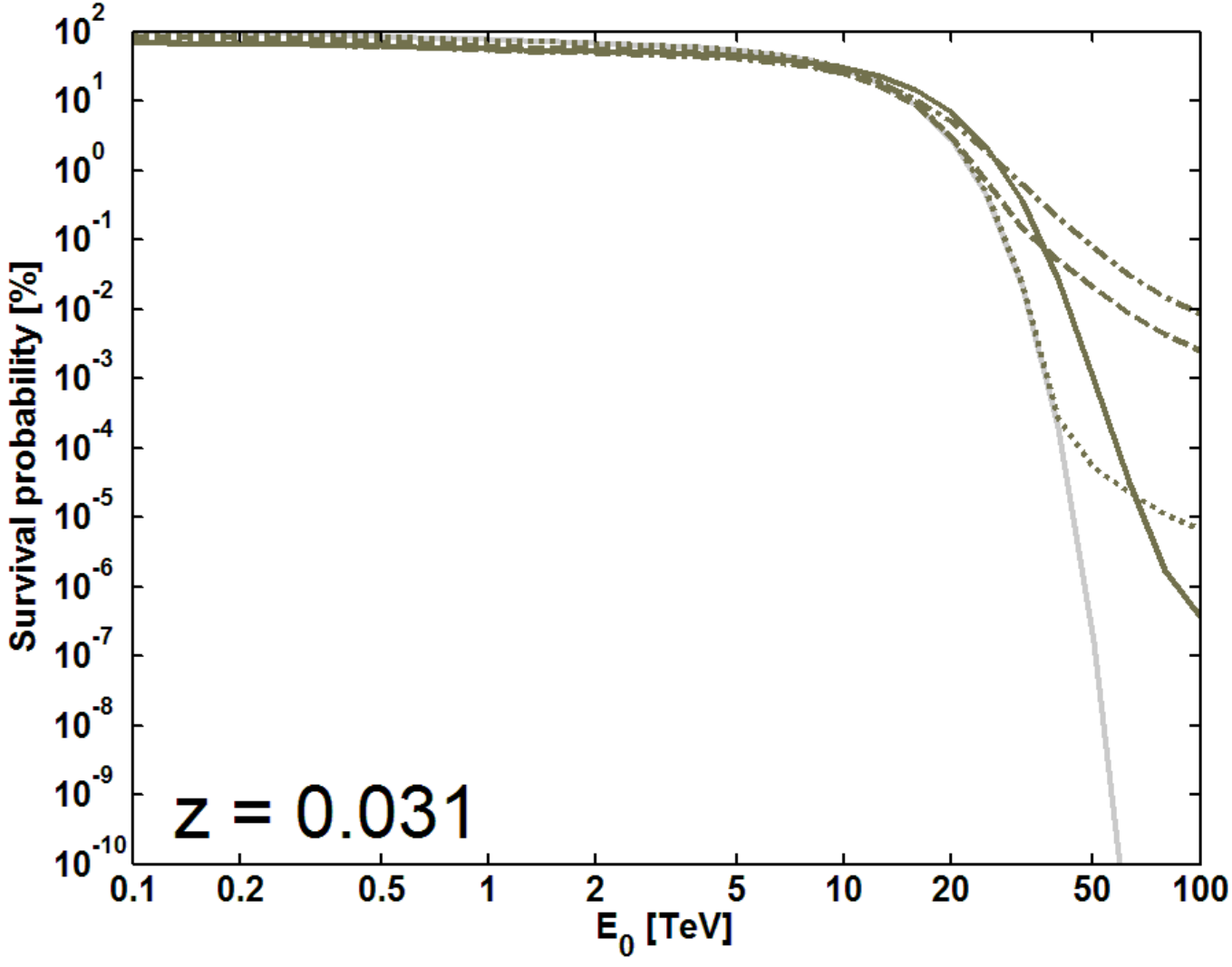

$L_{\mathrm{dom}} = 10\,\mathrm{Mpc}$

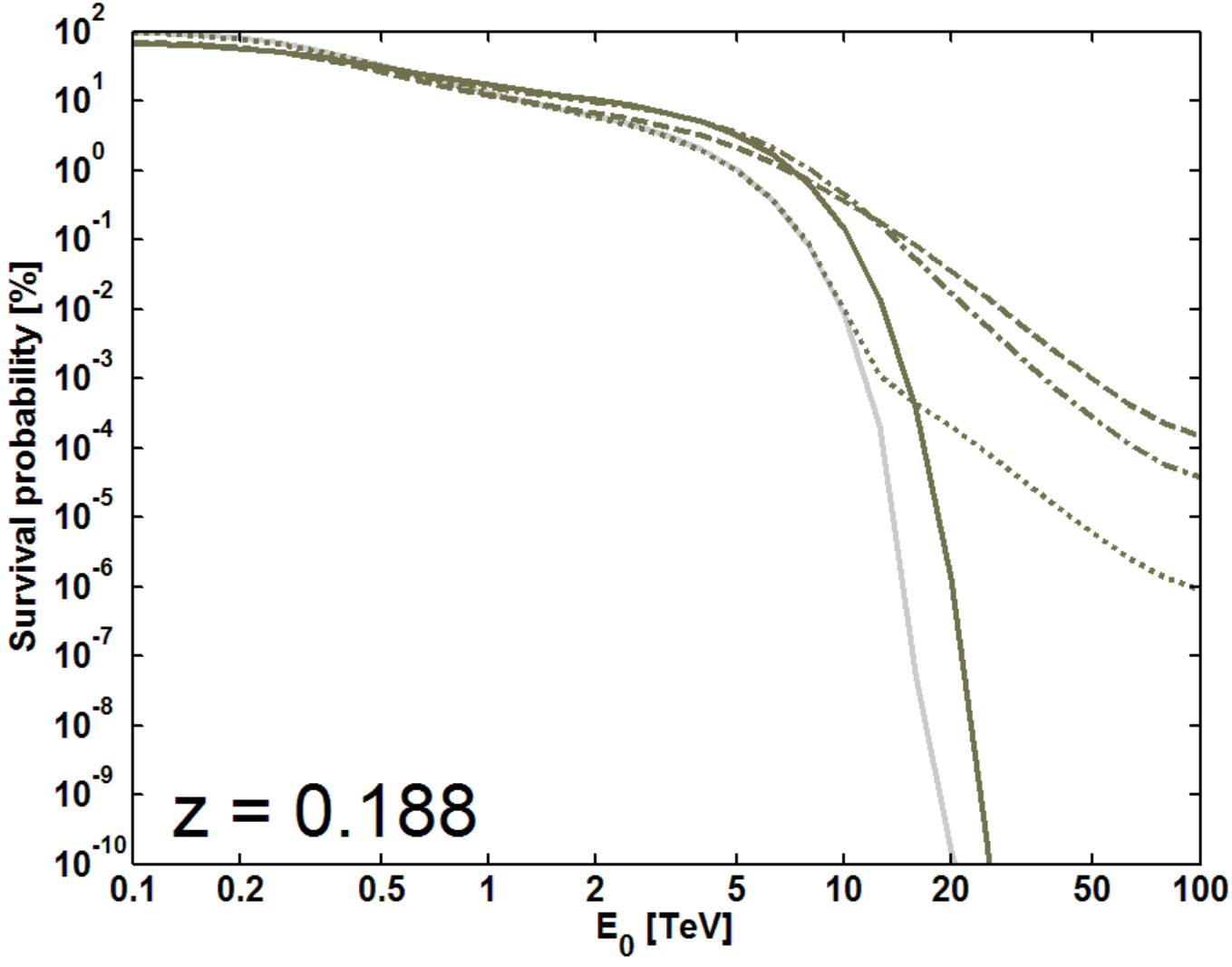

$L_{\mathrm{dom}} = 4\,\mathrm{Mpc}$

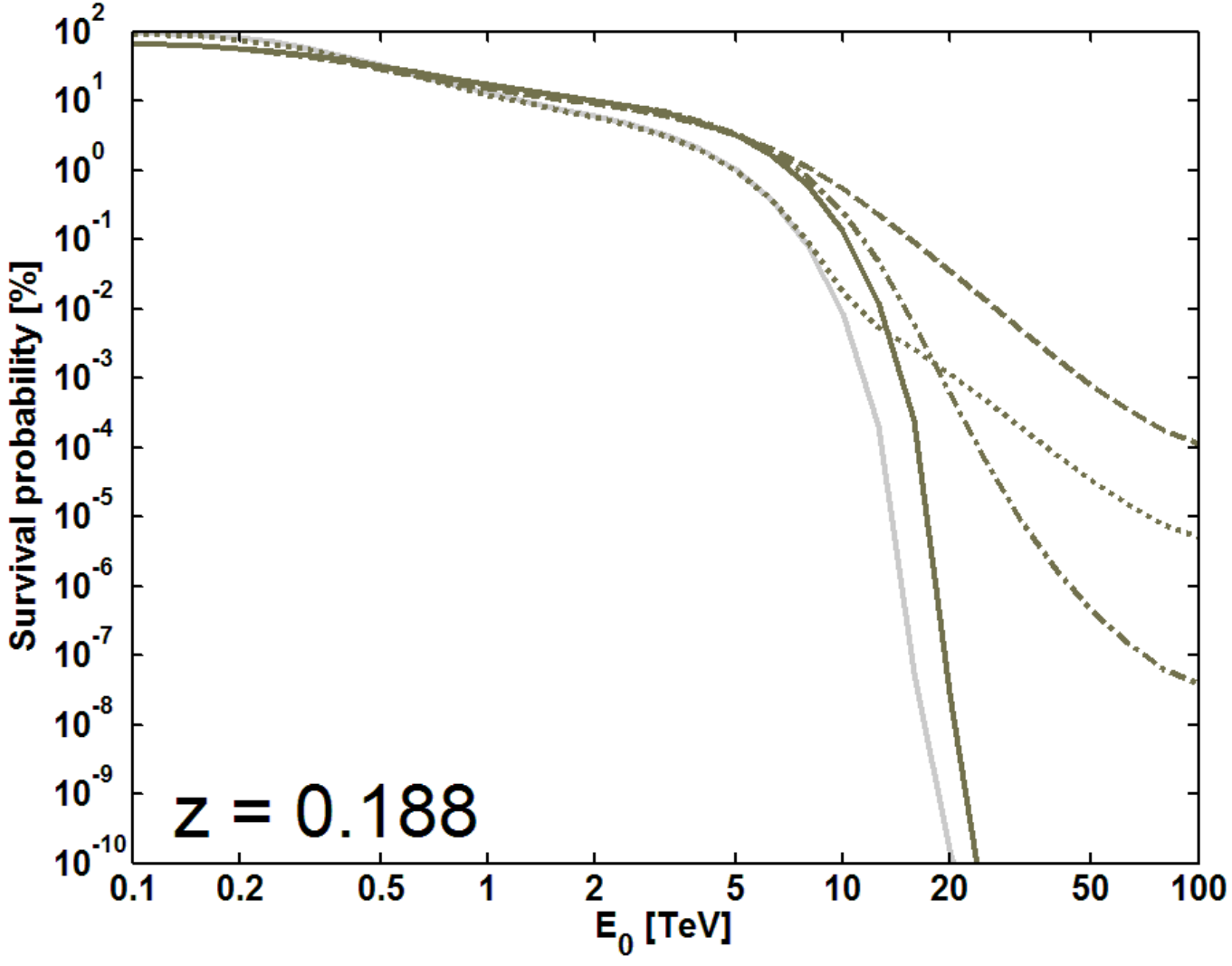

$L_{\mathrm{dom}} = 10\,\mathrm{Mpc}$

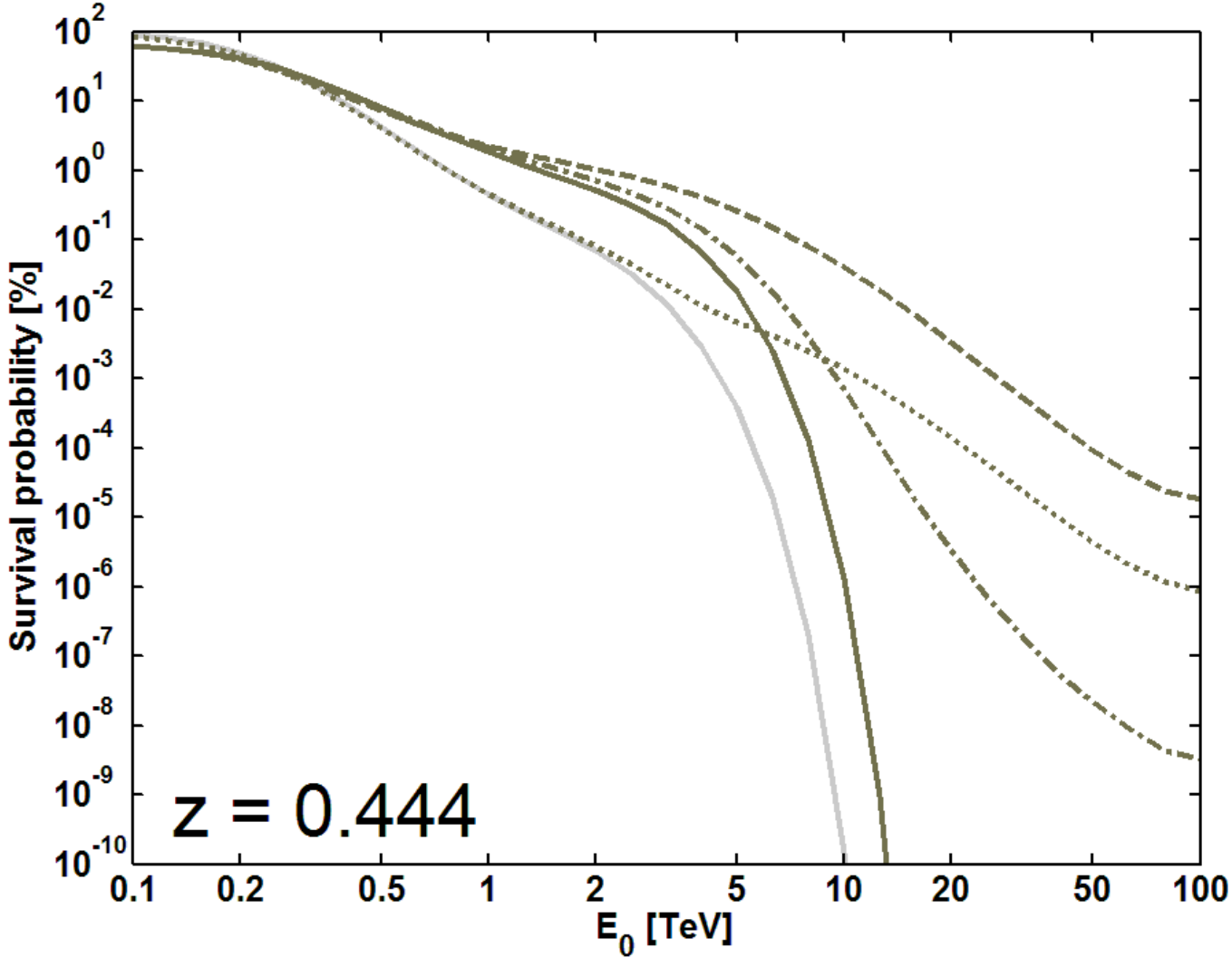

$L_{\mathrm{dom}} = 4\,\mathrm{Mpc}$

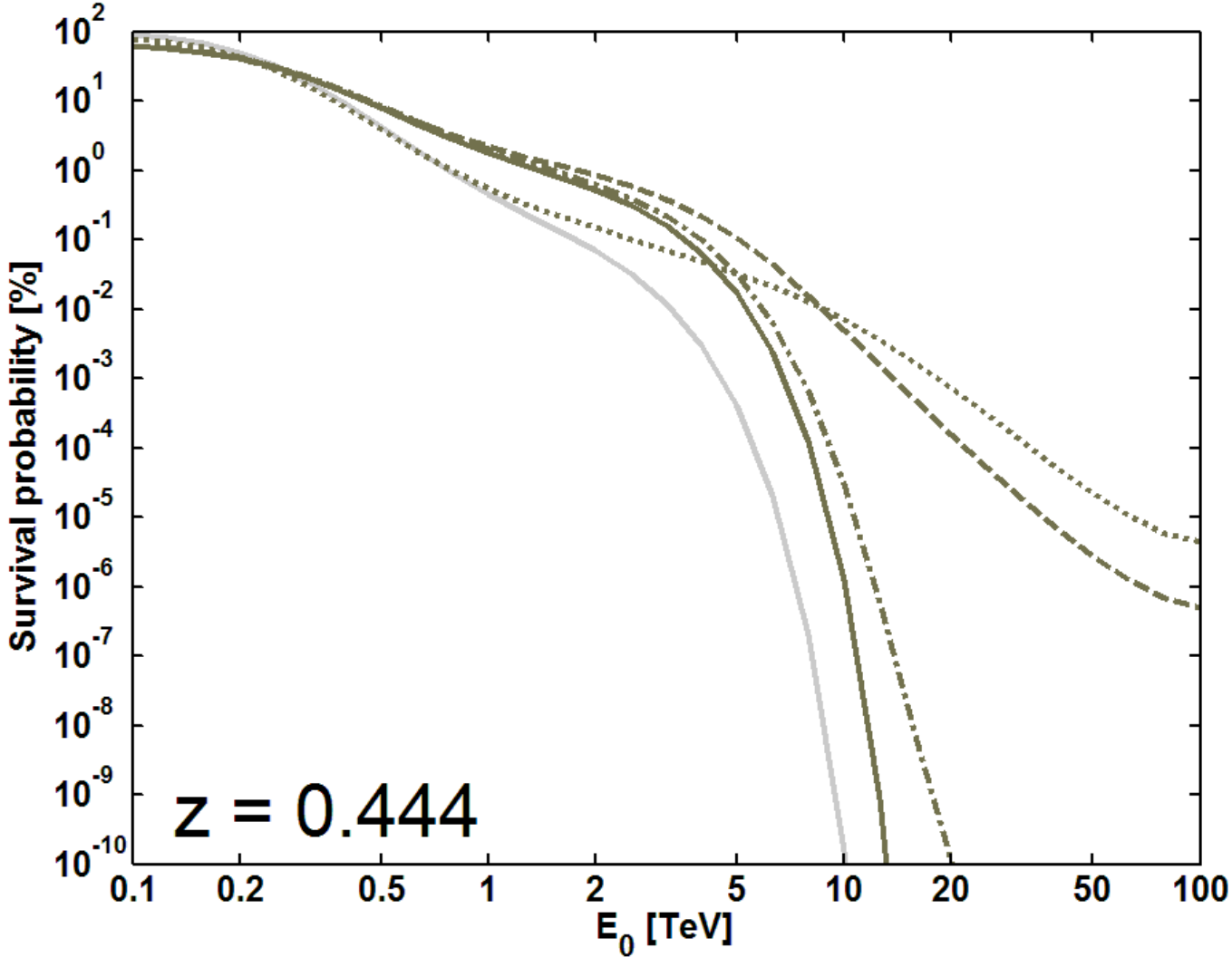

$L_{\mathrm{dom}} = 10\,\mathrm{Mpc}$

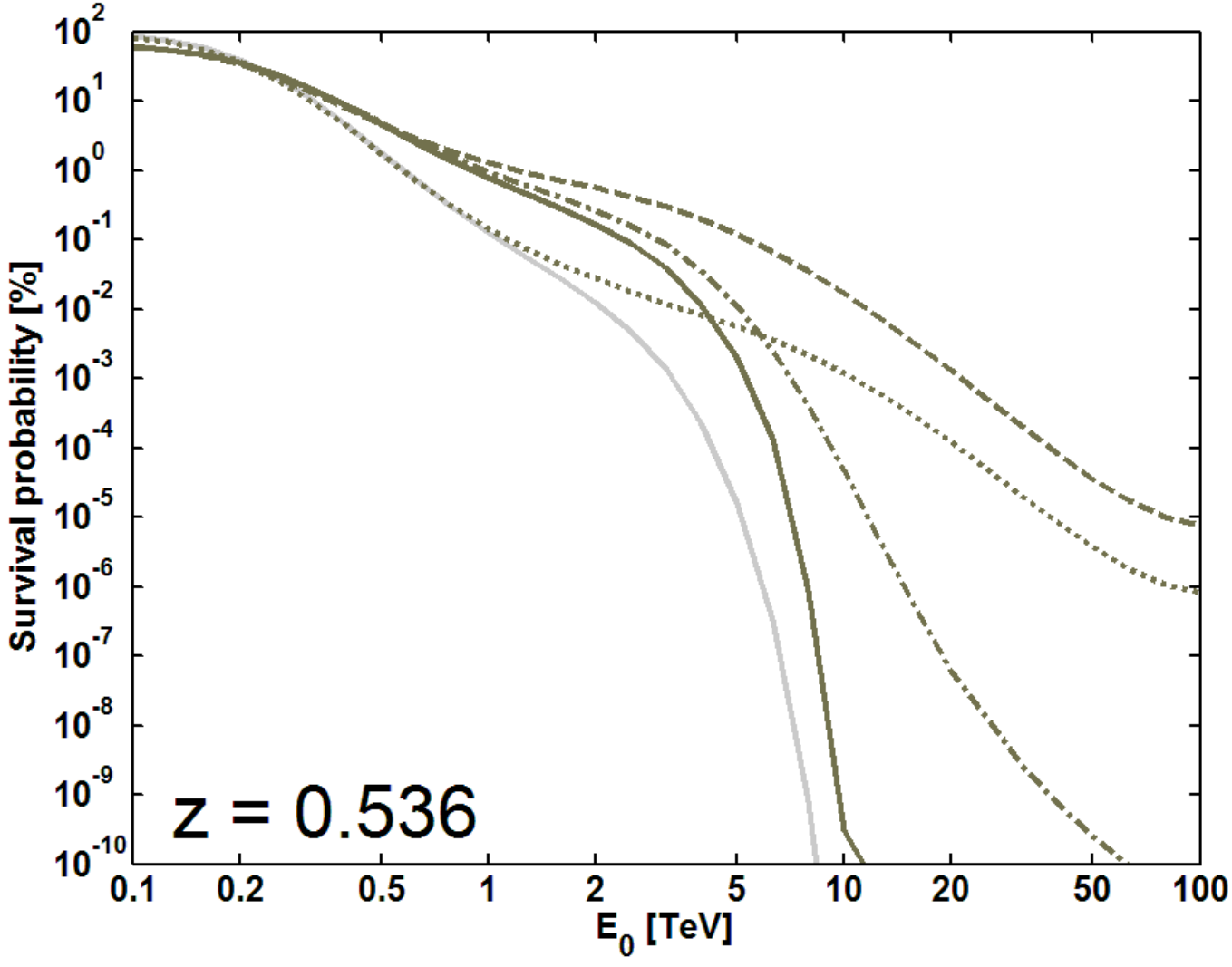

$L_{\mathrm{dom}} = 4\,\mathrm{Mpc}$

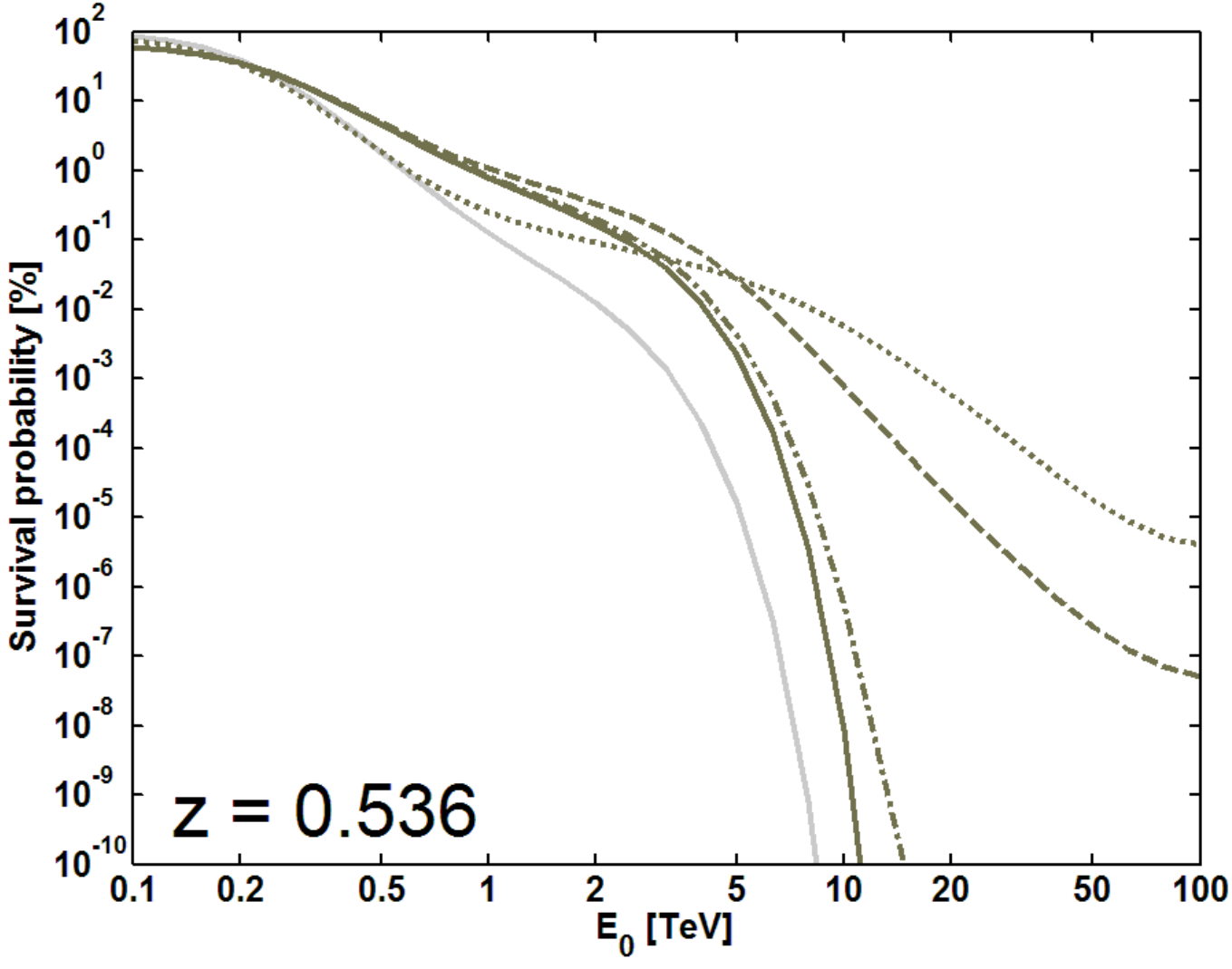

$L_{\mathrm{dom}} = 10\,\mathrm{Mpc}$

All plots show one common trend. At energies only slightly in excess of $100\,\mathrm{GeV}$, $P^{\mathrm{CP}}_{\gamma\to\gamma}(E_0, z)$ is LARGER than $P^{\mathrm{DARMA}}_{\gamma\to\gamma}(E_0, z)$, indeed in agreement with expectations. As the energy further increases, the situation reverses and $P^{\mathrm{DARMA}}_{\gamma\to\gamma}(E_0, z)$ gets progressively larger and larger than $P^{\mathrm{CP}}_{\gamma\to\gamma}(E_0, z)$ until the value $100\,\mathrm{TeV}$ is attained which is the highest energy value considered in the present analysis.

A somewhat surprising result emerges at large enough energies. Indeed, since ξ sets the strength of the photon-ALP oscillation mechanism, it would be natural to expect $P^{\mathrm{DARMA}}_{\gamma\to\gamma}(E_0, z)$ to monotonically increase with ξ. However, this is not the case. What is going on?

Owing to the random structure of the considered magnetic field, coherence is maintained only within ONE domain and so $P_{\gamma\to\gamma}^{\rm DARMA}(E_0, z)$ is ultimately controlled by two quantities: the photon-ALP conversion probability over a single domain $P_{\gamma\to a}(L_{\rm dom})$ and the photon absorption probability in Eq. (25). In order to clarify this issue in an intuitive fashion, we argue as follows, discarding cosmological effects for simplicity.
As far as $P_{\gamma\to a}(L_{\rm dom})$ is concerned, we have seen that it is given by Eqs. (21) in the case of photons linearly polarized in the direction parallel to **B**. This is not true in the present situation where the beam photons are assumed to be unpolarized, but for the sake of an order-of-magnitude estimate we can still suppose that $P_{\gamma\to a}(L_{\rm dom})$ has the form (21) and therefore we write it as

$$P_{\gamma\to a}(L_{\rm dom}) \simeq \sin^2\left[1.6\cdot 10^{-2}\,\xi\left(\frac{L_{\rm dom}}{\rm Mpc}\right)\right] \ . \qquad (80)$$

We distinguish two cases and we discuss them in turn:

A – As long as $\xi \ll 60\,(\mathrm{Mpc}/L_{\mathrm{dom}})$, Eq. (80) yields $P_{\gamma\to a}(L_{\mathrm{dom}}) \ll 1$ which entails that the fraction of ALPs produced over a single domain is very small. Since we are supposing the beam to be initially fully made of photons, it takes a length much larger that L_{dom} before a sizeable fraction of the beam consists of ALPs. In the same fashion, once such a situation is realized, a similar long length is needed in order for the beam to contain a sizeable amount of photons. Moreover, it follows from Eq. (80) that presently $P_{\gamma\to a}(L_{\mathrm{dom}})$ becomes a quadratic function of ξ which therefore increases monotonically with ξ. Accordingly, the picture outlined above is expected to emerge straightforwardly and this is confirmed by a numerical simulation in which ξ takes the above values but we assume $L_{\mathrm{dom}} = 0.05\,\mathrm{Mpc}$, which yields the behaviour shown in the plots reported in the next Figures.

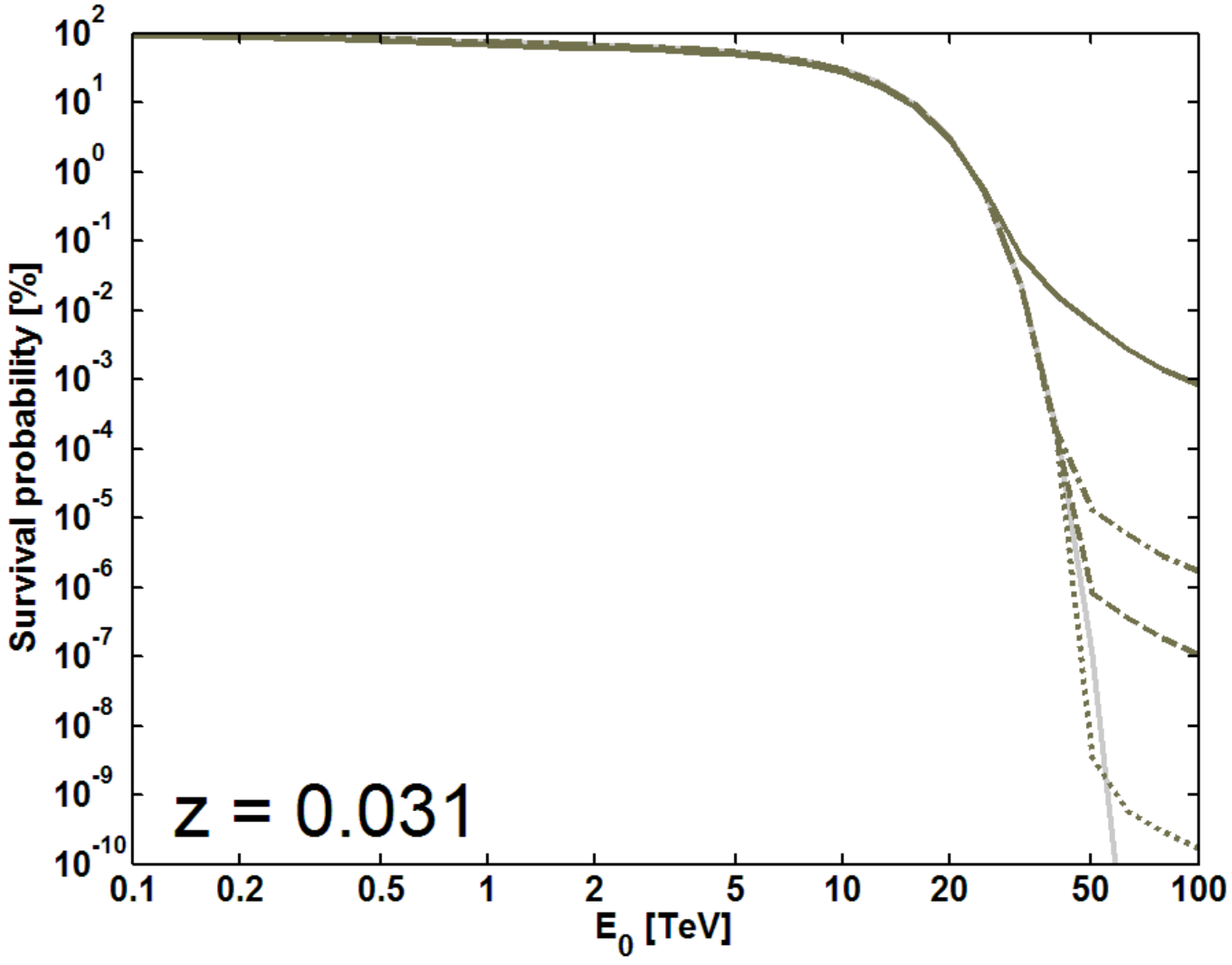
Survival probability [%]
10^{2}
10^{1}
10^{0}
10^{-1}
10^{-2}
10^{-3}
10^{-4}
10^{-5}
10^{-6}
10^{-7}
10^{-8}
10^{-9}
10^{-10}
z = 0.031
0.1
0.2
0.5
1
2
5
10
20
50
100
E_0 [TeV]

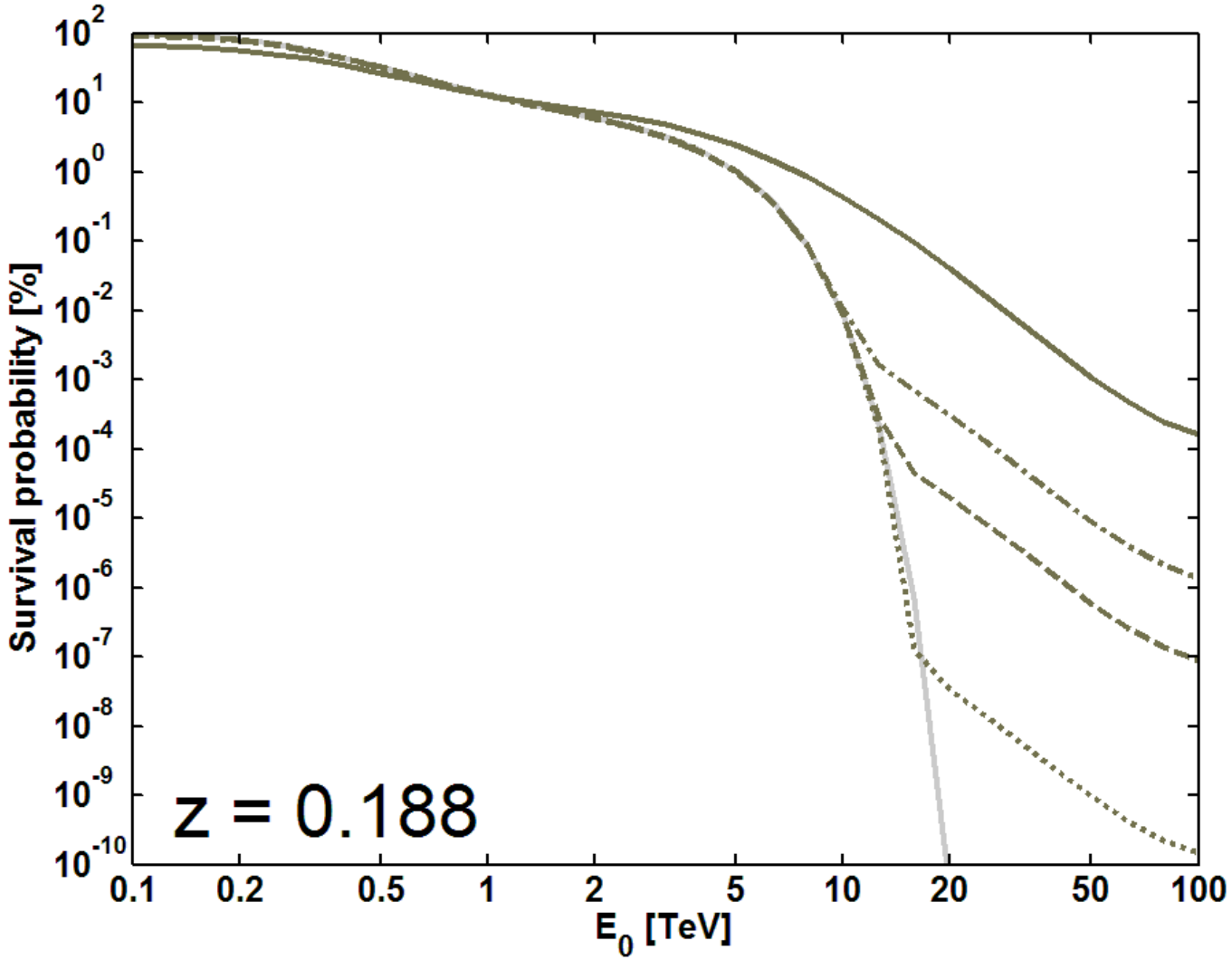
Survival probability [%]
10^{2}
10^{1}
10^{0}
10^{-1}
10^{-2}
10^{-3}
10^{-4}
10^{-5}
10^{-6}
10^{-7}
10^{-8}
10^{-9}
10^{-10}
z = 0.188
0.1
0.2
0.5
1
2
5
10
20
50
100
E_0 [TeV]

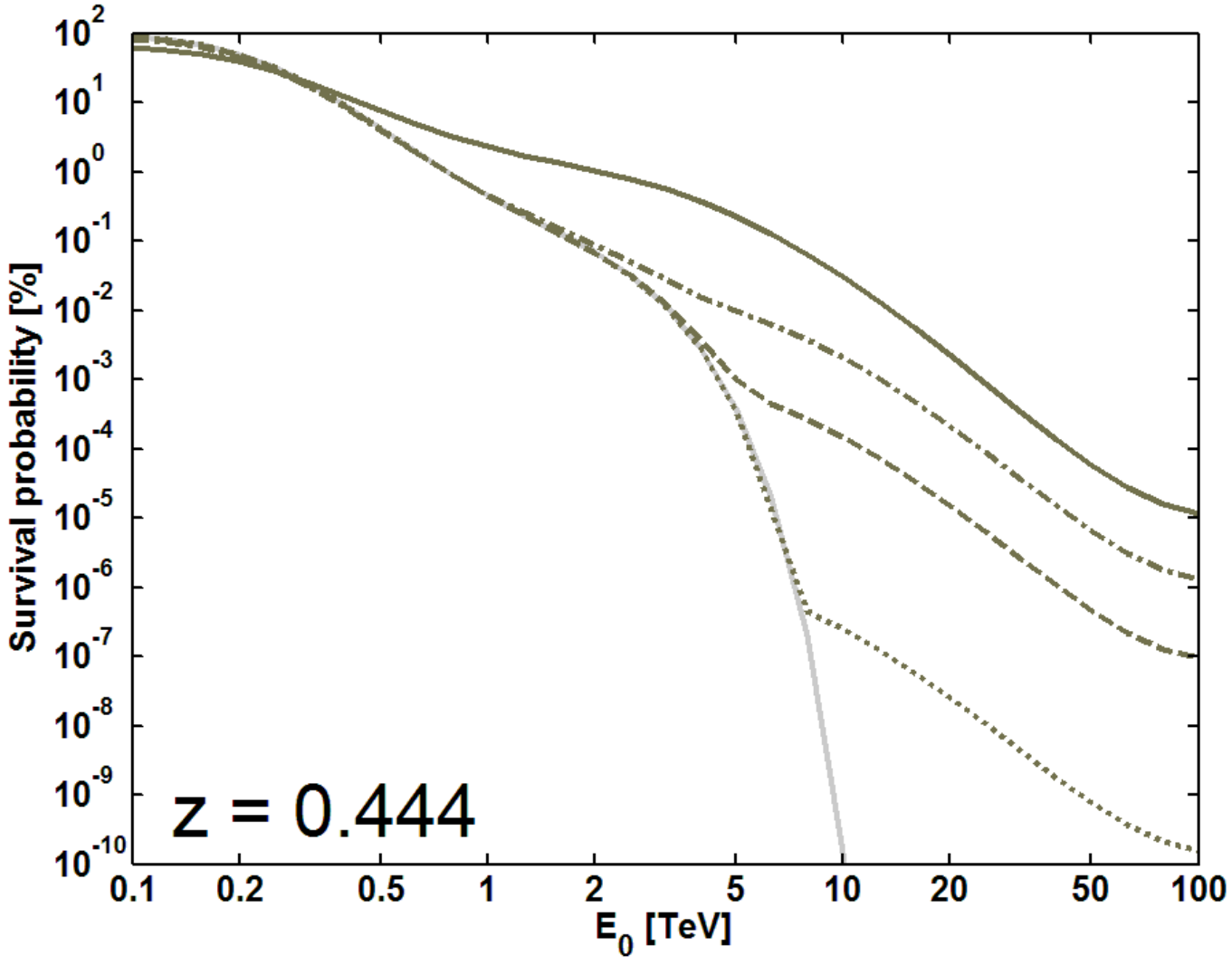
Survival probability [%]
10^{2}
10^{1}
10^{0}
10^{-1}
10^{-2}
10^{-3}
10^{-4}
10^{-5}
10^{-6}
10^{-7}
10^{-8}
10^{-9}
10^{-10}
z = 0.444
0.1
0.2
0.5
1
2
5
10
20
50
100
E_0 [TeV]

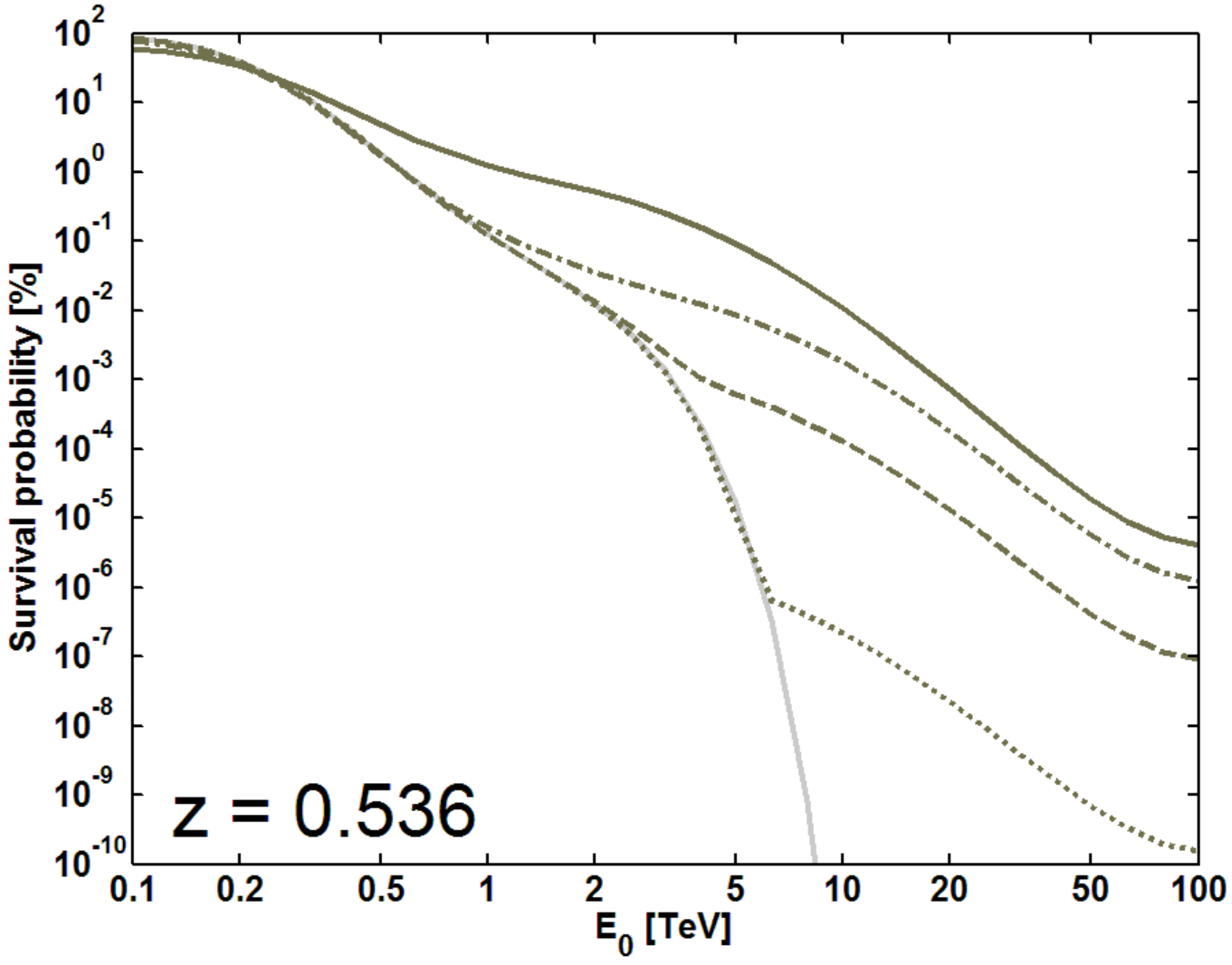
Survival probability [%]
10^{2}
10^{1}
10^{0}
10^{-1}
10^{-2}
10^{-3}
10^{-4}
10^{-5}
10^{-6}
10^{-7}
10^{-8}
10^{-9}
10^{-10}
z = 0.536
0.1
0.2
0.5
1
2
5
10
20
50
100
E_0 [TeV]

B – Otherwise the situation becomes considerably more complicated. First, $P_{\gamma\to a}(L_{\rm dom})$ fails to be a monotonically increasing function of ξ and it becomes oscillatory. So, depending on the actual value of $L_{\rm dom}$ it follows that $P_{\gamma\to a}(L_{\rm dom})$ can decrease as ξ increases. As stressed above, Eq. (80) can be taken at most to provide an order-of-magnitude estimate but it is clear that condition $\xi \ll 60\,({\rm Mpc}/L_{\rm dom})$ fails to be met for $L_{\rm dom} = 4\,{\rm Mpc}$ and $L_{\rm dom} = 10\,{\rm Mpc}$ along with the considered values of ξ. Hence, for a fixed source distance the behaviour exhibited in the above plots can arise. Still, this is not the end of the story, since in the present situation even after the domain closest to the source a relevant fraction of the beam consists of ALPs: a large enough number of $\gamma \to a$ and $a \to \gamma$ transitions take place inside a single domain. So, the overall effect is to have a larger number of photons per unit length between the source

and us as compared to the previous case. As a consequence, EBL absorption is now more effective thereby giving rise to a SMALLER observed photon flux. Moreover, this dimming evidently increases with the source distance, which explains why $P_{\gamma\to\gamma}^{\mathrm{DARMA}}(E_0, z)$ tends to decrease as z increases at fixed energy and eventually it behaves like $P_{\gamma\to\gamma}^{\mathrm{CP}}(E_0, z)$, which indeed occurs for $\xi = 5$.

In conclusion, it is evident from the above figures that in the most favourable case a boost factor of 10 in $P_{\gamma\to\gamma}^{\mathrm{DARMA}}(E_0, z)$ occurs at progressively lower energies as the source distance increases. Explicitly, for $z = 0.031$, $z = 0.188$, $z = 0.444$, $z = 0.536$ it takes place at $E_{10} \simeq 30\,\mathrm{TeV}, 8\,\mathrm{TeV}, 2\,\mathrm{TeV}, 1.2\,\mathrm{TeV}$, respectively. Above E_{10} the boost factor can be much larger.

10 – NEW INTERPRETATION OF VHE BLAZARS

Within conventional physics the values of $\Gamma_{\rm em}$ have to be tuned for every source in such a way to reproduce the corresponding values of $\Gamma_{\rm obs}$. No rational lies behind this procedure and a large spread in the values of $\Gamma_{\rm em}$ is demanded in order to account for the equally large spread in the values of $\Gamma_{\rm obs}$. While this procedure does not pose any technical problem, such a SYSTEMATIC FINE-TUNING lacks any conceptual appeal.

How is the situation within the DARMA scenario?
Our starting point is

$$\Phi_{\rm obs}(E_0, z) = P^{\rm DARMA}_{\gamma\to\gamma}(E_0, z)\, \Phi_{\rm em}\left(E_0(1+z)\right) \ , \qquad (81)$$

but since a good fit is provided by

$$\Phi_{\rm obs}(E_0, z) = K\, E_0^{-\Gamma_{\rm obs}(z)} \ , \qquad (82)$$

we have

$$K\, E_0^{-\Gamma_{\rm obs}(z)} = P_{\gamma\to\gamma}^{\rm DARMA}(E_0, z)\, \Phi_{\rm em}\left(E_0(1+z)\right) \ , \qquad (83)$$

from which we get $\Phi_{\rm em}\left(E_0(1+z)\right)$ for every detected VHE blazar. We next best-fit this function to a power-law expression

$$\Phi_{\rm em}\left(E_0(1+z)\right) = K\left[E_0(1+z)\right]^{-\Gamma_{\rm em}^{\rm DARMA}} \qquad (84)$$

over the energy range where the considered source is observed. We obtain in this way the values of $\Gamma_{\rm em}^{\rm DARMA}$.
For $\xi = 0.1$ there is no practical difference with respect to conventional physics, but as soon as the regime $\xi = 0.5$ is attained the difference becomes drastic. In particular the values of $\Gamma_{\rm em}^{\rm DARMA}$ fall in the SAME ballpark for both nearby and far-away sources.

It can be shown that the gist of the DARMA scenario for the observed VHE blazars is to drastically reduce the spread in the values of $\Gamma_{\rm em}$ as compared with what happens in conventional physics, thereby tracing the large spread in the values of $\Gamma_{\rm obs}$ to the wide spread in the blazar distances.

It seems therefore worthwhile to investigate this point in a quantitative fashion according the following strategy:

- As a zero-order approximation, we suppose that all blazars have the SAME value of $\Gamma_{\rm em}^{\rm DARMA}$, which for definiteness is taken to be the average value over all observed sources $\langle \Gamma_{\rm em}^{\rm DARMA} \rangle$ for a given choice of ξ and $L_{\rm dom}$.
- As a first-order correction – which is meant to improve on the above idealized situation – we allow for a SMALL SPREAD around $\langle \Gamma_{\rm em}^{\rm DARMA} \rangle$, which we tentatively take to be ± 0.2.

In order to keep the situation under control, we focus our attention on the single case $\xi = 1.0$ and $L_{\rm dom} = 4\,{\rm Mpc}$ which we regard as the most favourable one not only because $\Delta\Gamma_{\rm em}^{\rm DARMA}$ is very small – the case $\xi = 0.5$ and $L_{\rm dom} = 10\,{\rm Mpc}$ would be even better in this respect – but also because we feel that $L_{\rm dom} = 4\,{\rm Mpc}$ is more realistic than $L_{\rm dom} = 10\,{\rm Mpc}$. This amounts to take $\langle\Gamma_{\rm em}^{\rm DARMA}\rangle = 2.51$, which entails in turn $2.31 < \Gamma_{\rm em}^{\rm DARMA} < 2.71$ for all observed VHE blazars. The value 2.51 is close to the value 2.40 that we used in a previous discussion of the DARMA scenario, as well as to 2.47 which is the average value for the observed VHE blazars with $z < 0.05$ that undergo a negligible EBL attenuation.

Next, we evaluate for every source the *expected* observed spectral index $\Gamma_{\rm obs}^{\rm exp}(z)$. Basically, this amounts to run backwards the same procedure whereby we have got the values of $\Gamma_{\rm em}^{\rm DARMA}$ for $\xi = 1.0$. Quite explicitly

$$\Phi_{\rm obs}^{\rm exp}(E_0, z) = P_{\gamma\to\gamma}^{\rm DARMA}(E_0, z)\, K \left[E_0(1+z)\right]^{-2.51} . \qquad (85)$$

Since $P^{\rm DARMA}_{\gamma\to\gamma}(E_0, z)$ is known, $\Phi^{\rm exp}_{\rm obs}(E_0, z)$ can be computed exactly. Then we best-fit this function to a power-law expression, namely

$$\Phi^{\rm exp}_{\rm obs}(E_0, z) = K\, E_0^{-\Gamma^{\rm exp}_{\rm obs}(z)} \tag{86}$$

over the energy range where each source is observed. We find in this way the values of $\Gamma^{\rm exp}_{\rm obs}(z)$ for every source. As repeatedly stressed, the observed and emitted spectral indices are linearly related, and so they have the same error bars.

We check this view by performing a fit to all observed VHE blazars. This is shown in next figures, where the solid black line corresponds to $\Gamma^{\rm exp}_{\rm obs}(z)$ while the grey strip represents the range $\Gamma^{\rm exp}_{\rm obs}(z) \pm 0.2$.

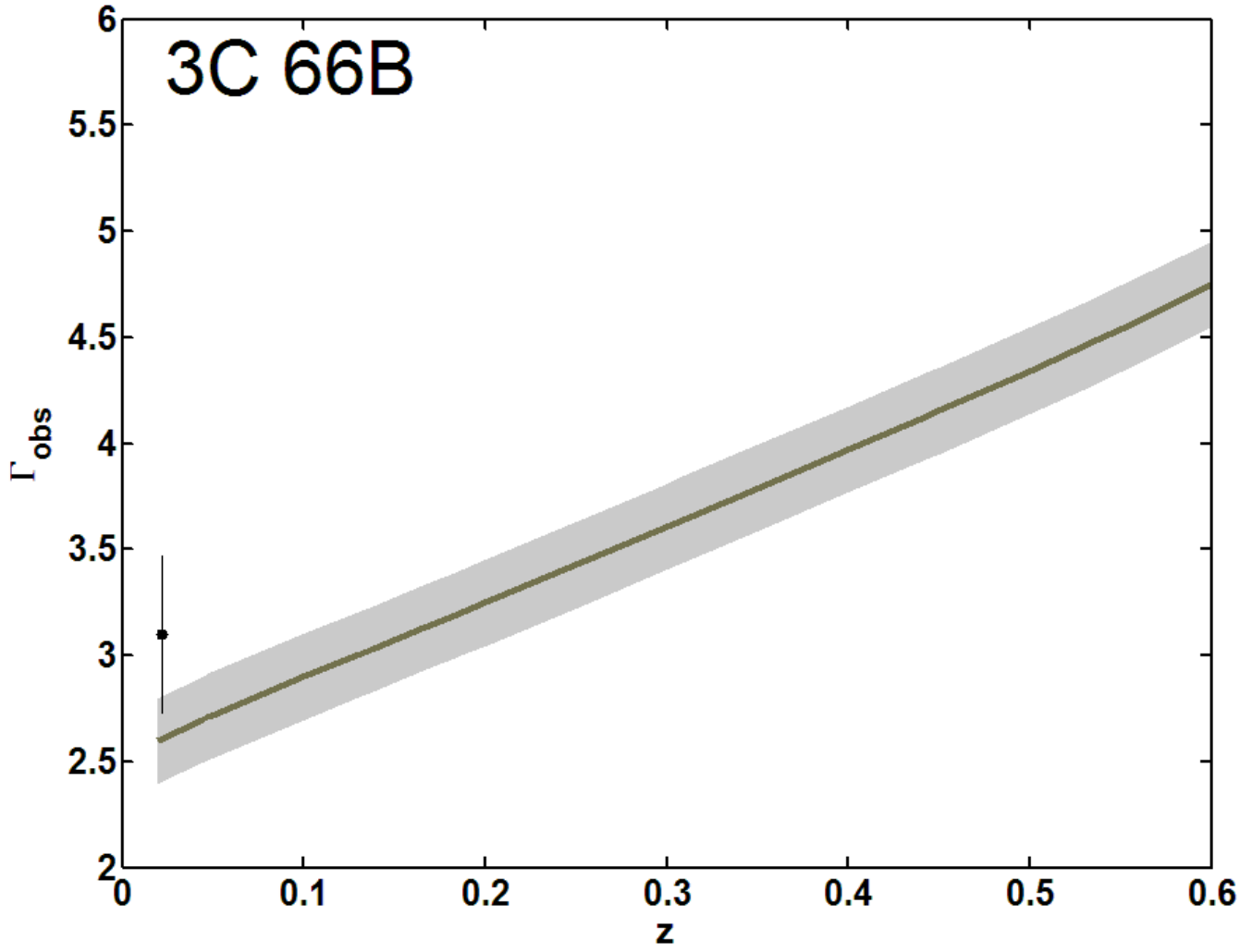
3C 66B
Γ_{obs}
z
6
5.5
5
4.5
4
3.5
3
2.5
2
0
0.1
0.2
0.3
0.4
0.5
0.6

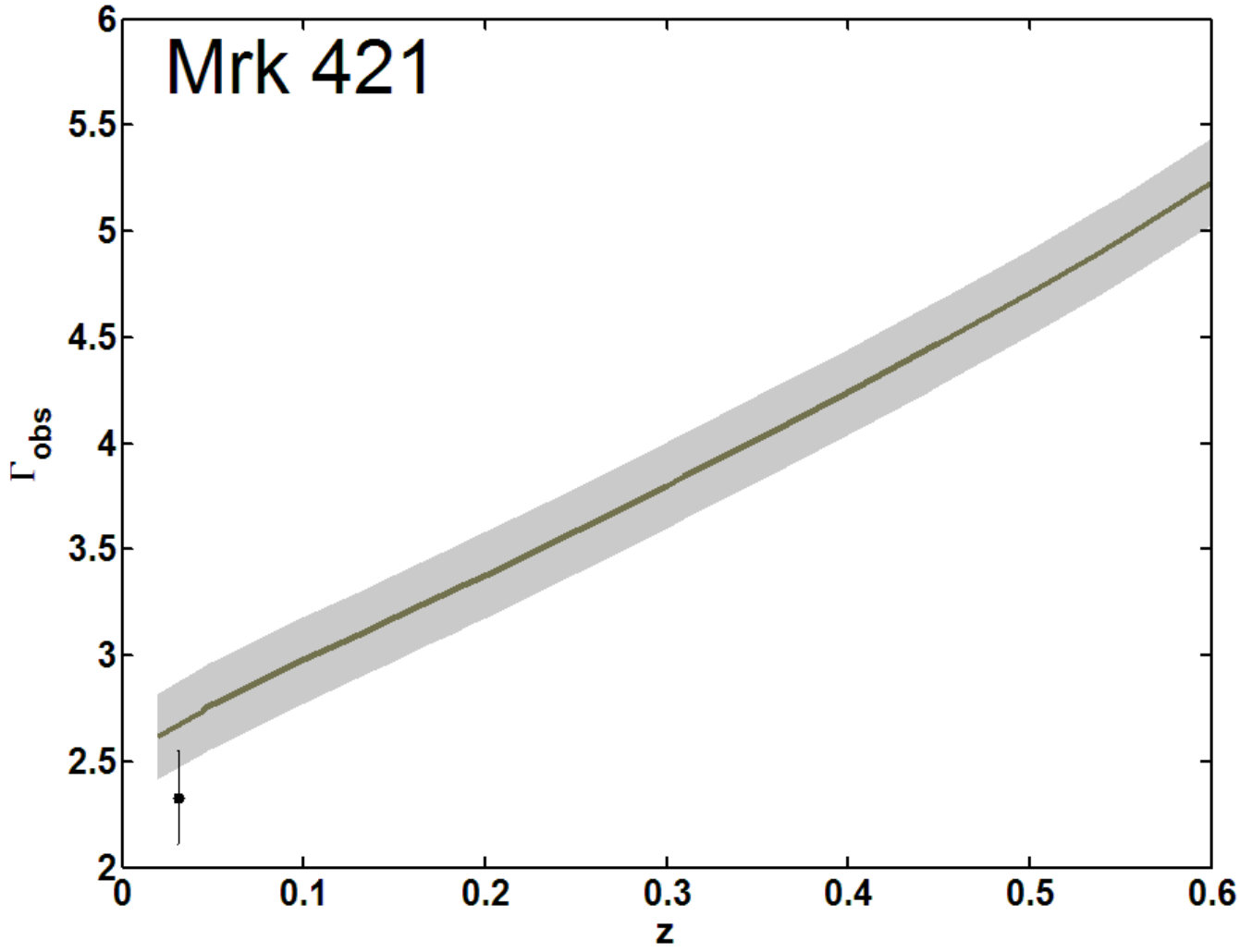
Mrk 421
Γ_{obs}
z
6
5.5
5
4.5
4
3.5
3
2.5
2
0
0.1
0.2
0.3
0.4
0.5
0.6

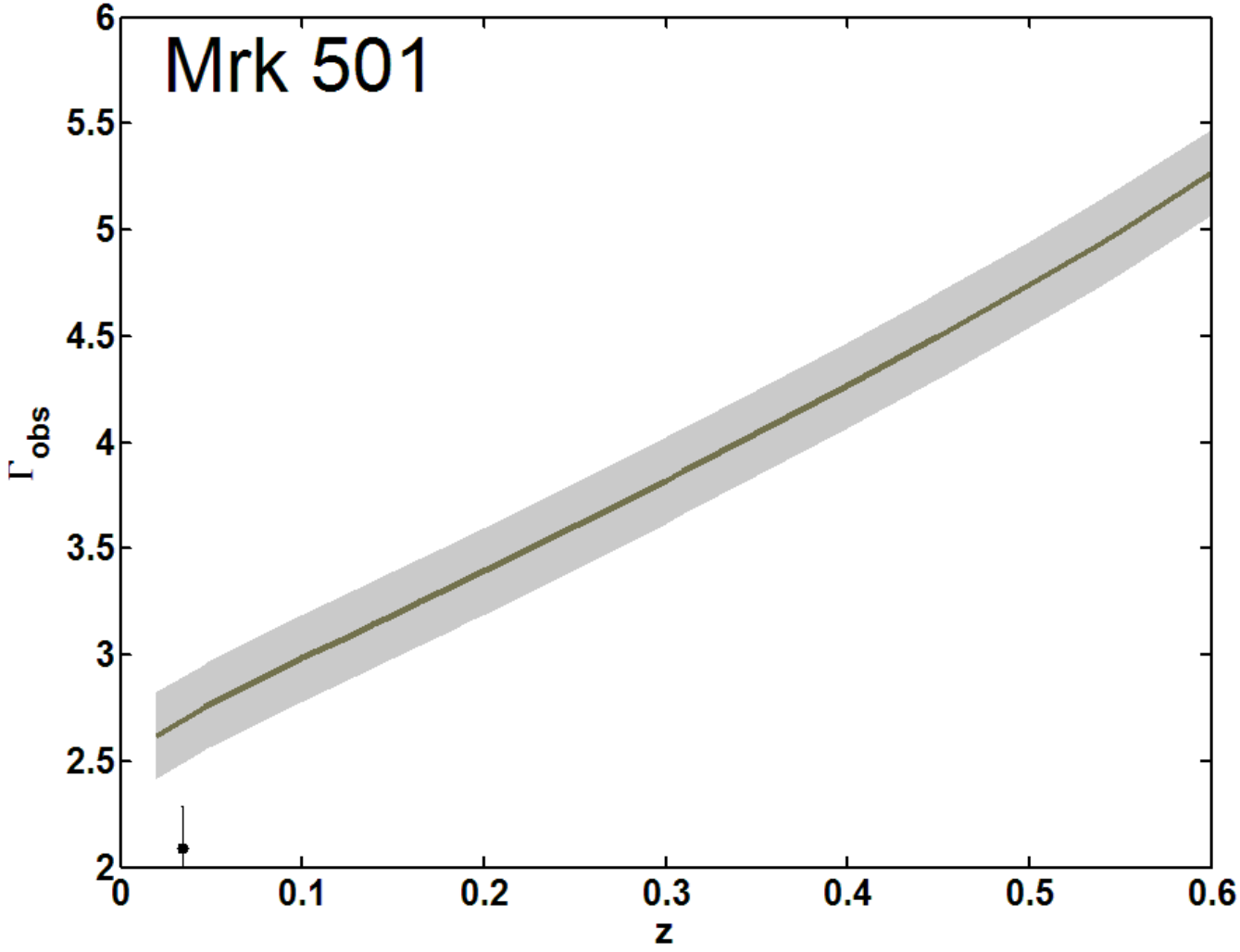
Mrk 501
Γ_{obs}
z
6
5.5
5
4.5
4
3.5
3
2.5
2
0
0.1
0.2
0.3
0.4
0.5
0.6

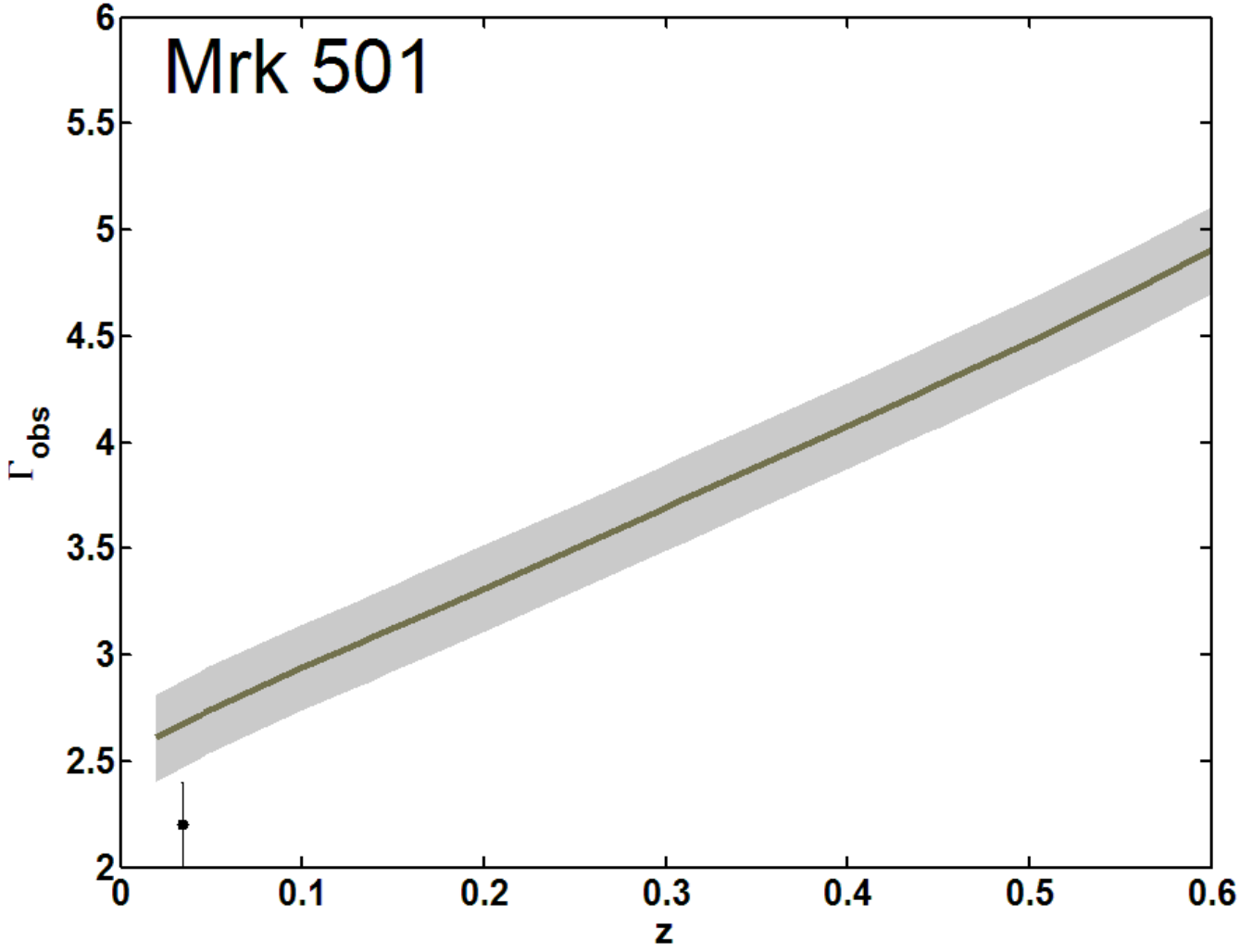
Mrk 501
Γ_{obs}
z
6
5.5
5
4.5
4
3.5
3
2.5
2
0
0.1
0.2
0.3
0.4
0.5
0.6

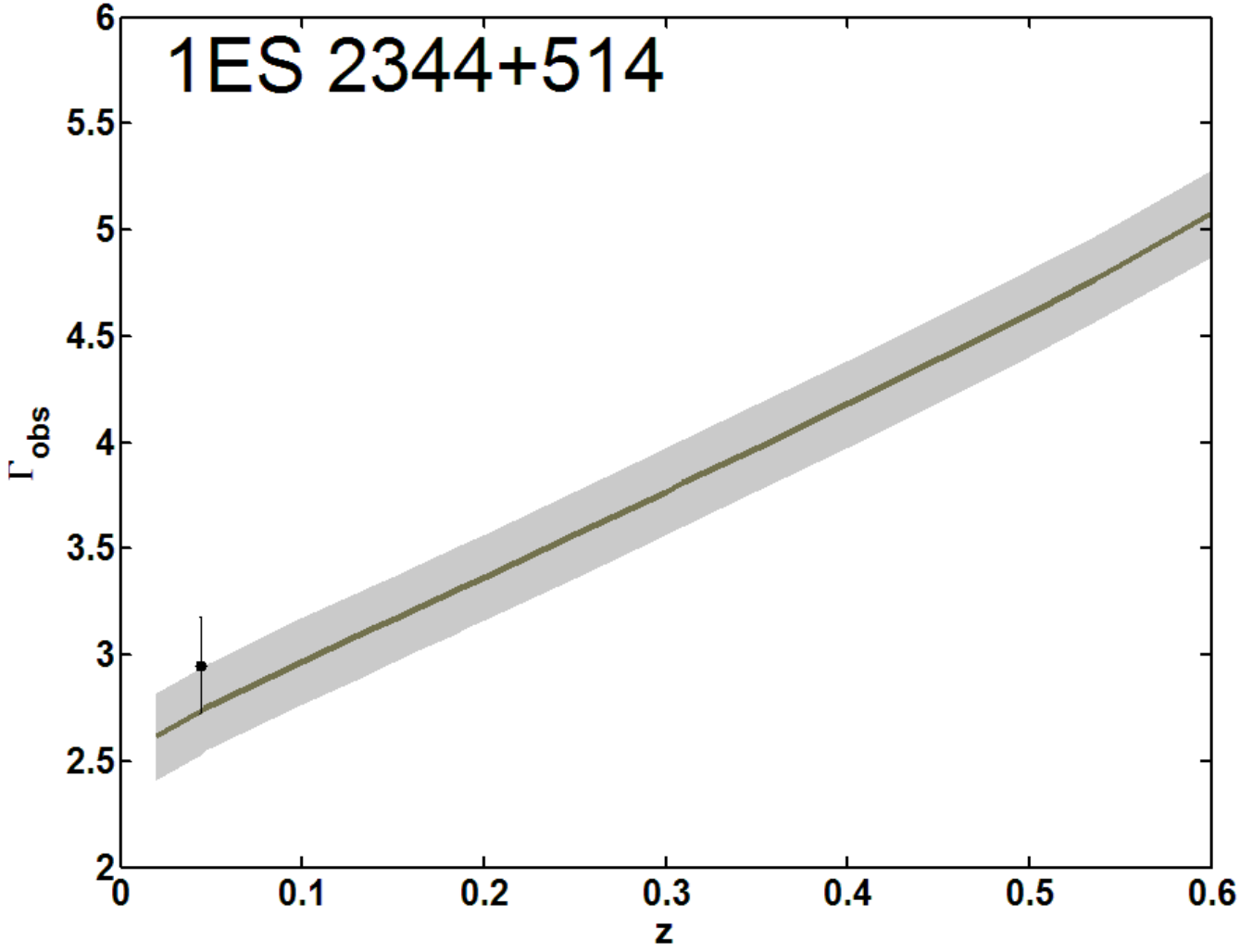
1ES 2344+514
6
5.5
5
4.5
4
3.5
3
2.5
2
0
0.1
0.2
0.3
0.4
0.5
0.6
z
Γobs

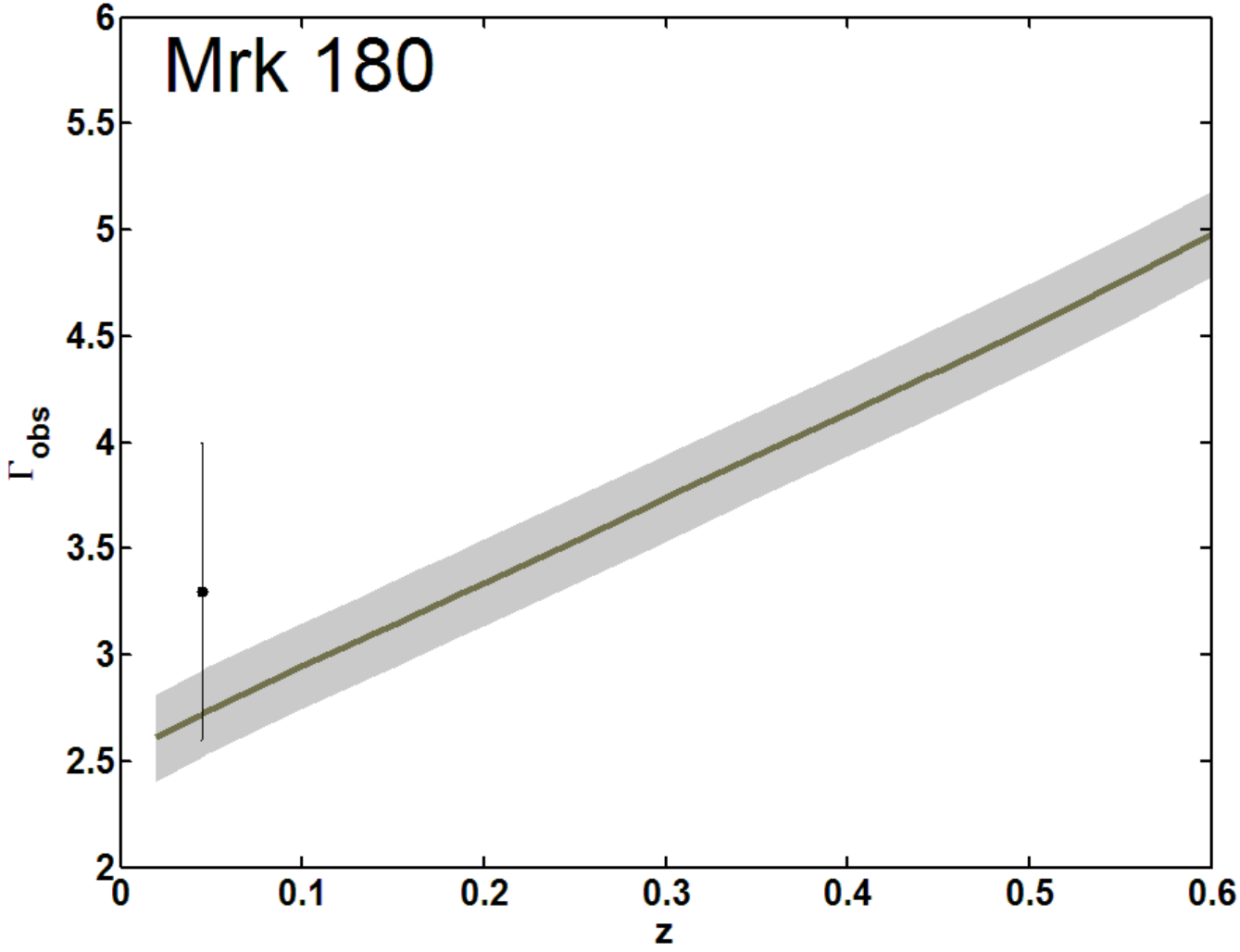
Mrk 180
Γ_{obs}
z
6
5.5
5
4.5
4
3.5
3
2.5
2
0
0.1
0.2
0.3
0.4
0.5
0.6

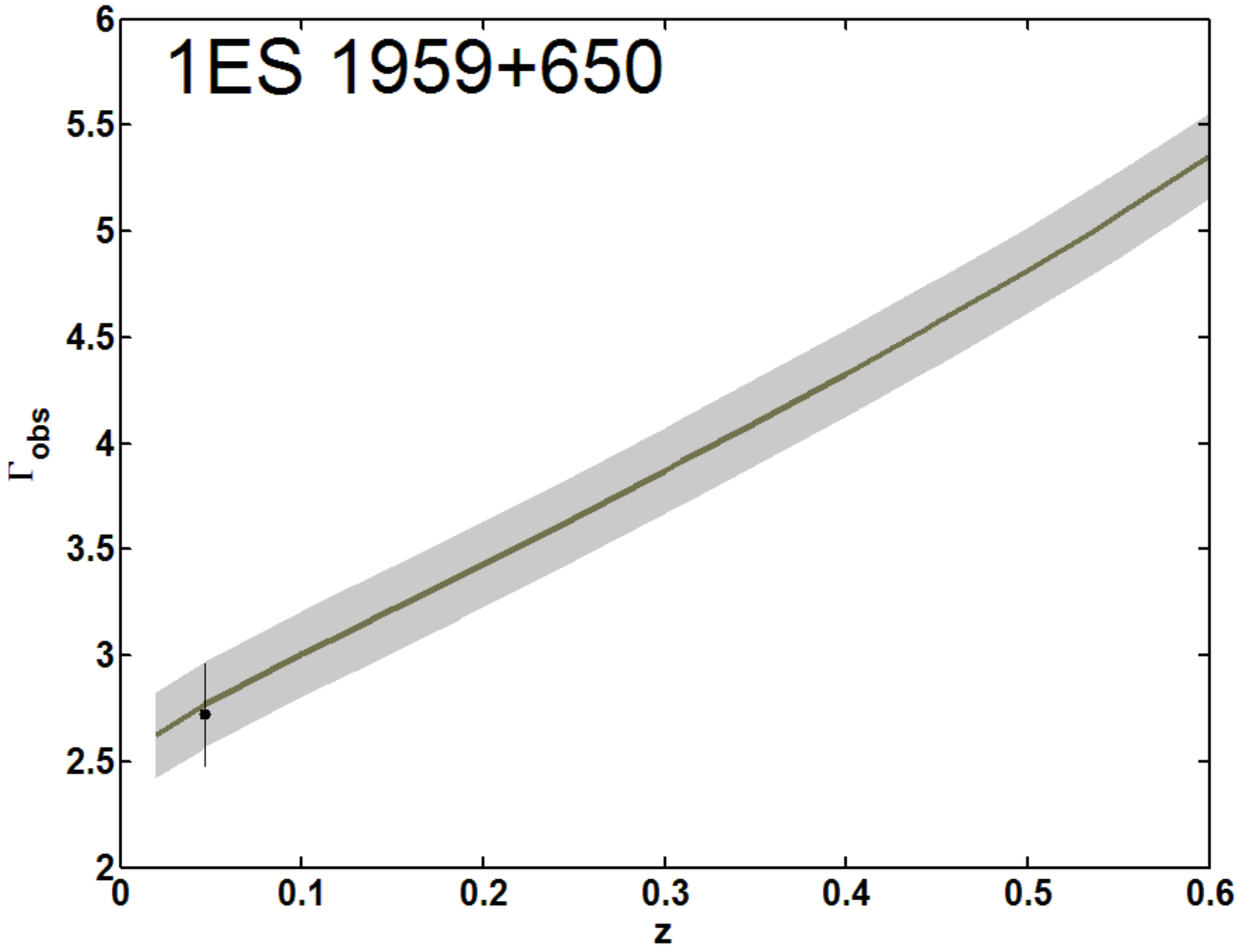
1ES 1959+650
Γ_{obs}
z
6
5.5
5
4.5
4
3.5
3
2.5
2
0
0.1
0.2
0.3
0.4
0.5
0.6

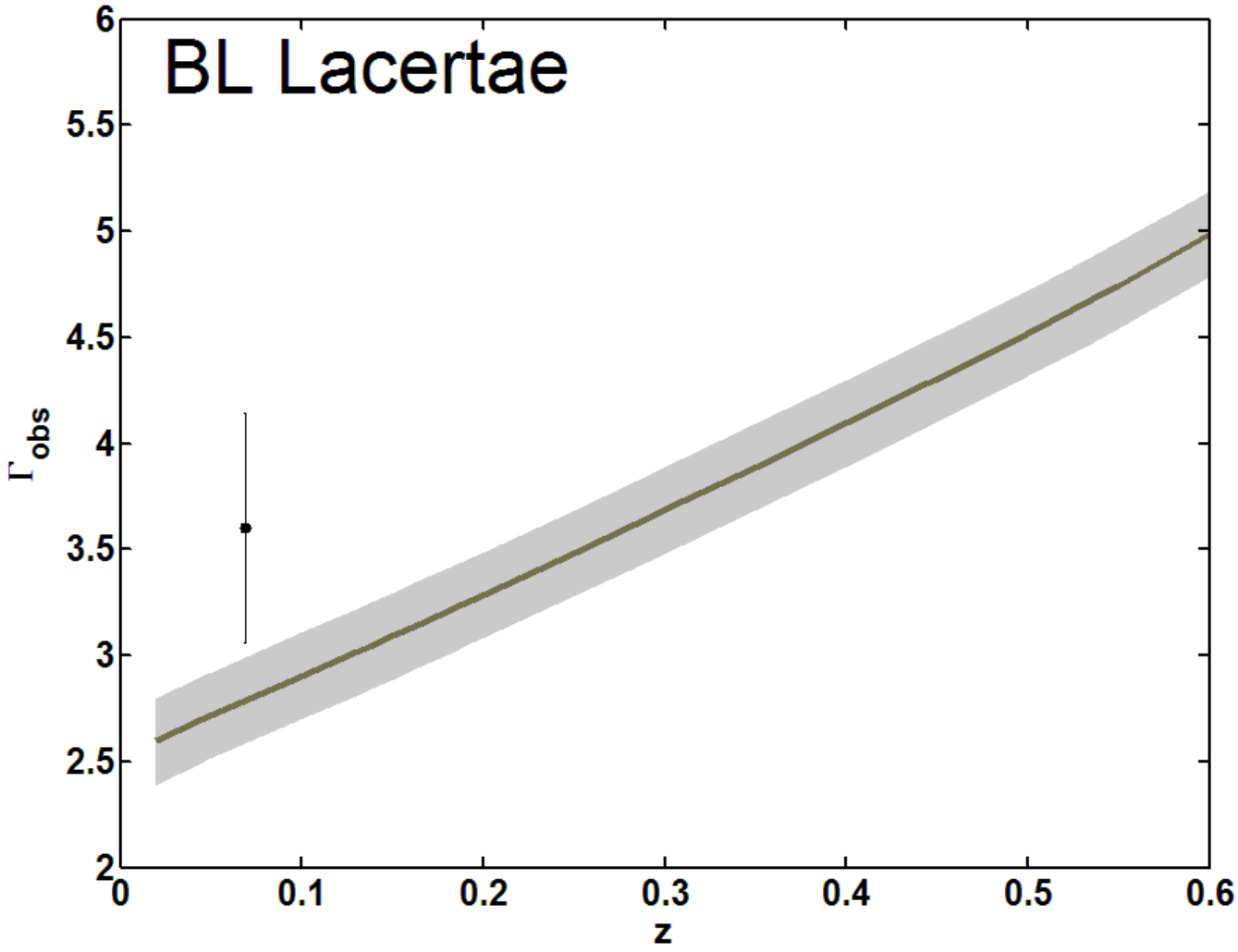
BL Lacertae
6
5.5
5
4.5
4
3.5
3
2.5
2
0
0.1
0.2
0.3
0.4
0.5
0.6
z
Γobs

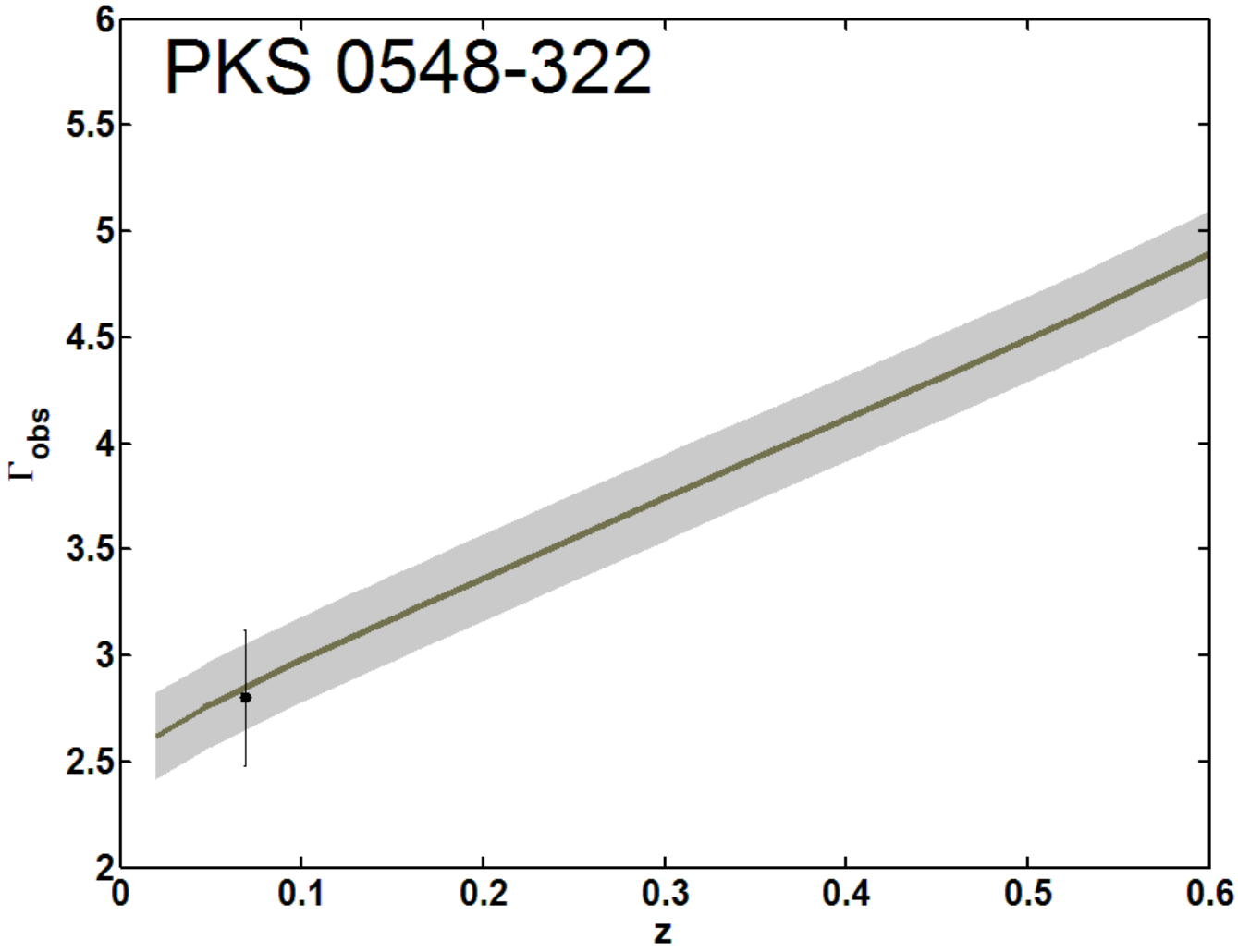
PKS 0548-322
Γ_{obs}
z
6
5.5
5
4.5
4
3.5
3
2.5
2
0
0.1
0.2
0.3
0.4
0.5
0.6

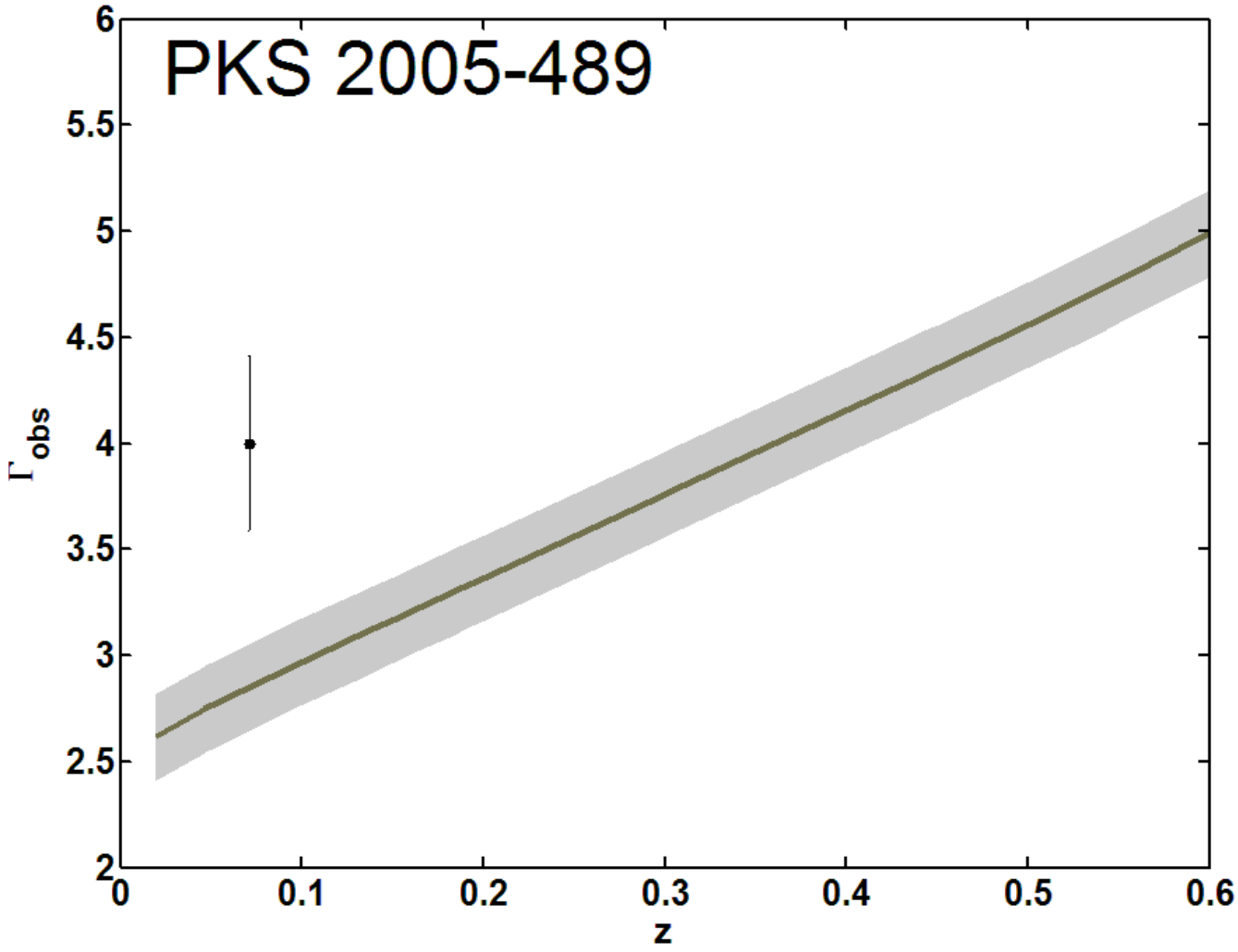
PKS 2005-489
Γ_{obs}
z
6
5.5
5
4.5
4
3.5
3
2.5
2
0
0.1
0.2
0.3
0.4
0.5
0.6

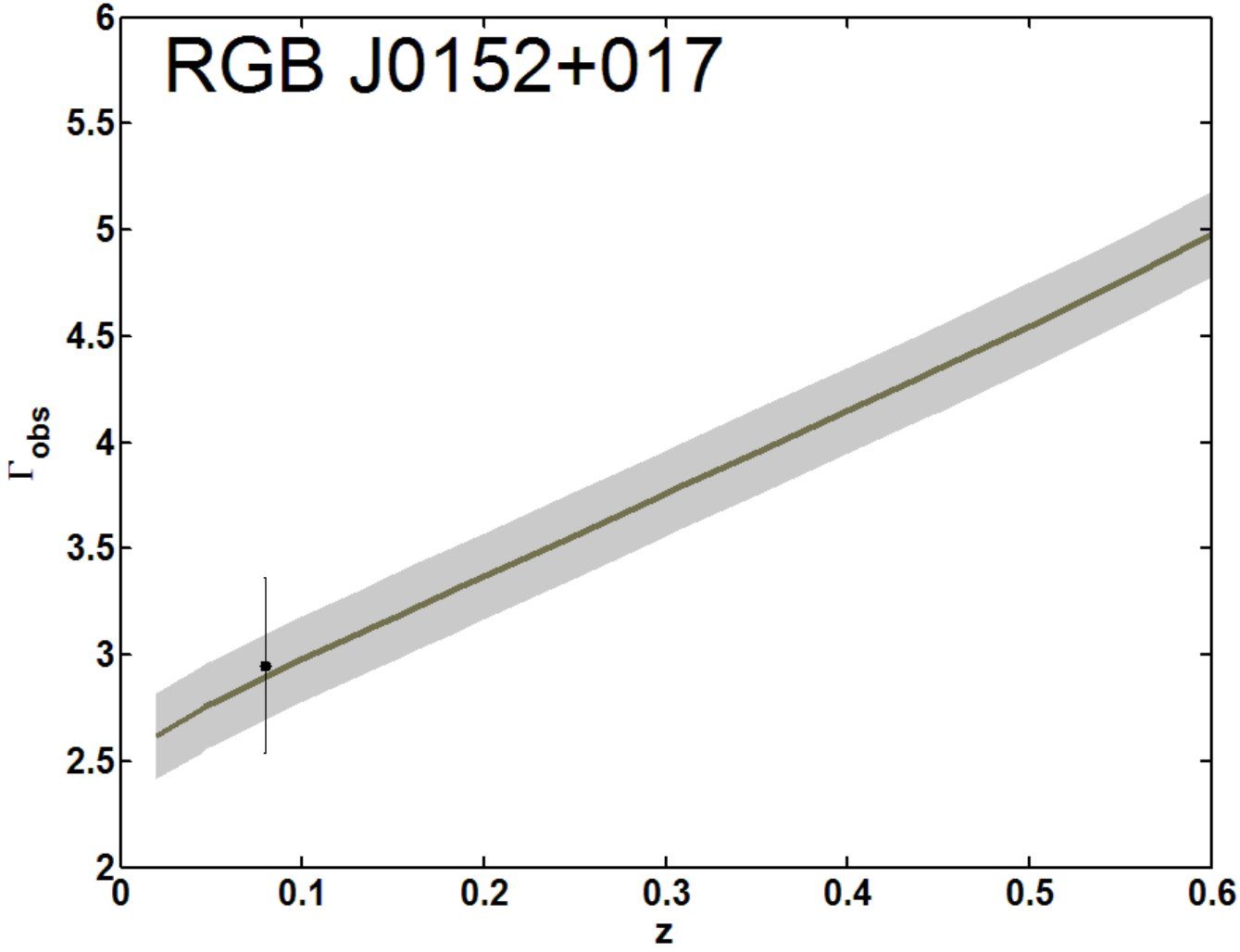
RGB J0152+017
6
5.5
5
4.5
4
3.5
3
2.5
2
0
0.1
0.2
0.3
0.4
0.5
0.6
z
Γobs

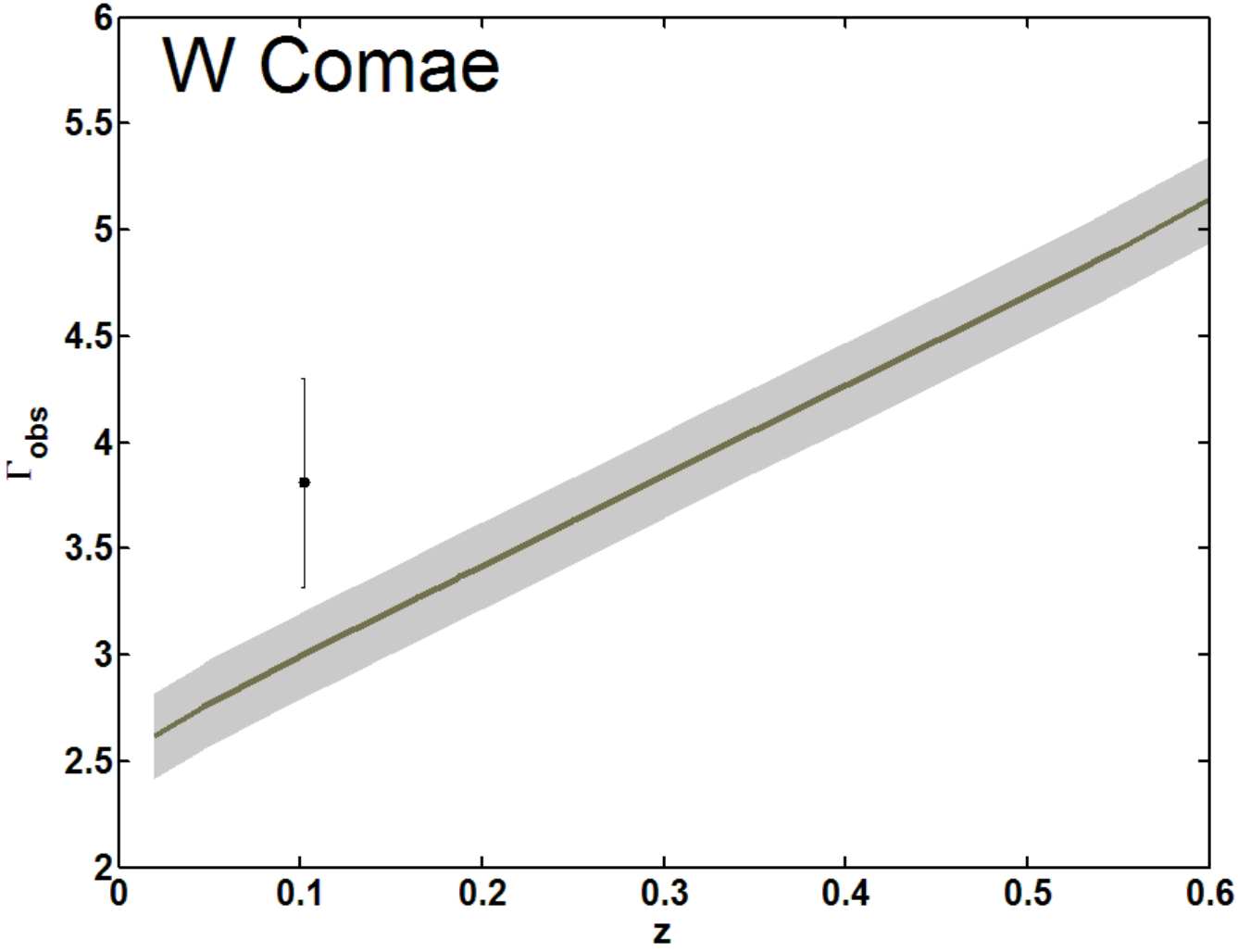
W Comae
6
5.5
5
4.5
4
3.5
3
2.5
2
0
0.1
0.2
0.3
0.4
0.5
0.6
z
Γobs

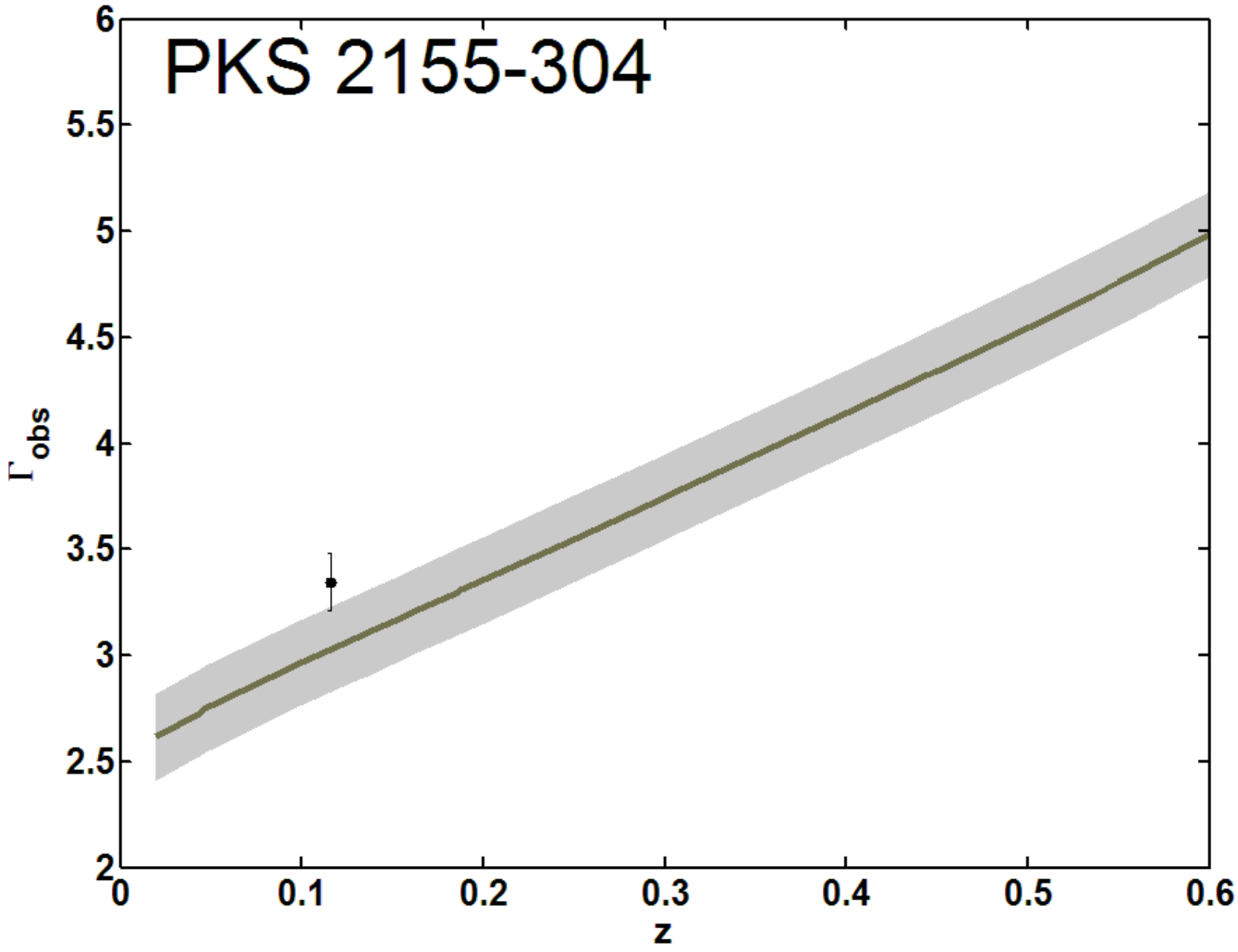
PKS 2155-304
Γ_{obs}
z
6
5.5
5
4.5
4
3.5
3
2.5
2
0
0.1
0.2
0.3
0.4
0.5
0.6

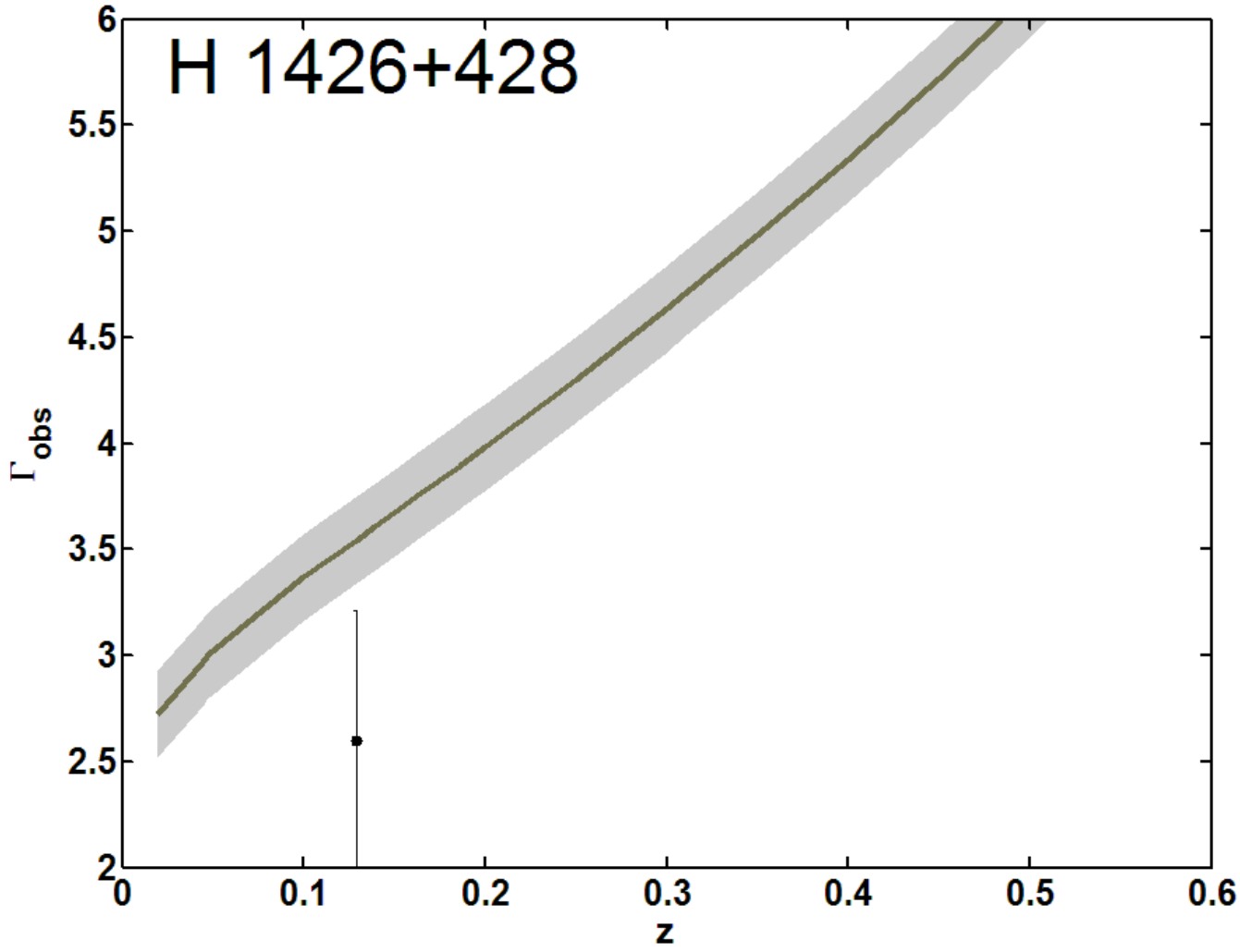
H 1426+428
Γ_{obs}
z
6
5.5
5
4.5
4
3.5
3
2.5
2
0
0.1
0.2
0.3
0.4
0.5
0.6

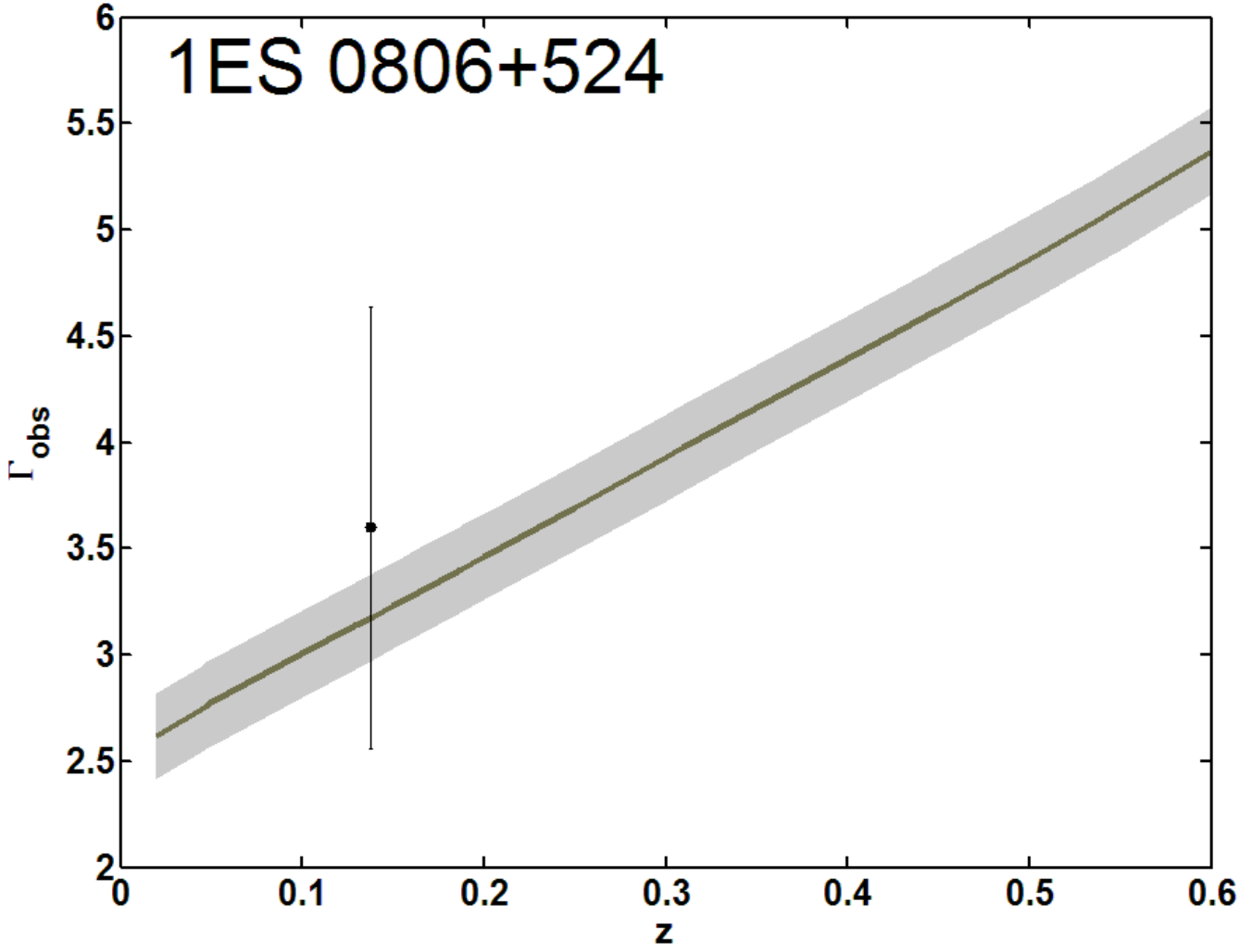
1ES 0806+524
Γ_{obs}
z
6
5.5
5
4.5
4
3.5
3
2.5
2
0
0.1
0.2
0.3
0.4
0.5
0.6

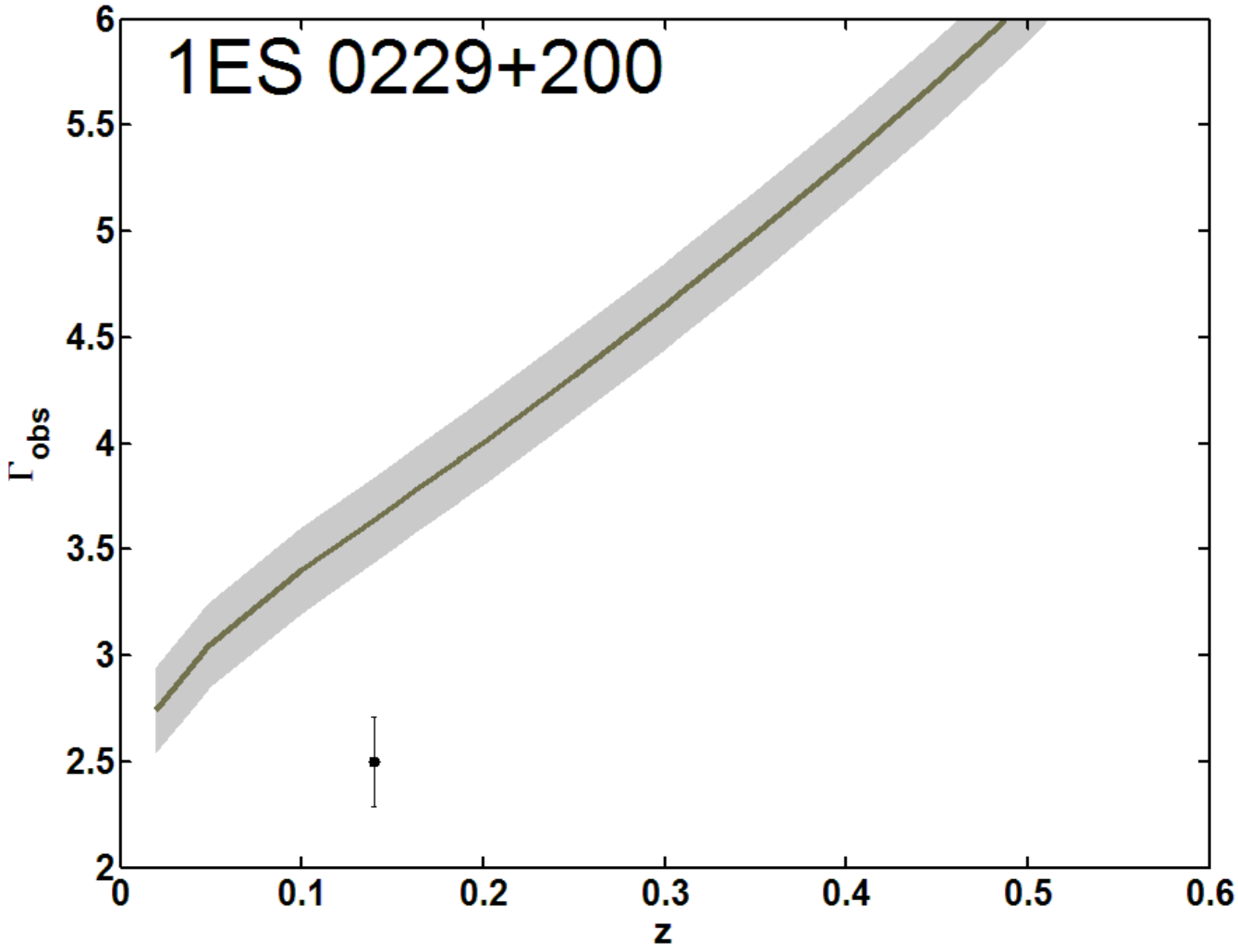
1ES 0229+200
Γ_{obs}
z
6
5.5
5
4.5
4
3.5
3
2.5
2
0
0.1
0.2
0.3
0.4
0.5
0.6

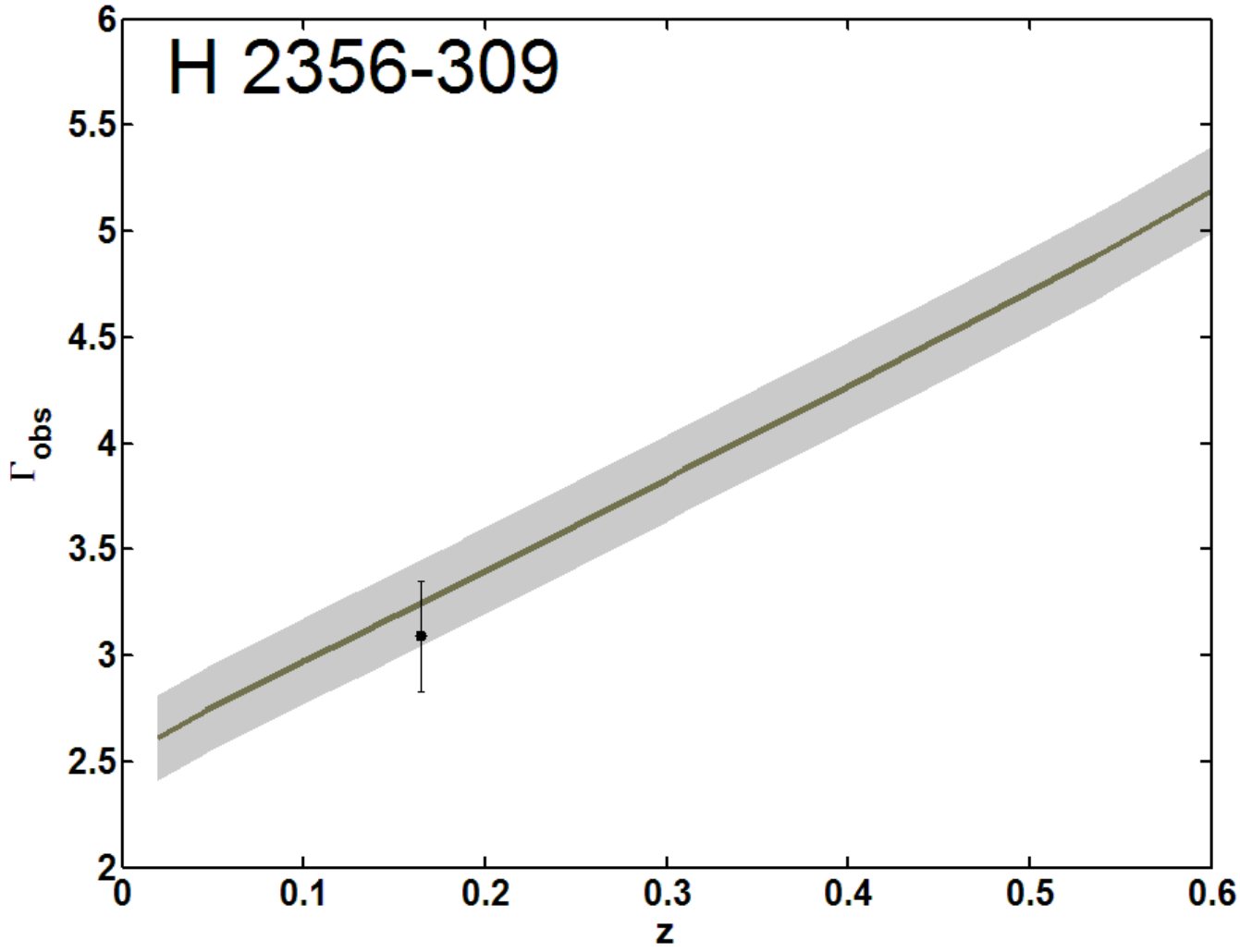
H 2356-309
Γ_{obs}
z
6
5.5
5
4.5
4
3.5
3
2.5
2
0
0.1
0.2
0.3
0.4
0.5
0.6

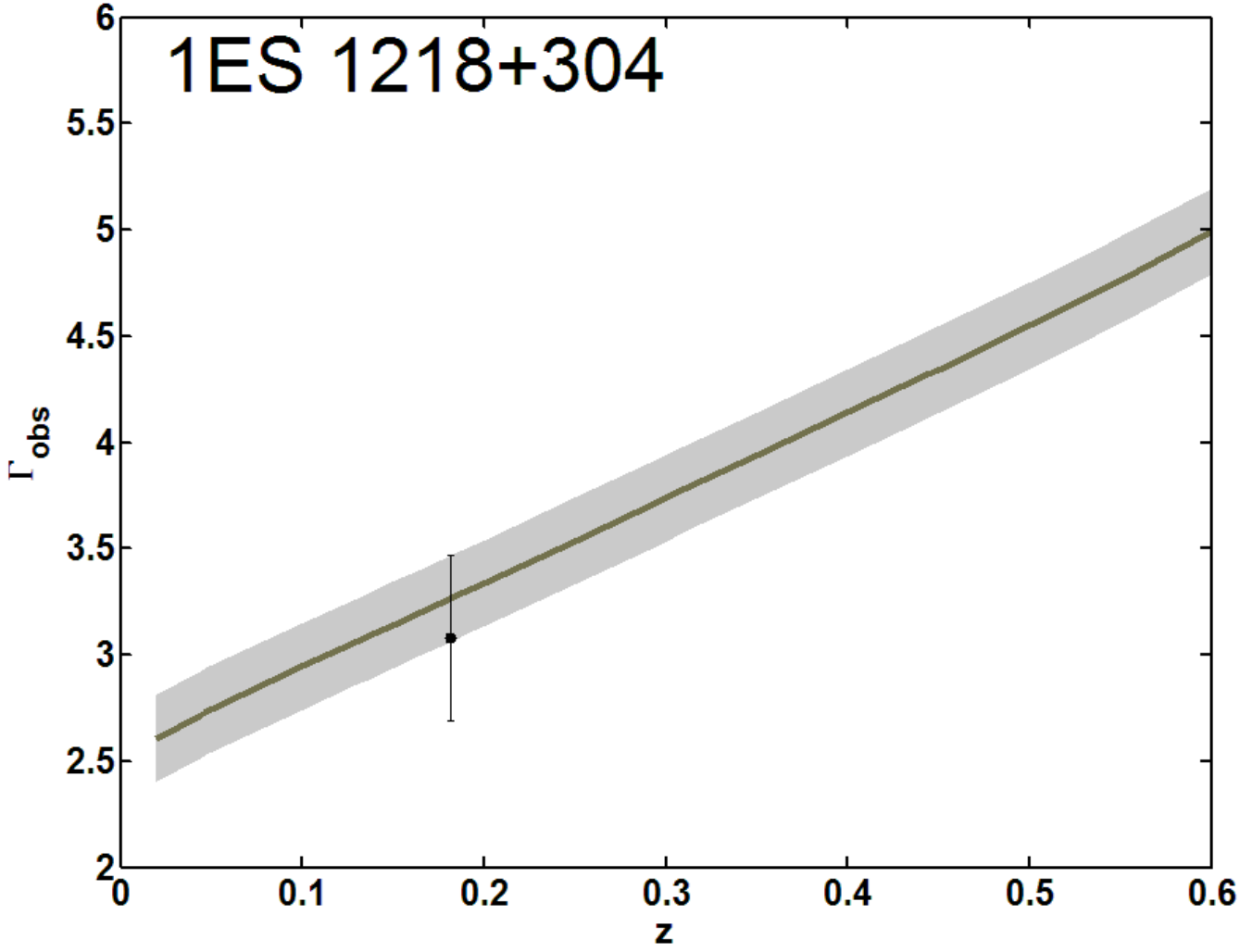
1ES 1218+304
Γ_{obs}
z
6
5.5
5
4.5
4
3.5
3
2.5
2
0
0.1
0.2
0.3
0.4
0.5
0.6

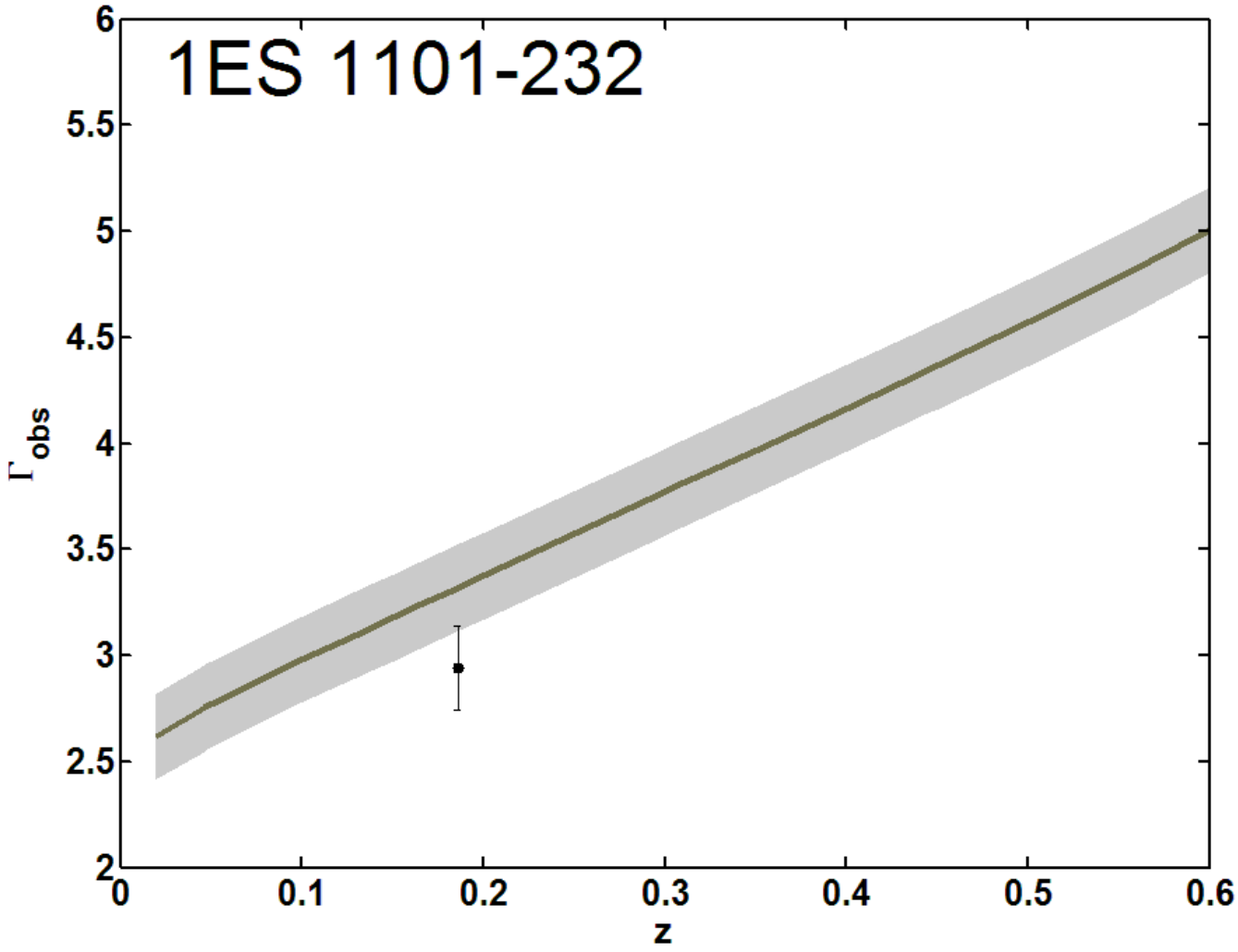
1ES 1101-232
Γ_{obs}
z
6
5.5
5
4.5
4
3.5
3
2.5
2
0
0.1
0.2
0.3
0.4
0.5
0.6

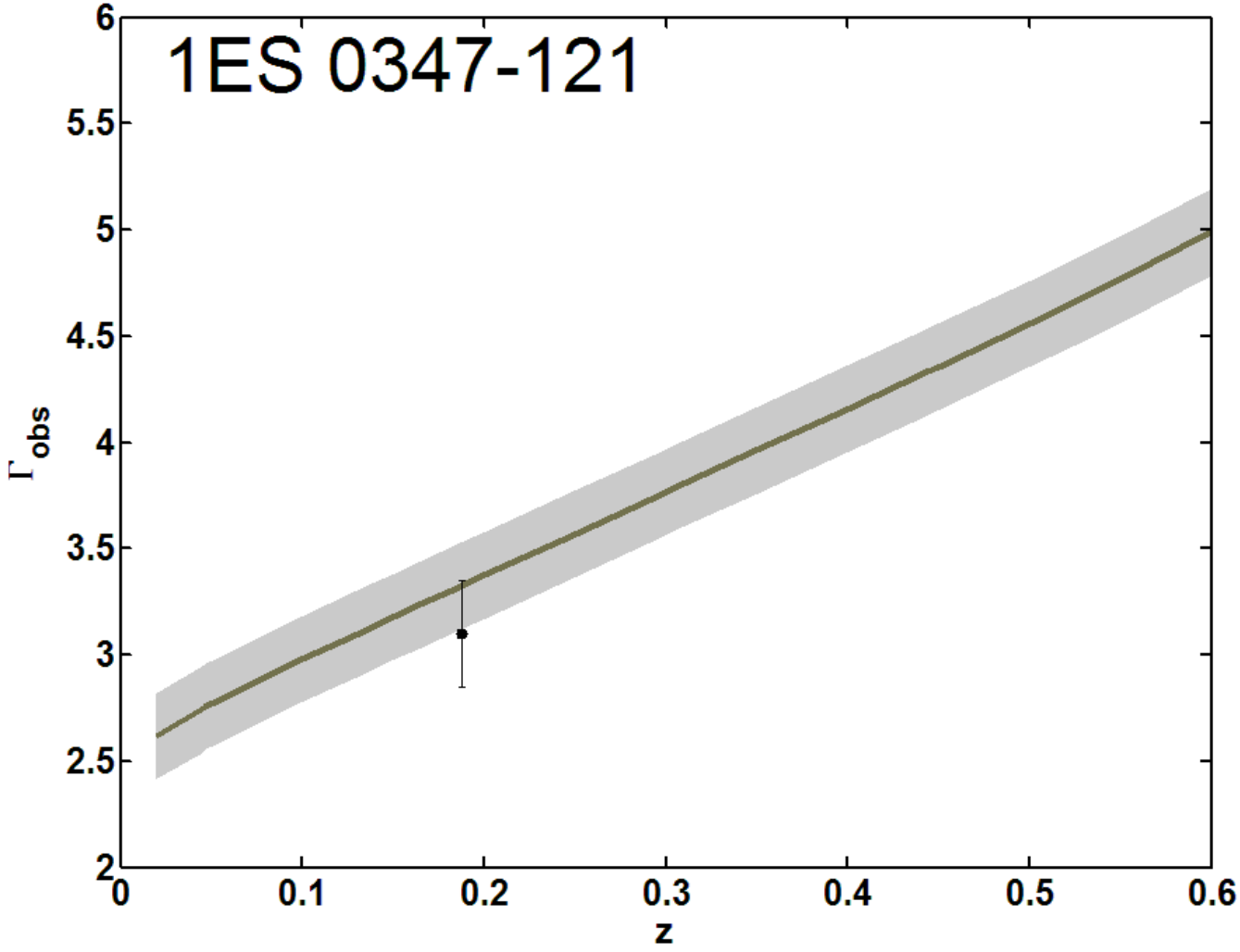
1ES 0347-121
Γ_{obs}
z
6
5.5
5
4.5
4
3.5
3
2.5
2
0
0.1
0.2
0.3
0.4
0.5
0.6

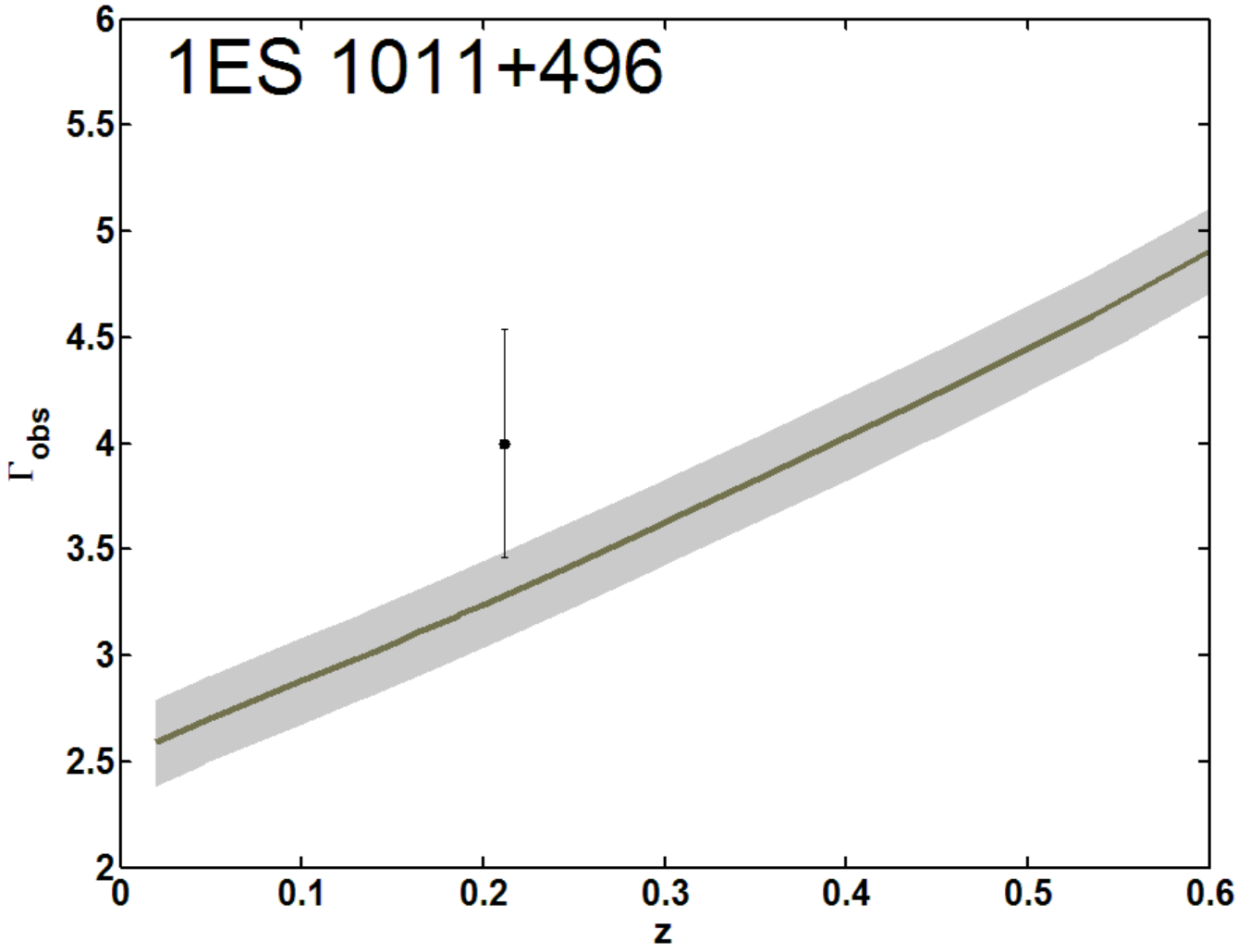
1ES 1011+496
Γ_{obs}
z
6
5.5
5
4.5
4
3.5
3
2.5
2
0
0.1
0.2
0.3
0.4
0.5
0.6

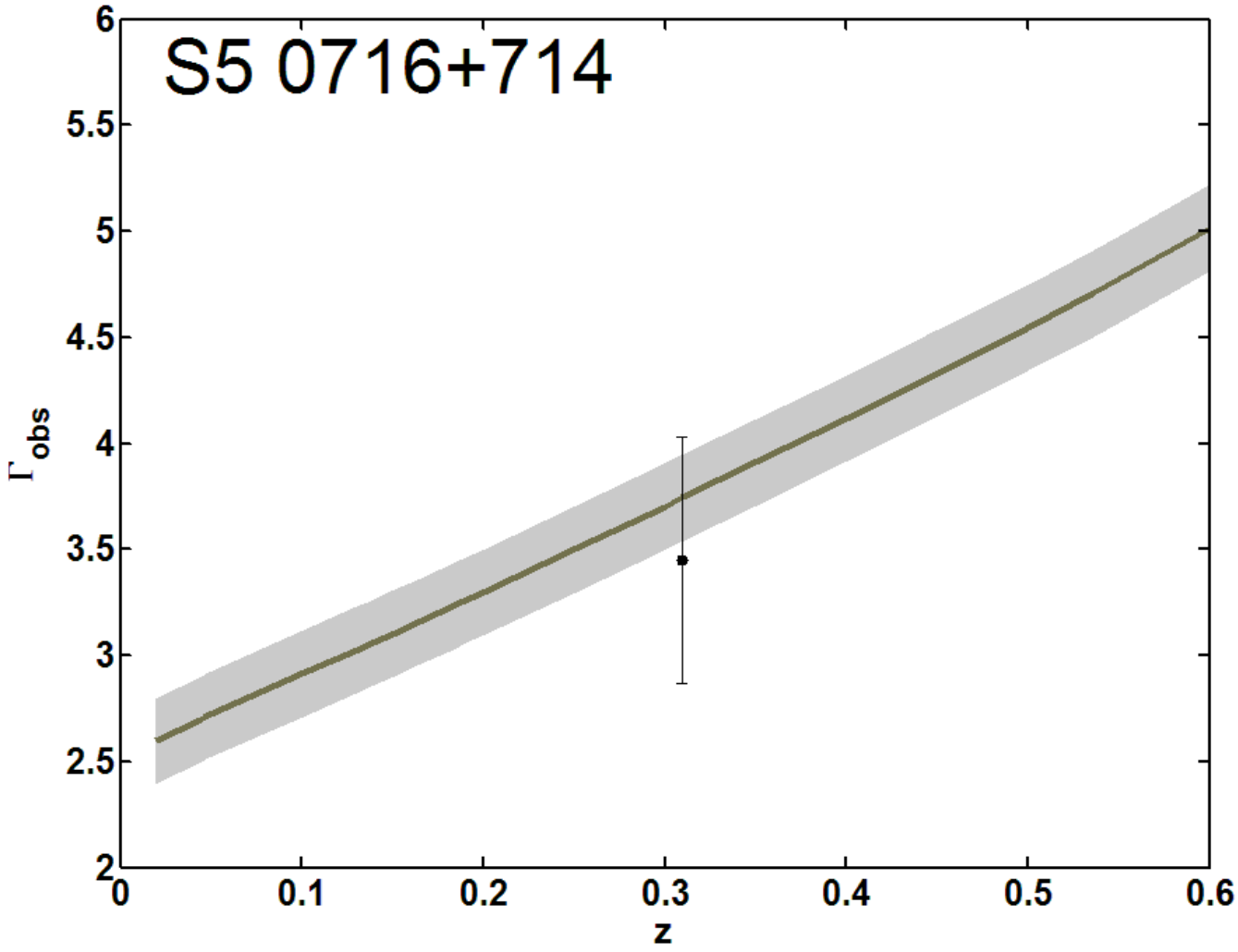
S5 0716+714
Γ_{obs}
z
6
5.5
5
4.5
4
3.5
3
2.5
2
0
0.1
0.2
0.3
0.4
0.5
0.6

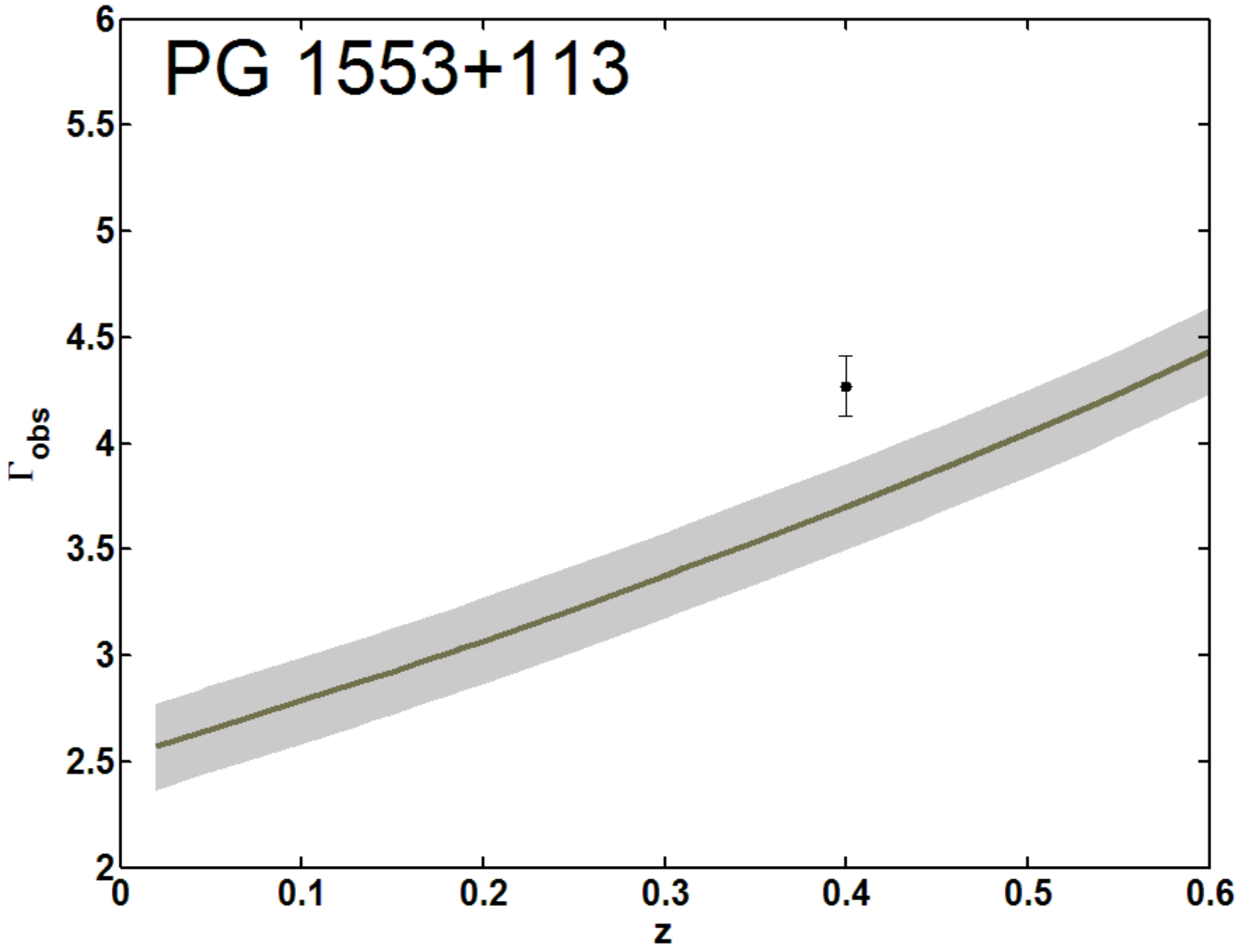
PG 1553+113
Γ_{obs}
z
6
5.5
5
4.5
4
3.5
3
2.5
2
0
0.1
0.2
0.3
0.4
0.5
0.6

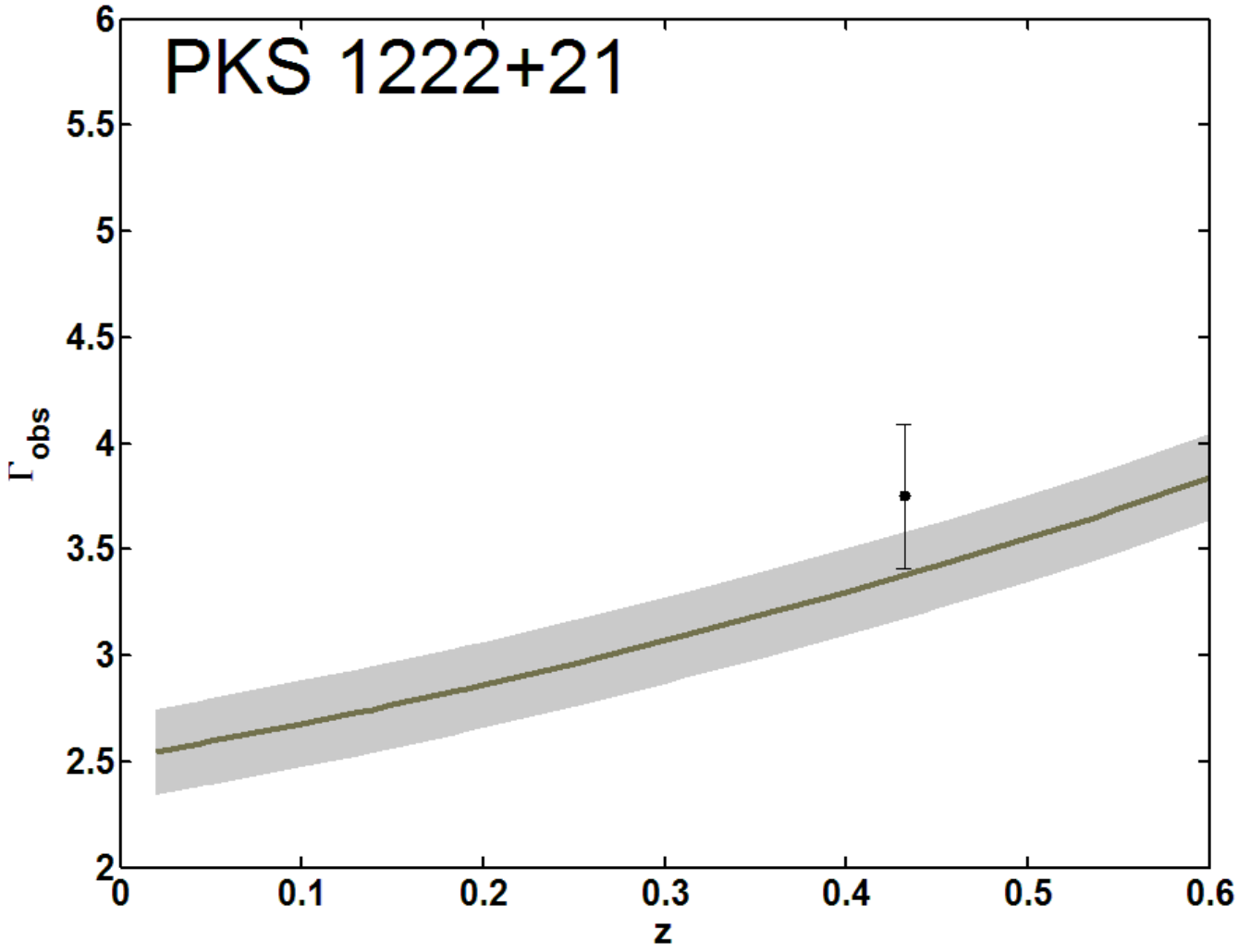
PKS 1222+21
6
5.5
5
4.5
4
3.5
3
2.5
2
Γ_{obs}
0
0.1
0.2
0.3
0.4
0.5
0.6
z

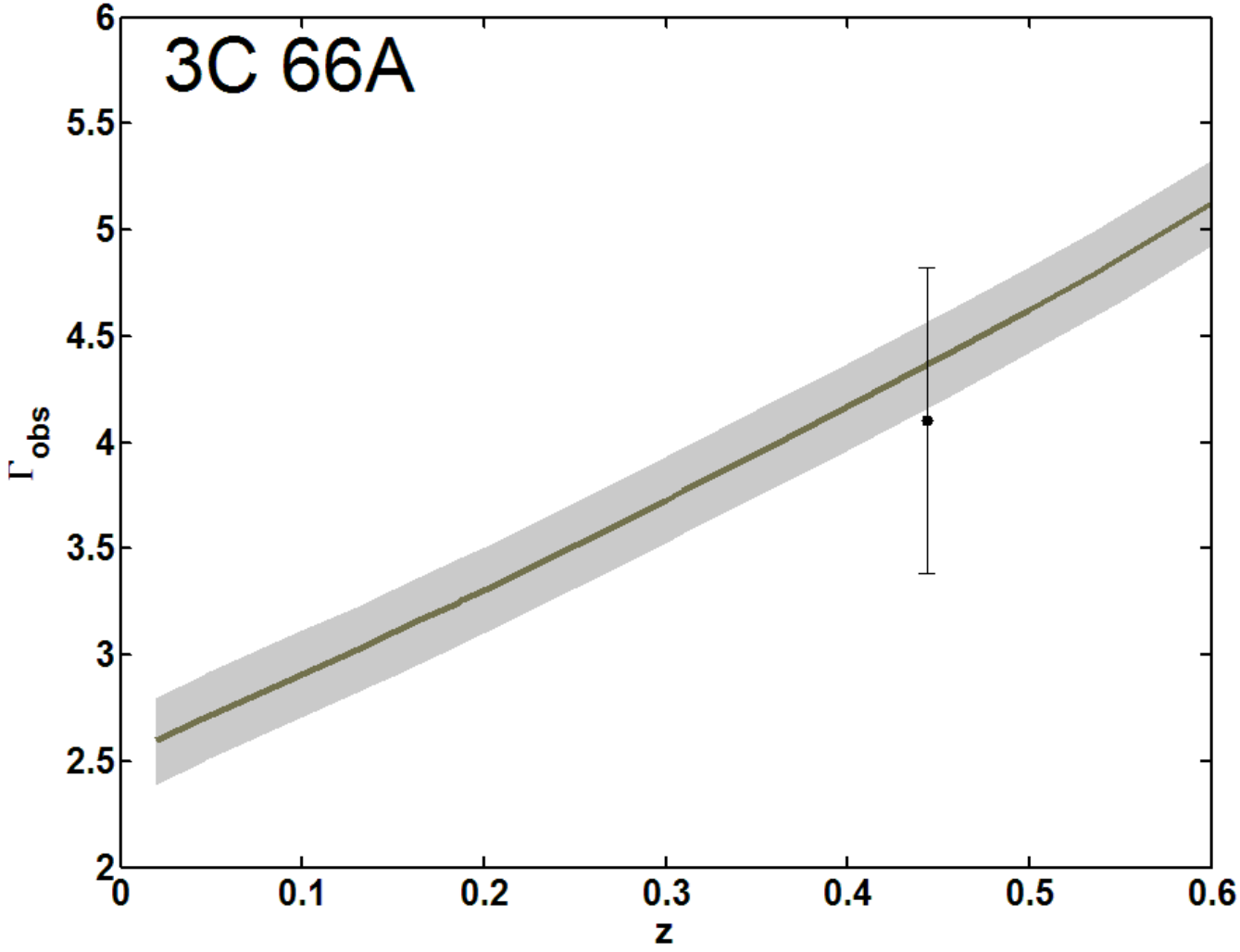
3C 66A
Γ_{obs}
z
6
5.5
5
4.5
4
3.5
3
2.5
2
0
0.1
0.2
0.3
0.4
0.5
0.6

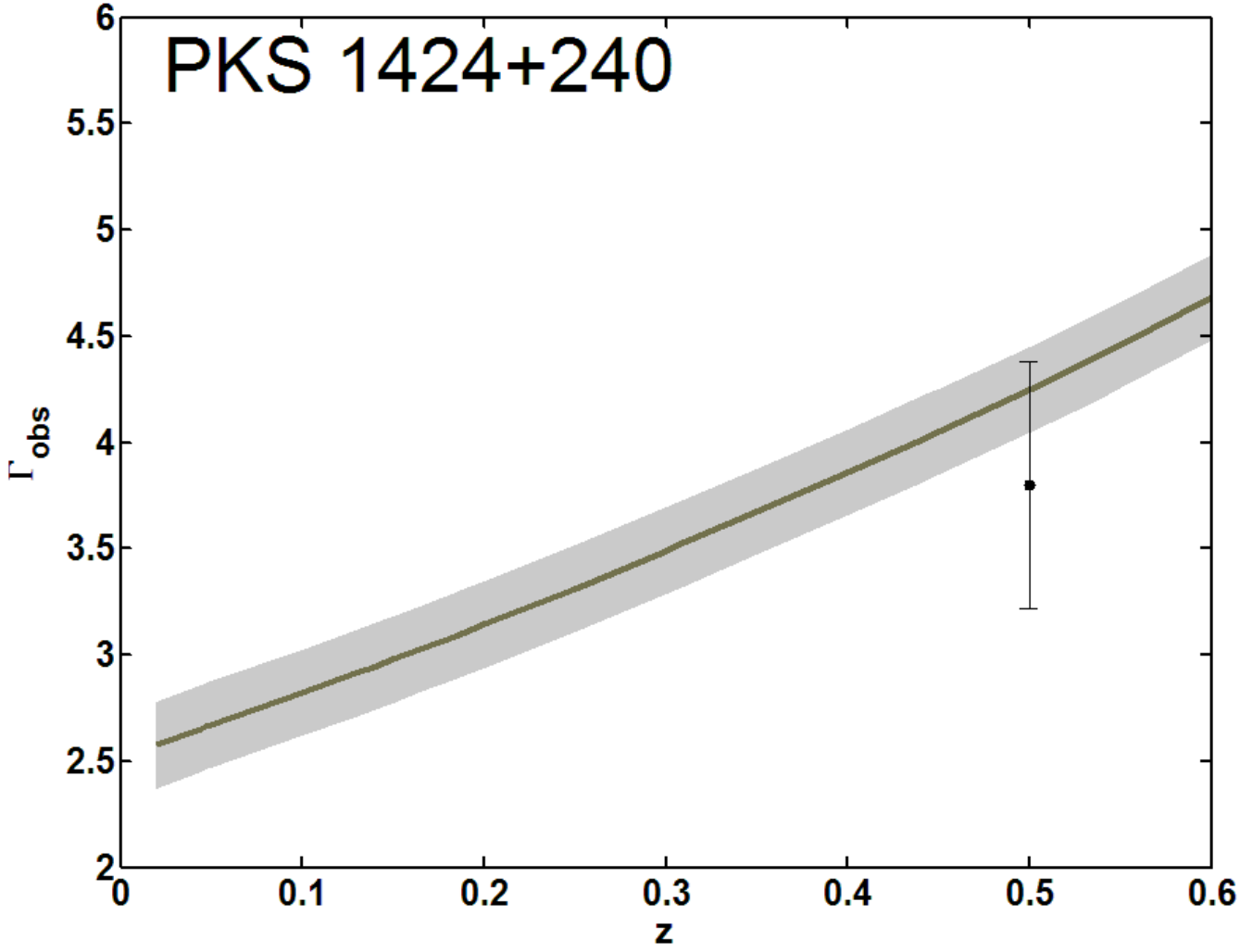
PKS 1424+240
Γ_{obs}
z
6
5.5
5
4.5
4
3.5
3
2.5
2
0
0.1
0.2
0.3
0.4
0.5
0.6

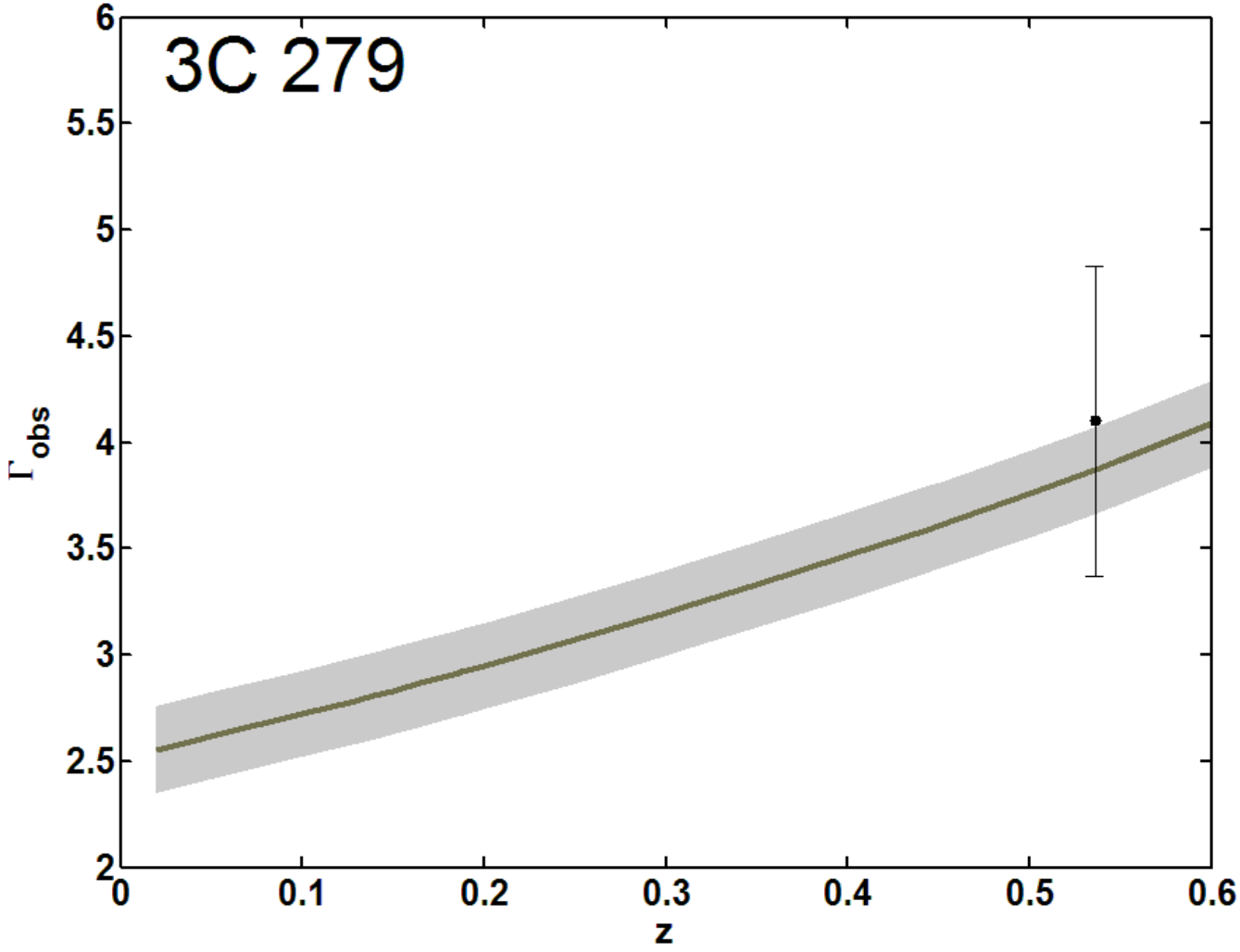
3C 279
Γ_{obs}
z
6
5.5
5
4.5
4
3.5
3
2.5
2
0
0.1
0.2
0.3
0.4
0.5
0.6

A look at those Figures shows that by assuming that ALL VHE blazars have $\Gamma_{\rm em} = 2.51 \pm 0.2$ allows to fit observations of 19 sources out of a total of 27 ones.

Yet, this statement is unfair. Because the role of photon-ALP oscillations is to partially offset EBL absorption, the DARMA scenario departs from conventional physics only to the extent that EBL attenuation becomes important. For instance, for $z \geq 0.100$ 12 sources out of a total of 16 ones are successfully fitted, whereas for $z \geq 0.138$ the fit becomes successful for 10 blazars out of a total of 11 ones. Clearly, even a small increase in the spread of $\Gamma_{\rm em}$ would improve the situation.

11 – CONCLUSIONS

Very light ALPs are a generic prediction of many extensions of the SM.

Our main assumptions are:

- Large-scale magnetic fields exist with a cellular morphology characterized by a coherence lenth in the $1 - 10\,\mathrm{Mpc}$ range and a strength not much smaller than the available upper bound $B_0 < 6\,\mathrm{nG}$.
- ALPs have to be very light in order to ensure that the strong-mixing regime is realized. The upper bound on their mass depends on the adopted value of the $a\gamma\gamma$ coupling constant B_0/M but in any case the condition $m < 5 \cdot 10^{-10}\,\mathrm{eV}$ has to be met. This prevents the axion needed to solve the strong CP problem from playing any role in the present context.

- The parameter M is consistent but fairly close to the strongest upper bound $M > 10^{11}\,\mathrm{GeV}$ coming from observations of supernova SN1987a. We remark that this bound is however affected by a large uncertainty and exceeds by one order of magnitude the robust bound $M > 10^{10}\,\mathrm{GeV}$ coming both from theoretical considerations of star cooling and from the negative result of the CAST collaboration.

We predict that a boost factor of 10 in the photon survival probability takes place for all VHE blazars observed so far well below the upper detection threshold of the planned CTA and HAWC water Cherenkov γ-ray observatory. Moreover, the energy E_{10} at which such a boost factor occurs decreases as the source distance increases and becomes e.g. as low as $2\,\mathrm{TeV}$ for the blazar 3C 279 at $z = 0.536$. Hence, our prediction can certainly be tested with the above planned detectors and possibly also with currently operating IACTs H.E.S.S., MAGIC, CANGAROO III, VERITAS as well as with the Extensive Air Shower arrays ARGO-YBJ and MILAGRO.

Remarkably, the DARMA scenario also offers a new interpretation of the observed VHE blazars, according to which the values of $\Gamma_{\rm em}$ for far-away VHE blazars are in the same ballpark of nearby ones and the large spread in the values of $\Gamma_{\rm obs}$ is mainly traced to the wide spread in the source distances.

As is well known, weakly interacting massive particles (WIMPs) can be detected either indirectly through astrophysical effects or directly at the Large Hadron Collider (LHC). The situation of ALPs characteristic of the DARMA scenario is in a sense similar. Besides being detectable indirectly through the astrophysical effects discussed in this paper, they lend themselves to a direct detection either in a planned photon regeneration experiment at DESY or with large xenon scintillation detectors developed for dark matter searches.